

Evaluation of highly variable water quality as basis for a sustainable water supply in the Dong Van karst region, Northern Vietnam

zur Erlangung des akademischen Grades einer

Doktorin der Naturwissenschaften

von der Fakultät für Bauingenieur-, Geo- und Umweltwissenschaften
des Karlsruher Instituts für Technologie (KIT)

genehmigte

DISSERTATION

von

M. Sc. Anna Franziska Ender

aus Freiburg i.Br.

Tag der mündlichen Prüfung:

29.03.2018

Referent: Prof. Dr. Nico Goldscheider

Korreferent: Prof. Dr.-Ing. Dr. h.c. mult. Franz Nestmann

Karlsruhe 2018

ABSTRACT

Karst aquifers are important groundwater resources, considering that many people across the world partly or even entirely depend on karst water. The special characteristics of karst aquifers result in a high variability in water availability and quality. Therefore, adapted water management strategies are crucial to use these water resources in a sustainable way. Especially in tropical and subtropical areas, like in Southeast Asia, the climate conditions with dry and rainy seasons hamper a continuous freshwater supply. In addition to severe water scarcity during dry seasons, a poor microbial water quality poses a threat to human health of the local population. The city Dong Van in Northern Vietnam faces increasing water scarcity and water quality problems. The designation as a UNESCO Global Geopark in 2010, called the Dong Van Karst Plateau, has led to a strong increase in tourist numbers, which enhance the pressure on the already tensed water supply situation. To meet the raising water demand and to protect groundwater resources against contamination and overexploitation, a profound understanding of the local hydrogeological conditions are essential.

Extensive field studies, including mapping, tracer tests and hydrochemical analyses were carried out and resulted in a hydrogeological conceptual model for the geologically complex karst area of Dong Van, which is presented in chapter 2 of the thesis. Four different physicochemical water types were identified, whereby the most important ones correspond to the karstified Bac Son and the fractured Na Quan aquifer. To evaluate the microbial water quality of the different water resources, analyses of three types of faecal indicator bacteria (FIB) *Escherichia coli* (*E. coli*), enterococci and thermotolerant coliforms were conducted. Although, all studied springs were faecally-impacted, the following relationships could be found: (1) Springs from the Bac Son formation displayed the highest microbial contamination, especially the springs that are involved in a polje series with connections to sinking streams. (2) The type of spring capture affects the water quality. Storage tanks are prone to contamination, since people might unknowingly pollute the water reservoirs. (3) FIB concentrations are dependent on seasonal variation, with higher values during wet season conditions.

Generally, water quality is affected by high fluctuations due to the high degree of hydrologic variability and spatial heterogeneity of transport parameters within karst aquifers. Therefore, the second study of this thesis (chapter 3) focuses on the characterization of flow and transport parameters within a karst conduit system. Six tracer tests were carried out with injections and monitoring at four sites along the flow system: a

swallow hole, two sites inside the cave, and two adjacent springs draining the system. Breakthrough curves (BTCs) were modelled with the one-dimensional Advection-Dispersion Model and the Two-Region-Non-Equilibrium Model. In order to obtain transport parameters in the individual sections of the flow system, an innovative evaluation approach was applied. The BTCs from one section were used as a multi-pulse input function for the next section. Using this approach, decreasing flow velocities along flow direction could be revealed due to decreasing gradients. However, dispersivity was highest in the middle section of the cave system. For the entire system, the tracer tests yielded an increase of mean flow velocities from 183 to 1,043 m/h with increasing discharge. Simultaneously, the proportion of immobile fluid regions decreased. Dispersivity was found to be minimal at intermediate discharge.

The water from the cave system described above is used for a projected and almost completed water supply system. For this reason, the water quality of the spring that drains the system is examined in the third study (chapter 4) of this thesis. Due to the high variability of karst springs, rapid assays are required that enable the observation of water quality fluctuations. In this study, the measurement of the enzymatic activity of *E. coli* is shown to be a valuable tool for water quality monitoring. The monitoring of β -D-glucuronidase (GLUC) activity was performed by using a prototype of a mobile, automated ColiMinder. With high temporal resolution, multiple hydrological, hydrochemical, physicochemical and microbiological parameters, including discharge, turbidity, particle-size distributions, and *E. coli* were measured during ten days of on-site monitoring to assess the relationship between GLUC activity, discharge dynamics and contamination patterns. Anthropogenic and agricultural activities led to a complex contamination pattern with high *E. coli* concentrations and GLUC activity with diurnal fluctuations. This daily dynamic could also be observed for the particle concentrations of small size classes (<10 μm), resulting in significant correlation coefficients. Stronger correlations between GLUC activity and *E. coli* or the concentration of 2-3 μm particles, were found for an event scale. However, GLUC activity and *E. coli* displayed significant differences in detail, which may be explained by viable but non-culturable cells. Nevertheless, the study showed that GLUC activity is a promising, complementary parameter for on-site and near real-time water quality monitoring, especially in combination with particle concentrations of small size classes.

The thesis presents a detailed view of water quality aspects in karst water resources on different scales. This holistic approach results in a better understanding of subtropical karst systems and delivers a valuable base in order to develop adapted and sustainable water management strategies. The presented methods and approaches are seen to be transferable and applicable to other remote karst areas under subtropical and tropical climate conditions.

KURZFASSUNG

Karstgrundwasserleiter sind wichtige Grundwasserressourcen, da weltweit viele Menschen teilweise oder sogar vollständig von Karstwasser abhängen. Aufgrund ihrer besonderen Eigenschaften ist die Verfügbarkeit und Qualität der Karstwässer hoch variabel. Daher sind für eine nachhaltige Nutzung dieser Wasserressourcen angepasste Bewirtschaftungsstrategien unerlässlich. Besonders in tropischen und subtropischen Gebieten, wie beispielsweise in Südostasien, erschweren die klimatischen Bedingungen mit Trocken- und Regenzeit, eine kontinuierliche Trinkwasserversorgung. Neben der Wasserknappheit in der Trockenzeit, stellt vor allem die schlechte mikrobielle Wasserqualität zur Regenzeit eine Bedrohung für die Gesundheit der Bevölkerung dar. Die Stadt Dong Van im Norden Vietnams sieht sich mit einer wachsenden Bedrohung durch Wasserknappheit und schlechter Wasserqualität konfrontiert. Die Ernennung des Dong Van Karst Plateaus zum UNESCO Global Geopark im Jahr 2010, führt zu stark steigenden Touristenzahlen, was den Druck auf die ohnehin bereits angespannte Wasserversorgungslage weiter verstärkt. Um den steigenden Wasserbedarf decken und die Grundwasserressourcen vor Verunreinigungen und Übernutzung schützen zu können, ist ein tiefgehendes Verständnis der hydrogeologischen Bedingungen vor Ort essentiell.

Umfangreiche Geländearbeiten wurden durchgeführt, einschließlich Kartierungen, Markierungsversuche und hydrochemischen Untersuchungen. Auf dieser Grundlage wurde ein hydrogeologisches Konzeptmodell für das geologisch komplexe Gebiet von Dong Van erstellt, das in Kapitel 2 vorgestellt wird. Vier Wassertypen konnten physikochemisch unterschieden werden, wobei die wichtigsten dem Bac Son Karstaquifer und dem Na Quan Kluftaquifer zugeordnet werden können. Um die mikrobielle Wasserqualität der verschiedenen Wasserressourcen beurteilen zu können, wurden die drei Fäkalindikatorbakterien (FIB) *Escherichia coli* (*E. coli*), enterococci und thermotolerante Gesamtcoliforme analysiert. Obwohl alle untersuchten Quellen mit Fäkalkeimen belastet waren, konnten folgende Zusammenhänge festgestellt werden: (1) Quellen der Bac Son Formation waren mikrobiell am stärksten belastet, vor allem wenn sie über die Poljenstaffelung mit Bachschwinden verbunden sind. (2) Die Quelfassung beeinflusst die mikrobielle Wasserqualität, da die üblichen Speichertanks anfällig für einen unwissentlichen Schadstoffeintrag durch die Quellanutzer sind. (3) Die Konzentrationen von FIB unterliegen jahreszeitlichen Schwankungen, mit höheren Werten in der Regenzeit.

Aufgrund der starken hydrologischen Variabilität und der räumlichen Heterogenität von Transporteigenschaften im Karst, unterliegt die Wasserqualität im Allgemeinen starken

Schwankungen. Daher konzentriert sich die zweite Studie (Kapitel 3) auf die Charakterisierung von Fließ- und Transportparametern in einem Karströhrensystem. Es wurden sechs Markierungsversuche durchgeführt, wobei die Eingaben und die Beprobungen an vier Stellen entlang des Fließsystems vorgenommen wurden: der Bachschwinde, zwei Stellen in der Höhle und an zwei benachbarten Quellen, die das System entwässern. Die Durchgangskurven wurden mit einem eindimensionalen Advektions-Dispersions-Modell und einem „Two-Region Non-Equilibrium“ Modell berechnet. Um Transportparameter für die einzelnen Abschnitte des Fließsystems zu erhalten, wurde ein innovativer Ansatz für die Datenauswertung gewählt. Dabei wurde die Durchgangskurve eines Abschnittes als Multi-Puls Eingabefunktion für den nächsten Abschnitt verwendet. Auf diese Weise konnte gezeigt werden, dass die Fließgeschwindigkeiten in Fließrichtung aufgrund abnehmender Gradienten abnehmen, die Dispersivität jedoch im mittleren Höhlenabschnitt am größten ist. Für das gesamte System ergaben die Untersuchungen, dass die mittlere Fließgeschwindigkeit mit steigender Schüttung von 183 auf 1,043 m/h ansteigt. Gleichzeitig nimmt der Anteil von immobilen Fluidbereichen im System ab. Es zeigte sich, dass die Dispersivität bei mittleren Schüttungen am kleinsten ist.

Das Wasser des Höhlensystems wird von einer geplanten und fast fertiggestellten Wasserversorgungsanlage genutzt werden. Daher wurde die Wasserqualität der Quelle, die das Höhlensystem entwässert, in der dritten Studie (Kapitel 4) dieser Arbeit untersucht. Aufgrund der hohen Variabilität von Karstquellen sind schnelle Untersuchungsmethoden erforderlich, um die Qualitätsschwankungen beobachten zu können. In dieser Studie erwies sich die Bestimmung der Enzymaktivität von *E. coli* als wertvolles Werkzeug. Mit einem mobilen, automatischen Prototypen des ColiMinders, konnte die Aktivität von β -D-Glucuronidase (GLUC) überwacht werden. Mehrere hydrologische, hydrochemische, physikochemische und mikrobiologische Parameter, wie Schüttung, Trübe, Partikelgrößenverteilung und *E. coli* wurden bei einer zehntägigen Monitoring-Kampagne zeitlich hochaufgelöst gemessen, um die Beziehung zwischen GLUC Aktivität und Schüttungsdynamiken bzw. Kontaminationsmustern zu untersuchen. Dabei zeigte sich, dass anthropogene und landwirtschaftliche Aktivitäten zu einem komplexen Kontaminationsmuster mit hohen *E. coli* Konzentrationen und GLUC-Aktivitäten führen, die tageszeitlichen Schwankungen unterliegen. Diese Tagesschwankungen konnten auch in den Partikelkonzentrationen der kleinen Größenklassen ($<10\mu\text{m}$) beobachtet werden, was sich in signifikanten Korrelationskoeffizienten widerspiegelt. Deutlich stärkere Korrelationen zwischen GLUC Aktivität und *E. coli* bzw. Konzentrationen der 2-3 μm Partikel konnten für ein einzelnes Regenereignis erzielt werden. Dennoch unterscheiden sich die Ergebnisse der GLUC Aktivität und *E. coli* im Detail, was durch lebende, aber nicht kultivierbare Zellen (VBNC) erklärt werden kann. Die Studie zeigt aber, dass die GLUC Aktivität ein

vielversprechender, ergänzender Parameter für ein vor Ort und nahezu Echtzeit-Monitoring der Wasserqualität ist, besonders in Kombination mit den kleinen Partikelgrößenklassen.

In dieser Arbeit wird die Wasserqualität subtropischer Karstwasserressourcen mit einem differenzierten Blick auf verschiedenen Ebenen betrachtet. Dieser ganzheitliche Ansatz führt zu einem besseren Verständnis von subtropischen Karstsystemen. Außerdem liefert es eine wichtige Grundlage für die Entwicklung von angepassten Strategien zur nachhaltigen Wasserbewirtschaftung. Die vorgestellten Methoden und Ansätze können auf andere entlegene Karstgebiete unter subtropischen und tropischen Klimabedingungen übertragen und bei deren Untersuchung eingesetzt werden.

TABLE OF CONTENTS

1	INTRODUCTION	1
1.1	General motivation.....	1
1.2	Karst in Southeast Asia	5
1.2.1	<i>General karst characteristics</i>	5
1.2.2	<i>Subtropical and tropical karst</i>	6
1.3	Water management in Vietnam.....	9
1.3.1	<i>Water resources in Vietnam and their management</i>	9
1.3.2	<i>Water management in Dong Van</i>	12
1.3.3	<i>KaWaTech project</i>	15
1.4	Objectives and approaches.....	17
1.5	Structure of the thesis.....	19
2	HYDROGEOLOGICAL CONTROLS OF VARIABLE MICROBIAL WATER QUALITY IN A COMPLEX SUBTROPICAL KARST SYSTEM IN NORTHERN VIETNAM	21
2.1	Introduction.....	22
2.2	Materials and methods	23
2.2.1	<i>Study site</i>	23
2.2.2	<i>Sampling campaigns</i>	25
2.3	Results and discussion.....	29
2.3.1	<i>Tracer tests</i>	29
2.3.2	<i>Physicochemical characterization</i>	31
2.3.3	<i>Hydrogeological conceptual model</i>	34
2.3.4	<i>Microbiological water quality</i>	37
2.4	Conclusions	44
2.5	Acknowledgements.....	46
3	SPATIAL RESOLUTION OF TRANSPORT PARAMETERS IN A SUBTROPICAL KARST CONDUIT SYSTEM DURING DRY AND WET SEASONS.....	49
3.1	Introduction.....	50
3.2	Materials and methods	51
3.2.1	<i>Study Site</i>	51
3.2.2	<i>Tracer Tests</i>	53
3.2.3	<i>Modelling of the results</i>	55
3.3	Results	58
3.3.1	<i>Variability of flow parameters</i>	58
3.3.2	<i>Spatial resolution by using the multiple pulse injection approach</i>	64

3.4	Discussion.....	67
3.4.1	<i>Variability of flow parameters</i>	67
3.4.2	<i>Multiple-pulse-injection approach</i>	69
3.5	Conclusions.....	70
4	EVALUATION OF β-D-GLUCURONIDASE AND PARTICLE-SIZE DISTRIBUTION FOR MICROBIOLOGICAL WATER QUALITY MONITORING IN NORTHERN VIETNAM ...	73
4.1	Introduction.....	74
4.2	Materials and methods.....	77
4.2.1	<i>Site selection and sampling campaign</i>	77
4.2.2	<i>Sensor measurements</i>	78
4.2.3	<i>Correlation analysis</i>	81
4.3	Results & discussion.....	82
4.3.1	<i>Time series</i>	82
4.3.2	<i>Variations in time series during one rain event</i>	85
4.3.3	<i>Correlation analysis</i>	86
4.3.4	<i>Comparison of β-D-glucuronidase activity and <i>E. coli</i></i>	91
4.4	Conclusion.....	93
5	CONCLUSIONS AND OUTLOOK.....	97
5.1	General overview.....	97
5.2	Scientific aspects.....	97
5.3	Project related aspects.....	101
5.4	Regional transferability aspects.....	103
	ACKNOWLEDGEMENTS.....	107
	DECLARATION OF AUTHORSHIP.....	111
	REFERENCES.....	113
	SUPPLEMENTARY INFORMATION.....	127
	Supplementary Material – Chapter 2.....	127
	Supplementary Material – Chapter 3.....	131
	Supplementary Material – Chapter 4.....	133

LIST OF FIGURES

Fig. 1-1	Location of the study site in the province Ha Giang, district Dong Van, Northern Vietnam (DEM: Zindler et al. 2015).	3
Fig. 1-2	Left: Quan Ba Twin Mountains (Tam Son city, Quan Ba district) with conical karst landforms in the background. Right: Small depression, enclosed by steep karst cones, south of Dong Van.	6
Fig. 1-3	Schematic illustration (inspired by Goldscheider and Drew 2007) of a heterogeneous tropical karst aquifer system with the typical duality of infiltration (point/diffuse) and groundwater flow within matrix, fractures and conduits.	7
Fig. 1-4	Fenglin karst at the Li River in Yangshuo, south of Guilin in South China (left, www.pixabay.com) and in Ha Long Bay, Vietnam (right, photographed by Anh Tran Diep).	8
Fig. 1-5	Dong Van polje (photographed from west to east) with an alluviated flat floor, several karst springs at the western and northern margins and a sinking stream at the eastern margin.	8
Fig. 1-6	Mean precipitation (climate station Dong Van District, 2000–2012) and mean air temperature (climate station Ha Giang District, 1990–2010; Vietnam National Centre for Hydro-Meteorological Forecasting, NCHMF).	13
Fig. 1-7	Left: Girls carrying 40 L cans full of water from the spring to their homes. Right: Even small springs with discharge rates < 0.2 L/s are intensively used for personal hygiene.	13
Fig. 1-8	Hanging Pools as water storage in the Dong Van region.	14
Fig. 1-9	Seo Ho water supply system that was planned and built within the KaWaTech and KaWaTech Solution project (modified after Oberle et al. 2017).	16
Fig. 1-10	Studies that were carried out on different scales in the Dong Van region (Satellite Image: Google Earth, photo: karst spring ML 4, where the monitoring was performed, March 2014).	20
Fig. 2-1	a Location of the study site (close to the Chinese border) is shown on a section of the world karst aquifer map. The distribution of carbonate rocks in Vietnam and the adjacent countries is shown in blue (based on the WOKAM approach after Chen et al. 2017). b Lithostratigraphic and hydrostratigraphic profile. c Geological map of the Dong Van area (the digital elevation model (DEM) in the background is from B Zindler, A Degen, H Stolpe, RUB Bochum, unpublished data, 2015. d Cross-section through the Dong Van Valley from North to South. The location of the photos is shown with labels P1 and P2. P1: Dong Van Valley (from W to E), P2: Sang Ma Sao Valley (from SW to NE)	24

Fig. 2-2	a Injection and major sampling points for the tracer tests conducted in Dong Van and the identified connections (arrows), and b the observed breakthrough curves (DEM: B Zindler, A Degen, H Stolpe, RUB Bochum, unpublished data, 2015).....	30
Fig. 2-3	a Principal component analysis (PCA) of the samples (n = 108) taken in the Dong Van area. The variables are shown with blue lines and the individual observation in colored points, depending on the different sampling points. One outlier (W2) was excluded from the PCA. b Hydrochemical groups according to the Ca ²⁺ /Mg ²⁺ molar ratio versus Ca ²⁺ . The blue group “Others” include observations from springs of the Song Hien Fm. and the Mia Le Fm. The group “Mixed Water” includes the samples of the Ma Le cave system (SSML, CST1, CST2, CSP3, CSP4), since the Ma Le River drains a catchment area where all the geological units are represented	33
Fig. 2-4	Schematic model of the Dong Van polje. The recharge area of the karst aquifer lies, at least partly, in the northern mountainous region. Water from the cave and corresponding spring CSP1 is used for the water supply system of Dong Van. Additionally, groundwater is extracted by private (W1, W4) and public wells. Colors correspond to the geological map (Fig. 2-1c).....	35
Fig. 2-5	a Hydrogeological map of the Dong Van region. The different hydrogeological zones are related to the Bac Son karst aquifer. The less important fractured Na Quan aquifer is not considered in this figure. Geological information can be found in Fig. 2-1 (DEM in the background: B Zindler, A Degen, H Stolpe, RUB Bochum, unpublished data, 2015). b North-south cross-section through the Dong Van Valley	36
Fig. 2-6	Concentrations of a <i>Escherichia coli</i> (<i>E. coli</i>) and b enterococci (ENT), dependent on hydrogeology, seasons and the type of sampling points. Considered values are from dry and transient season 2015, and rainy season 2016. The group “Other Fm.” includes samples from surface streams and the spring from the Toc Tat Fm. (OS6)	38
Fig. 2-7	Categories for fecal indicator bacteria depending on a hydrological conditions and b on aquifer type. The group “wet season” contains analysis from three campaigns (July 2014, September 2015 and June 2016) and the group “dry season” from two campaigns (February 2014, March 2015). Samples from wells are not considered within the comparison of seasons	39
Fig. 2-8	Monitoring at the spring CSP1 for a time period of 24 days with daily measurements. In total, eight samples were taken for the analysis for <i>Escherichia coli</i> (<i>E. coli</i>)	41
Fig. 2-9	Forty-eight-hour monitoring at the spring KS2 for the evaluation of short-term water quality dynamics. Although no precipitation event occurred, daily	

	contamination events could be identified with <i>E. coli</i> levels of >2,420 MPN/100 ml (>UDL)42
Fig. 2-10	Comparison of contamination levels of 45 samples (n) collected at springs with and without a direct connection to a swallow hole: five springs are known to be directly connected to a swallow hole (KS1, KS2, CSP3, CSP4 and SRDV), and four springs are assumed to have no direct connection to a swallow hole (CSP1, CSP2, KS3 and KS6).....43
Fig. 3-1	a Study area in Northern Vietnam near the Chinese border. The overview map is a section of the world karst aquifer map that exhibits the distribution of carbonate rocks (blue) in Vietnam (Chen et al. 2017). b The Ma Le cave system (D Lagrou, SPEKUL, unpublished report, 2005), shown on the 1:50,000 geological map (Vietnam Institute of Geosciences and Mineral Resources, unpublished data, 2017) with a digital elevation model in the background (B. Zindler, A. Degen, H. Stolpe, RUB Bochum, unpublished data, 2015). c Cross section, following the course of the caves. The course of the caves is not to scale, but is, however, in the range of measured dimensions.....52
Fig. 3-2	Flow chart illustrating the procedure of the multiple pulse injection application, exemplified with the section ML 3–ML 4 and marked with the circled numbers 1 and 2. Cross section follows the course of the caves (Fig. 3–1b).57
Fig. 3-3	Breakthrough curves observed at the spring ML 4 under different hydrologic conditions. Discharge (<i>Q</i>) and recovery rate (<i>R</i>) were determined for the spring ML 4.....58
Fig. 3-4	Variation of flow and transport parameters for the complete cave system (ML 1–ML 4) dependent on the spring discharge (ML 4), modelled with a ADM and b 2RNE59
Fig. 3-5	Breakthrough curves, modelled with the advection-dispersion model, for each sampling site within the cave system for both a dry and b wet season (<i>Q</i> discharge, v_m mean flow velocity, α dispersivity, <i>R</i> recovery rate). The Dirac input function was applied. Note the different scales of the time axes.....60
Fig. 3-6	For ML 3, a multiple pulse injection (MPI) was applied to model the BTC in ML 4 (number 2), for a dry season 2014, and b rainy season 2014. For comparison, the ADM, modelled with a Dirac injection in ML 1, is also shown (number 1; note, numbers 1 and 2 refer to Fig. 3-2). In the descending branch, the MPI approach resulted in a better fitting of the tailing that is indicated by smaller residuals64
Fig. 3-7	Spatial resolution of flow and transport parameters within the cave system. Mean flow velocity (v_m) and dispersivity (α) are calculated with an ADM and a Dirac input for the first segment and a MPI input function for all subsequent segments. The parallel flow path ML 3–SH 1 is not considered in this figure, but exhibits lower mean flow velocities and higher dispersivity than ML 3–ML 4

	(Table 3–5 and Table3– 6). Cross section follows the course of the caves (Fig. 3-1b). 67
Fig. 4-1	Study area in Northern Vietnam near the Chinese border. The blue color on the overview map (left) exhibits the distribution of carbonate rocks in Vietnam (Chen et al. 2017). The Ma Le Valley is drained by the Ma Le River, which enters an underground cave system and emerges at the spring to form the Seo Ho River. A water quality monitoring program was performed at the Seo Ho spring. Grey numbers indicate the elevation in meters above sea level (modified after Zindler et al. 2015). 77
Fig. 4-2	Time series of precipitation, discharge, electrical conductivity, turbidity, concentration of three different particle size classes, and enzymatic activity. Grab samples for the determination of TTC and <i>E. coli</i> by using Colisure, were taken every 4 h. The upper detection limit (dotted line) was set to 24,200 MPN/100 ml, due to a dilution factor of 10. The grey bar highlights the period illustrated in Fig. 4-3. Time series signify a strong daily pattern in the data set of particle concentration, turbidity, and enzymatic activity that is not related to precipitation..... 83
Fig. 4-3	Time series during a moderate rainfall: All parameters, measured with an interval of 30 min (blueish bars = 60 min), display a fast reaction on the precipitation event. However, GLUC activity and small particle concentrations respond faster than <i>E. coli</i> and exhibit their first maxima at the minimum of the electrical conductivity, which marks the arrival of the lower mineralized rain water at the spring. 86
Fig. 4-4	a) Autocorrelation of time series of enzymatic activity (GLUC), turbidity, different particles size classes (1–2 μm , 2–3 μm and 5–10 μm), water temperature (water temp), and <i>E. coli</i> . b) Cross correlation between time series of GLUC and different particle size classes, turbidity, water temperature, and <i>E. coli</i> . There is no considerable time lag between the maxima of particle concentrations and GLUC..... 88
Fig. 4-5	Means at different times of the day of GLUC activity measurements (black line) with its range of values (grey) and the corresponding <i>E. coli</i> . Two outliers (4 pm: 5,170 MPN/100 ml and 8 pm: >24,200 MPN/100 ml) are not shown in this graph..... 92
Fig. 5-1	Schematic cross-section from the Seo Ho River in the west to the Nho Que River in the east. Spring water quality decreases from west to east due to the anthropogenic and agricultural impact within the poljes. It is assumed that there is a confining fault in the Sang Ma Sao valley. Otherwise the hydraulic gradient to the Seo Ho River would be too steep. Furthermore, the local occurrence of gabbro gives evidence for a fault zone. Colours correspond to Fig. 2–1b and Fig. 2–4. The geology east of the Nho Que River is not considered.... 98

Fig. 5-2	Extent of the Dong Van Karst Plateau Global Geopark (DEM: SRTM, NASA). The Geopark border corresponds to the external borders of the four districts Dong Van, Meo Vac, Yen Minh and Quan Ba.	104
Fig. 5-3	Distribution of carbonate rocks in Southeast Asia (modified after Chen et al. 2017).....	105

LIST OF TABLES

Table 1-1	Maximum and minimum discharge rates of some Vietnamese main rivers (Statistical Yearbook of Vietnam 2016).....	10
Table 1-2	Agricultural production in Ha Giang province (Statistical Yearbook of Vietnam 2016). Values for 2016 are preliminary (prel.) projections and percentage increase is calculated for 2016 compared to 2010.	12
Table 2-1	Sampling points	26
Table 2-2	Flow and transport parameters for the tracer tests conducted in Dong Van and shown in Fig. 2-2. Parameters are given for the major springs.....	31
Table 2-3	Correlation matrix of the physicochemical parameters included in the PCA....	32
Table 2-4	Factor loadings of the variables	32
Table 2-5	Main characteristics of the different aquifer types.....	45
Table 3-1	Tracer tests conducted in the Ma Le cave system.....	54
Table 3-2	Different flow velocities that can be yielded by tracer tests (Käss 2004).....	55
Table 3-3	Flow and transport parameters for the sampling sites within the cave system and the karst springs by using a Dirac injection in ML 1, for tracer tests from February, July and August 2014.	61
Table 3-4	Flow and transport parameters for the sampling sites within the cave system and the karst springs by using a Dirac injection in ML 1, for tracer tests from September and October 2015.....	62
Table 3-5	Flow and transport parameters for the tracer tests in February and July 2014 for the individual cave sections by using the multiple pulse injection approach and the ADM as well as the 2RNE.....	65
Table 3-6	Flow and transport parameters for the tracer tests in September and October 2015 for the individual cave sections by using the multiple pulse injection approach and the ADM as well as the 2RNE.....	66
Table 4-1	Spearman`s rank correlation r_s with significance p and the number of measurements n for the entire period (left, white) and the measurements during the rain event on October 1 st (right, blue). The Spearman`s rank correlation analysis yielded higher correlation coefficients for a single rain event.....	90

LIST OF ABBREVIATIONS

2RNE	Two-Region Non-Equilibrium Model
AC	Autocorrelation
ADB	Asian Development Bank
ADM	Advection-Dispersion-Model
BTC	Breakthrough Curve
CCF	Cross-Correlation Function
CDOM	Coloured Dissolved Organic Matter
CERWASS	National Center for Rural Water Supply and Sanitation
<i>E. coli</i>	<i>Escherichia coli</i>
ENT	Enterococci
FC	Faecal Coliforms
FIB	Faecal Indicator Bacteria
GLUC	β -D-Glucuronidase
IWRM	Integrated Water Resources Management
MARD	Ministry of Agriculture and Rural Development
MFU	Modified Fishman Units
MONRE	The Ministry of Natural Resources and Environment
MPI	Multiple Pulse Injection
MPN	Most Probable Number
MU	4-methylumbelliferone
MUG	4-methylumbelliferyl- β -D-glucuronide
NAWAPI	National Center of Water Resources Planning and Investigation
NCHMF	Vietnam National Centre for Hydro-Meteorological Forecasting
PCA	Principal Component Analysis
PSD	Particle-Size Distribution
RMSE	Root Mean Square Error
SAC254	Spectral Absorption Coefficient at 254 nm
SM	Supplementary Material
TTC	Total Thermotolerant Coliforms
UDL	Upper Detection Limit
VBNC	Viable But Non-Culturable
VIGMR	Vietnam Institute of Geosciences and Mineral Resources
WSR	Water Sector Review

Further abbreviations and notations are discussed as they occur.

CHAPTER 1

1 INTRODUCTION

1.1 GENERAL MOTIVATION

Freshwater is an essential environmental resource and groundwater constitutes one of the most important components of usable global freshwater resources (Filimonau and Barth 2016). According to the United Nations Development Program (UNDP), more than 40 % of the people around the world suffer from water scarcity. While 2.1 billion people have no access to safely managed drinking water services, 844 million do not even have a basic drinking water service (WHO 2017). Since 2.3 billion people still lack basic sanitation services (year 2015), human health is often threatened by faeces-impacted water (UNICEF 2017). The wide-spread lack of wastewater management strategies exacerbates the situation. More than 80 % of the world's wastewater is released into the environment without being treated. In some of the least developed countries, this percentage increases to 95 % (UNESCO 2017a). Although groundwater resources are usually in a qualitatively better condition than surface waters, they are often affected by a contaminant input from intense agricultural activities. In addition, they are threatened by overexploitation, especially in densely populated areas. Unfortunately, the worldwide water situation is expected to worsen in future. Climate change will directly affect the water cycle and therefore, the quantity and quality of water resources. The impacts can include floods, droughts, higher frequency of extreme weather events, raising sea levels and higher water temperatures among others. To face these challenges, many efforts have to be taken to investigate water resources and to develop adapted water management strategies to ensure a sustainable water supply. The development of all societies and cultures is strongly dependent on the availability of water. However, a progressive growth of the agriculture, energy and industry sector, enhance the pressure on water resources (WWAP 2015). Therefore, in 2015, countries of the United Nations adopted the 2030 Agenda for Sustainable Development including 17 Sustainable Development Goals. These goals aim to ensure availability and sustainable management of water and sanitation for all, by 2030

(Goal 6), whereby problems of water quantity, as well as water quality, should be solved. In the light of the fast-growing world population with about 80 million people per year (USCB 2017), the world community faces a huge challenge, which is intensified by the fact that water demand is not linearly correlated with population growth. Instead, the rate of water demand has doubled the rate of population growth over the last decades due to rising living standards, changing consumption patterns and trade globalization (WWAP 2015). Especially, countries with outstanding economic growth, like Vietnam, struggle with the achievement of a sustainable water management strategy and a safe access to freshwater for all.

While in 1960, the Vietnamese population amounted to 34.7 million, 92.7 million people were living in Vietnam in 2016. At the same time, their gross national income per capita increased from 110 US\$ in 1991 to 2,100 US\$ in 2016 (World Bank 2017), which resulted in an immense reduction of poverty rate from 58 % in 1992 to 13.5 % in 2014 (UNDP 2017). This amazing transformation from one of the world's poorest nations to a middle-income country in less than three decades is unfortunately associated with several growing pains. For many years, the main task of water resources management in Vietnam was to ensure a sufficient availability of freshwater for agriculture. However, in context of Vietnam's economic transformation process, the water sector has undergone several reforms. Although various attempts were made to integrate environmental concerns, many challenges still need to be overcome regarding water resources management (Waibel 2010). In the public perception, water-related problems are gaining more importance due to intensified reporting in the daily news. Topics like pollution of water reservoirs due to uncontrolled wastewater discharge and overloading landfills, contamination of groundwater caused by mining activities, as well as catastrophic pollution of coastlines and beaches leave an alarming impression (e.g. vietnamnews.vn). Furthermore, flooding constitutes another threat caused by severe storms and by the rising sea level due to climate change.

While large areas of the country are burdened by too much water, the karst areas of the northern highlands suffer from water scarcity. The subtropical climate in Northern Vietnam, with its dry and rainy seasons, results in a high variability of water availability with less precipitation between November and April and more precipitation between May and October. Ceaseless droughts during dry seasons for years exacerbate the already hard life of the local population (Vietnam News 2015). Furthermore, the water demand has strongly increased due to increasing tourist numbers. The northernmost Vietnamese province Ha Giang registered an increase of tourist numbers from 257,621 in 2011 to 511,819 in 2015 (Statistical yearbook Ha Giang 2015). This dramatic increase is likely related to the designation of the UNESCO Global Geopark, called Dong Van Karst Plateau, in 2010. The Geopark includes the four districts Dong Van, Meo Vac, Yen Minh and Quan Ba and

consists a total area of 2,356 km² (UNESCO 2017b). The Dong Van District is the northernmost district of the Ha Giang province (Fig. 1-1) with the identically named capital city Dong Van, located at the northern rim of the karst plateau. According to the report No. 470 (November 15, 2016) from the Dong Van People's Committee, 6,856 inhabitants are living in Dong Van City.



Fig. 1-1 Location of the study site in the province Ha Giang, district Dong Van, Northern Vietnam (DEM: Zindler et al. 2015).

Since Dong Van is the northernmost city within the geopark, where tourists can stay overnight, and it is a popular starting point for tours to the northern flag tower Lung Cu,

most of the Geopark tourists visit Dong Van City. The tourist numbers are expected to further increase. The geopark estimates that tourist numbers will reach 800,000 in 2020 and 1.1 million in 2030 (Hanoitimes 2017). As a result of such a high increase in tourism, Dong Van City has grown very fast with numerous hotels sprouting up. This worsens the already tense situation in terms of a continuous freshwater supply and an adequate wastewater handling.

Additionally, the characteristics of karst hamper the access to water resources and its adequate management. High infiltration rates and scarce surface water storage capacities restrict the water availability. The access to karst water resources is further complicated by the high anisotropy and heterogeneity of karst aquifers. They are characterized by a triple porosity (matrix/fractures/conduits) and a duality of both recharge (autogenic/allogenic) and infiltration (diffuse/concentrated). Within karst conduits, groundwater flow is partly turbulent with high flow velocities and short residence times, which result in a fast transport of contaminants. Karst springs respond rapidly to precipitation events including changes in discharge, turbidity and physicochemical parameters. Since contaminants can easily reach the groundwater via swallow holes and are rapidly transported to springs, karst aquifers are seen as particularly vulnerable (Bakalowicz 2005; Goeppert and Goldscheider 2008; Goldscheider and Drew 2007; Kačaroğlu 1999). In anticipation of increased frequency of extreme events due to climate change, the karst water management faces many challenges. The high variability in water availability and water quality requires adapted management and groundwater protection strategies to ensure a sustainable water supply.

There are only few published studies dealing with karst water resources in Northern Vietnam (Liu et al. 2004; Nguyen et al. 2013; Nguyet and Goldscheider 2006; Nguyet et al. 2016; Tam et al. 2001; Tam and Batelaan 2011; Van Nguyen et al. 2013). Reasons for this paucity could be the very remote location, limited financial resources, lack of required equipment and complicated geological settings (Van Nguyen et al. 2013). However, since the water demand is strongly rising in broad areas, a detailed and systematic investigation of the water resources is crucial for the development of a sustainable water management strategy in karst areas.

The main motivation of this thesis is the evaluation of the water quality and its strong spatiotemporal variability in the Dong Van region. As basis for this evaluation, a hydrogeological conceptual model was developed, based on detailed field investigations. Due to the specific characteristics of karst aquifers, a combination of different hydrogeological methods was applied, including geological mapping, artificial tracer tests, hydrochemical sampling and determination of physicochemical parameters. For the evaluation of microbial water quality, numerous analyses of faecal indicator bacteria (FIB)

were done and their relationships to geological settings, hydrological conditions and type of spring (tapped/untapped) were assessed. Furthermore, the transport parameters within an active cave system were studied by means of tracer tests. Using an innovative evaluation approach spatial resolved transport parameters could be obtained. Based on this information, water quality fluctuations at the karst spring, which drains the cave system, can be evaluated. The high variability of water quality at this spring could be observed with an innovative device, which enables the near real-time and on-site monitoring of the enzymatic activity of the FIB *Escherichia coli* (*E. coli*). In combination with measurements of particle-size distribution, a promising tool was found to monitor microbial contamination patterns. Prior to the presentation of the detailed local investigations, an overview of the general characteristics of karst and specifically of tropical karst is given. Furthermore, an introduction of the current water management strategies in Vietnam and in particular, the situation for Dong Van City will emphasize the significance of these studies.

1.2 KARST IN SOUTHEAST ASIA

1.2.1 *General karst characteristics*

Karst aquifers are of particular importance, since they provide freshwater for about 25 % of the world's population (Ford and Williams 2007). At the same time they are particularly interesting for hydrogeologists due to their complex nature. Since they consist of soluble rocks like limestone, dolostone and evaporites, the CO₂ in the percolating water dissolves carbonate rocks and enhances the primary low porosity of the rock matrix. Hot and wet climate conditions in tropical areas lead to high biogenic carbon dioxide concentrations and consequently, to significant carbonate dissolution (Waltham 2008). The resulting fissured network causes a secondary porosity. In a hierarchical manner, some fissures were progressively enlarged by dissolution that resulted in a conduit network and therefore, in a triple porosity. Furthermore, there is a duality of recharge and infiltration in karst areas. Recharge is either autogenic (from the karst area itself) or allogenic (from adjacent non-karst areas), whereby the infiltration may either take place concentrated via swallow holes or diffusely into fissures or even through overlying soils (Goldscheider and Drew 2007). Hence, karst aquifers exhibit an extreme heterogeneity of groundwater flow that might be completely independent of topography. Consequently, they are poorly characterized using conventional hydrogeological methods like pumping tests and potentiometric surface mapping. Rather they require techniques that have large volumes of investigations, like natural and artificial tracer tests (Maliva 2016).

1.2.2 Subtropical and tropical karst

In Southeast Asia about 10 % of the region is covered by karst (Mouret 2004). In the countries of Myanmar, Thailand, Laos, Vietnam, Cambodia, and mainland Malaysia karst occurs mostly on carbonate rocks, of which the Permian and Carboniferous carbonates are most important. However karst can be also found in carbonates of Ordovician, Silurian, and Devonian ages. In the middle Triassic, the Indosinian orogeny led to an intense compression between Indochina and South China resulting in an elevation of the active North Vietnam margin and, thereby, exposure of carbonates (Cai and Zhang 2009). The following erosion episode resulted in a prolonged karstification period. In combination with the effects of the Himalayan orogeny and the opening of the South China Sea, a regional uplift started 65 million years ago. Consequently, large-scale erosion took place, shaping the actual landscape (Mouret 2004).

The dissolution processes, which are strongly influenced by rock structure and lithology, create a karst terrain characterized by sinking streams, caves, enclosed depressions, fluted rock outcrops, and large springs (Ford and Williams 2013). Dependent on the geographical position and the prevailing climatic conditions, the formation and appearance of karst landforms can be very different (Stevanovic 2015). Under subtropical and tropical climate conditions, like in Vietnam, tower karst and cone karst (Fig. 1-2) are developed.



Fig. 1-2 Left: Quan Ba Twin Mountains (Tam Son city, Quan Ba district) with conical karst landforms in the background. Right: Small depression, enclosed by steep karst cones, south of Dong Van.

The generally conical carbonate hills (cones) can have overlapping flanks and can be separated by more-or-less enclosed depressions (Fig. 1-3). This results in a polygonal arrangement of depressions, surrounded by deeply serrated ridges (Day 2004; Ford and Williams 1989).

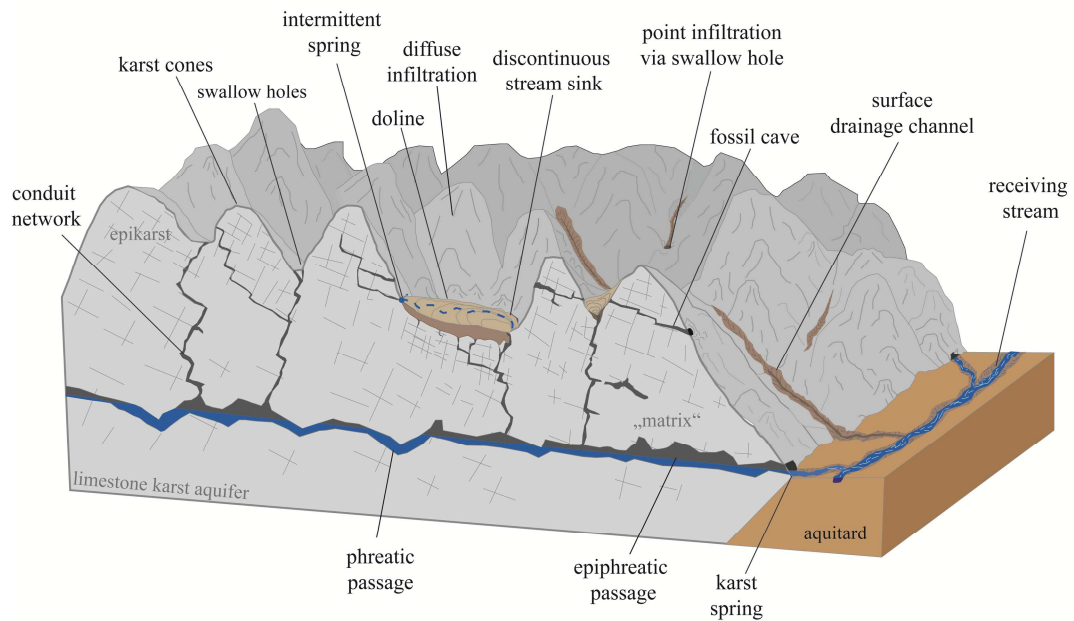


Fig. 1-3 Schematic illustration (inspired by Goldscheider and Drew 2007) of a heterogeneous tropical karst aquifer system with the typical duality of infiltration (point/diffuse) and groundwater flow within matrix, fractures and conduits.

The Chinese terminology distinguishes the tropical karst types by the presence or absence of a karst plain between the hills, instead of by the shape of their hills (Ford and Williams 2007; Waltham 2008). *Fengcong* is used to describe a karst terrain with an egg-box topography, meaning roughly equal-spaced conical hills and deep dolines (Fig. 1-2, right). Thereby the local relief can range from 30 m to over 300 m. In such a karst system, water infiltrates either by fissure percolation or concentrated through swallow holes, where short ephemeral stream courses end. Since the water table lies generally far below the doline floors, the development of large vadose, dendritic cave systems is possible (Waltham 2008). In contrast, the Chinese term *Fenglin* indicates isolated steep-sided towers on an alluviated plain (Ford and Williams 2007), as can be seen in the Guilin region in South China (Fig. 1-4, left) or in Ha Long Bay in Vietnam (Fig. 1-4, right).

Depressions can also be classified as *polje*, if they exhibit a flat floor in rock or in unconsolidated sediments, such as alluvium, if they are closed by steep marginal slopes at least at one side and, if they show karstic drainage (Ford and Williams 2007). One example is the *polje*, in which the city Dong Van is located (Fig. 1-5). Typically, the groundwater table is close to the *polje* bottom (Nicod 2003).



Fig. 1-4 Fenglin karst at the Li River in Yangshuo, south of Guilin in South China (left, www.pixabay.com) and in Ha Long Bay, Vietnam (right, photographed by Anh Tran Diep).



Fig. 1-5 Dong Van polje (photographed from west to east) with an alluviated flat floor, several karst springs at the western and northern margins and a sinking stream at the eastern margin.

The evolution of cone karst is seen as a natural progression from doline karst. With an ongoing dissolution of limestone by rainwater diversion, dolines become enlarged and residual hills remain. These hills emerge from a bedrock base and commonly surround

closed depressions between the peak clusters (Williams 1987). Fractures or individual beds within steeply dipping limestone sequences play an important role concerning the shape of the cones, whereby the alignment of dolines and the formation of corridors is more determined by fault and fold zones. Valleys between the cones can be formed if the saddles between lined-up dolines break (Waltham 2008). However, former surface drainage systems can also influence the alignment of karst cones and therefore, affect the karst morphology (Day 2004). With the development of an efficient underground drainage system, a progressive deepening of the valleys takes place (Waltham 2008). A rapid or intermittent tectonic uplift is a key factor for the evolution of mature cone karst, since the doline deepening continues until it reaches the floor of the limestone or the regional base level. The relation between the karstic and non-karstic rocks can also play an important role in the development of the karst morphology, since it controls the proportion of diffuse autogenic and concentrated allogenic recharge (Williams 1987). In addition, collapse features might affect the morphology of cone karst, but seems to be of minor significance (Day 2004; Waltham 2008).

In cone karst areas, water supply is a special challenge. The drainage occurs mainly underground, either by fissure percolation or concentrated trough swallow holes. Usually, the water table is far below doline floors, resulting in large vadose cave systems of dendritical type (Waltham 2008). The localization and access to groundwater are difficult, especially because there is no correlation between cave passages and surface topography. In addition, groundwater flow is strongly influenced by geological structures. While lateral groundwater movement is rather controlled by stratigraphy, downward groundwater flow is mainly bound to deeply penetrating fault systems (Gremaud et al. 2009; Tran et al. 2013). In areas that experienced multiple regional deformation events, like northeastern Vietnam, karst systems are overprinted by tectonic structures, which can strongly influence groundwater flow and, therefore, further complicate the localization of groundwater (Tran et al. 2013).

1.3 WATER MANAGEMENT IN VIETNAM

1.3.1 Water resources in Vietnam and their management

Vietnam is shaped by a river network, consisting of 2,360 rivers (>10 km length), whereby the Mekong and the Red River are the most important (Waibel 2010). However, 60 % of Vietnam's total river flow originates in riparian countries, leading to an increased water insecurity (ADB 2013). Table 1-1 presents maximum and minimum discharge rates of some

main rivers traversing Vietnam, emphasising the extreme high variability in discharge. Although, the total surface water discharge is high (Vietnam: 9,856 m³/a per person, international standard: 1,700 m³/a per person), the spatial and temporal variation between river basins and dry and wet seasons result in water scarcity in some regions (ADB 2009b).

Table 1-1 Maximum and minimum discharge rates of some Vietnamese main rivers (Statistical Yearbook of Vietnam 2016).

River	Station		Year				
			2010	2013	2014	2015	2016
			Discharge [m ³ /s]				
Da river	Lai Chau	<i>Max</i>	2,940	4,690	5,150	2,820	3,200
		<i>Min</i>	362	89	96	25	26
	Hoa Binh	<i>Max</i>	3,040	3,070	4,030	2,840	3,220
		<i>Min</i>	70	69	15	15	15
Thao river	Yen Bai	<i>Max</i>	3,070	5,340	3,400	3,800	6,970
		<i>Min</i>	135	98	88	89	134
Red river	Son Tay	<i>Max</i>	9,220	13,100	6,810	7,250	9,610
		<i>Min</i>	485	640	640	557	667
	Hanoi	<i>Max</i>	5,450	6,960	6,370	5,730	7,290
		<i>Min</i>	175	145	58	132	145
Luc Nam river	Chu	<i>Max</i>	2,450	2,070	2,560	2,640	
		<i>Min</i>	1		1	1	
Ma river	Xa La	<i>Max</i>	683	1,240	1,600	3,250	1,430
		<i>Min</i>	30	26	25	17	29
	Cam Thuy	<i>Max</i>	2,360	2,480	1,920	4,250	
		<i>Min</i>	83	94	75	75	
Ca river	Dua	<i>Max</i>	3,640	5,280	2,040	3,020	3,660
		<i>Min</i>	52	48	65	39	40
	Yen Thuong	<i>Max</i>	5,060	5,280	2,160	2,860	3,300
		<i>Min</i>	69	66	95	26	54

With about 3,600 reservoirs, groundwater resources also play an important role regarding water availability, but its abundance varies regionally strongly (Waibel 2010). Estimations of the total renewable groundwater potential amount to 63 billion m³/a (ADB 2013).

The historical development of water management in Vietnam is detailed described in Waibel (2010). Based on this working paper, a short overview is given in the following sections. Before the modern state of Vietnam was formed, water management was mainly under local responsibility. Between 1947 and 1975, the country experienced a setback, due to the two Indochina wars, which also affected its water resources development. After the reunification of Vietnam in 1975, water resources management gained more attention, since

the agriculture in the South had to be rebuilt. In the mid-1980s, the introduction of the market economy (Doi Moi) resulted in the reorganization of property rights. Consequently, water was an economic good for the first time and pricing of water was introduced. Due to the reformations, a change in agriculture production and irrigation practices was possible, leading to large scale investments of foreign funds. In 1995, the Ministry of Agriculture and Rural Development (MARD) was founded, which was responsible for water resources management functions. However, the responsibilities of aspects such as urban water supply or water quality control were given to other ministries. This fragmentation hampered the development of an integrated water resources management approach. In 1998, the Law on Water Resources was promulgated, which states that water should be the property of all people and universally managed by the state. The Ministry of Natural Resources and Environment (MONRE) was established in 2002, to combine water and environmental policies and to separate water resources functions from the responsibility of public service delivery. The latter stayed in the responsibility of MARD, at least in rural areas.

In 2006, the water law was complemented by the National Water Resources Strategy towards the year 2020, issued by MONRE (2006), and approved by the Prime Minister through decision 81/2006/QĐ-TTg (Vietnam Law & Legal Forum 2006). This policy paper intends to provide a comprehensive framework for all water-related policies and implementation plans by setting up “guiding principles, objectives, missions and implementation measures regarding the protection, exploitation, use and development of water resources, as well as the prevention, and mitigation of adverse impact caused by water” (MONRE 2006). This national strategy was supported by the Water Sector Review (WSR), which aimed to review the state of Vietnam’s water sector, based on the best information available at that time (ADB 2009b). The WSR concluded that the water sector was facing immense problems and that fundamental changes were essential to start the development towards an integrated water resources management (IWRM) (ADB 2009a). In 2012, the Order No.15/2012/L-CTN was issued by the State President for the official promulgation of the Law on Water Resources No. 17/2012/QH13 (Nguyen 2013). Various attempts have been made to integrate environmental concerns to the water sector and the protection of water resources has become important in the past years, resulting in a new Law on Water Supply and a new Law on Sewerage and Wastewater Treatment, which will be promulgated in 2019 and 2020, respectively (Linh 2017). Though the legislative regulations are well developed, the execution is still facing many challenges, especially on a local scale.

1.3.2 Water management in Dong Van

People are living in far-flung settlements in mountainous areas or in the district capital city Dong Van. While the majority of people are sustaining themselves on agriculture, especially in the mountainous villages, people in Dong Van City profit by the strongly increasing tourism. The economic development leads to a demographic growth in the region and, in combination with the high tourist numbers the pressure on agricultural production has increased. Table 1-2 illustrates the strong increase in agricultural production between 2010 and 2016 in Ha Giang. Consequently, in both agriculture and tourism sectors, the water demand is raising.

Table 1-2 Agricultural production in Ha Giang province (Statistical Yearbook of Vietnam 2016). Values for 2016 are preliminary (prel.) projections and percentage increase is calculated for 2016 compared to 2010.

Product	Unit	2010	2013	2014	2015	prel. 2016	Increase [%]
Paddy	[10 ³ Tons]	194.2	206.9	207.9	203.5	210.4	8
Maize	[10 ³ Tons]	136.3	176.9	178.4	186.5	185.1	36
Sweet Potatoes	[10 ³ Tons]	6.8	6.9	7.9	10.4	9.2	35
Cassava	[10 ³ Tons]	34.2	40.3	39.5	36.3	39.8	16
Pigs	[10 ³]	431.7	435.4	460.2	485.4	490.7	14
Poultry	[10 ³]	3,041	3,403	3,876	4,042	4,056	33
Fishery	[Tons]	1,422	1,827	1,871	1,901	1,923	35
Aquaculture	[Tons]	1,341	1,683	1,729	1,756	1,802	34

The few surface streams are deeply incised, resulting in a difference of hundreds of meters in altitude between the rivers and the mountainous villages. For this reason, the water supply is decentralized and individual in rural areas. During rainy season, people collect the rain water, e.g. from the roof tops. Most of the precipitation occurs between May and October; the months June and July are generally the peak of the rainy season (Fig. 1-6). There are no long term measurements of air temperature within the Dong Van district. Therefore, the mean air temperature for Ha Giang district is exhibited in Fig. 1-6. In Dong Van, slightly lower mean air temperatures are expected due to higher altitude.

During dry season, people are dependent on small springs, where great effort is necessary to collect the water with cans that must be carried back home. This job is mostly carried out by children and young women. Furthermore, these springs are also used for personal hygiene and for doing the laundry (Fig. 1-7).

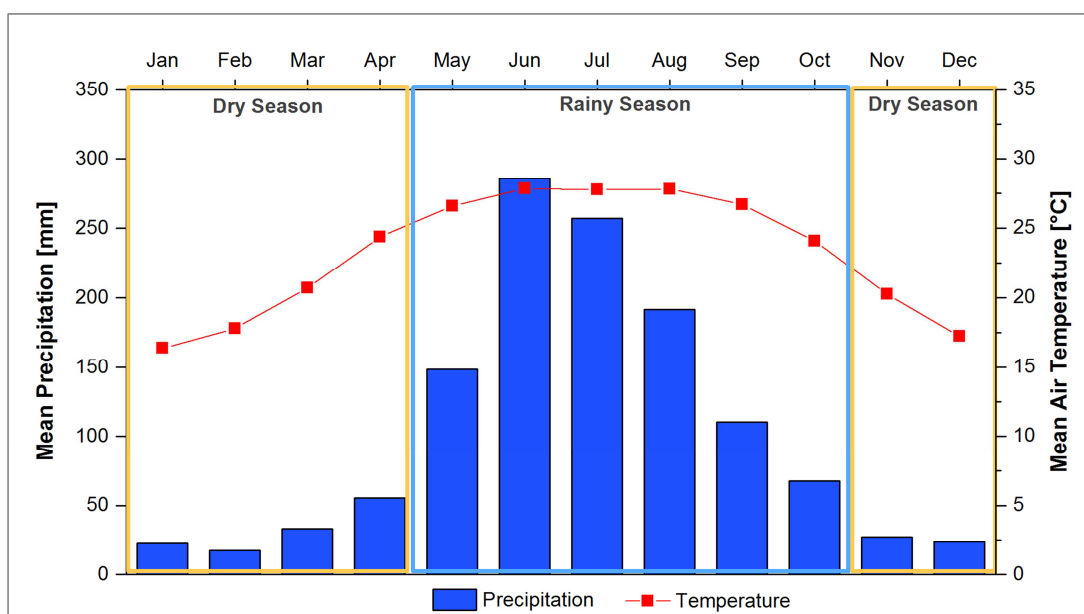


Fig. 1-6 Mean precipitation (climate station Dong Van District, 2000–2012) and mean air temperature (climate station Ha Giang District, 1990–2010; Vietnam National Centre for Hydro-Meteorological Forecasting, NCHMF).



Fig. 1-7 Left: Girls carrying 40 L cans full of water from the spring to their homes. Right: Even small springs with discharge rates < 0.2 L/s are intensively used for personal hygiene.

In the last years, the Vietnamese government has invested a lot of money to build reservoirs, called “*Hanging Pools*” to store the water from rainy season for the dry season (Fig. 1-8). However, these constructions are not sustainable for several reasons. First, the region is tectonically quite active, leading to a relatively short life-time of the concrete basins due to cracks, for instance. Furthermore, the basins consist of a large open water surface, resulting in a high evaporation and an increasing deterioration of water quality. On

one hand the water quality decreases due to natural contamination from microbial and algae growth. On the other hand, the basins might also be used as recreational water, causing an anthropogenic input of contaminants.



Fig. 1-8 Hanging Pools as water storage in the Dong Van region.

In Dong Van City, most households of the city centre are connected to a main system operated by the National Center for Rural Water Supply and Sanitation (CERWASS). The water originates from one karst spring and two groundwater wells, whereby the karst spring supplies the main proportion of water in the rainy season. During dry season, the water contribution of the wells increases, if the spring discharge is too low. The water is distributed intermittently, since the spring discharge is not high enough to ensure a continuous water supply for the whole city, especially during dry season. For this reason, each household has its own storage tank, generally installed on the housetop. However, karst springs are seen to be highly vulnerable, leading to fluctuations in water quality. The quality also worsens within the poor supply system, due to the combination of leakages and intermittent water supply, which enables an input of bacteria to the pipe network and, in some cases, bacterial growth (Kumpel and Nelson 2013; Kumpel and Nelson 2014; Kumpel and Nelson 2016).

The presented work was embedded in a Vietnamese-German cooperation for the development of sustainable technologies for karst water management (KaWaTech project) and was funded by the German Federal Ministry of Education and Research (BMBF, grant number 02WCL1291A). Within the framework of KaWaTech, an assessment of water demand was conducted for Dong Van. Within the rural areas, the current mean water consumption amounts to 20 litre per capita and day (lpcd), including the water consumption of animals (Germany: 123 lpcd, BMUB 2017). In Dong Van City, water availability is improved by the supply system, leading to a significantly higher mean water consumption of 90 lpcd (Zindler and Stolpe in preparation). According to the survey of Zindler and Stolpe (in preparation), in the rural areas, 45 % of the population suffers from water scarcity

during rainy season and 97 % during dry season. In contrast, in Dong Van City, 5 % of the population is faced with water shortages during rainy season and 35 % during dry season.

To meet the further increasing water demand of Dong Van City due to population growth and increasing tourist numbers, public and private wells have been drilled to extract water from the karst aquifer below Dong Van City. However, there is no information about the extent of the aquifer, the recharge rates and residence times of groundwater. Thus, no management strategy was developed for a sustainable use of this valuable groundwater resource. In the worst case, the uncontrolled groundwater extraction could lead to severe groundwater depletion. In addition, several wells were constructed inexpertly, leading to a potential hydraulic connection between surface water and groundwater. This potential connection could lead to a deterioration of the groundwater quality.

1.3.3 KaWaTech project

The main intention of the KaWaTech project was to develop innovative solutions for a sustainable karst water supply system, wherefore German and Vietnamese partners from universities, research institutes, industries and authorities have worked together since November 2013. The project is subdivided into four work packages, including (1) investigations, exploration and monitoring; (2) hydropower and water production; (3) water distribution and supply, and (4) resource protection and socio-cultural aspects. By closely interlinking these topics, an adapted hydropower-driven water supply system will be implemented that is able to pump water from the Seo Ho River to a distribution tank in Ma U (Fig. 1-9). Thereby, a total difference in static head of 390 m has to be overcome (Oberle et al. 2017). By using a mechanically coupled unit of one “pump as turbine” (PAT) and one pump, even small discharge rates during dry season can be efficiently used to supply the water to the distribution tanks (Fritz et al. 2012; Oberle et al. 2017). Furthermore, an innovative multiple chamber system was developed for the distribution tanks. Hence, a fair gravitationally water distribution from the tank Ma U to the mountainous villages and Dong Van City is possible and is adapted to the variable water quantities (Oberle et al. 2017). Within the project, several field studies were carried out to determine the water availability and the current and expected future water demand to design the dimensioning of the water supply system.

The completion of the water supply and distribution system is part of the subsequent project KaWaTech Solutions (BMBF, grant number 02WCL1415), which runs from November 2016 to October 2019. Beside the implementation of the supply and distribution system, water purification is also an important part of the second project phase. Based on the

information yielded from the first project phase, a central treatment plant will be designed to ensure the supply of water with fair quality. The large scale implementation of the treatment plant is expected to take place by the Vietnamese partners close to the Ma U distribution tank.

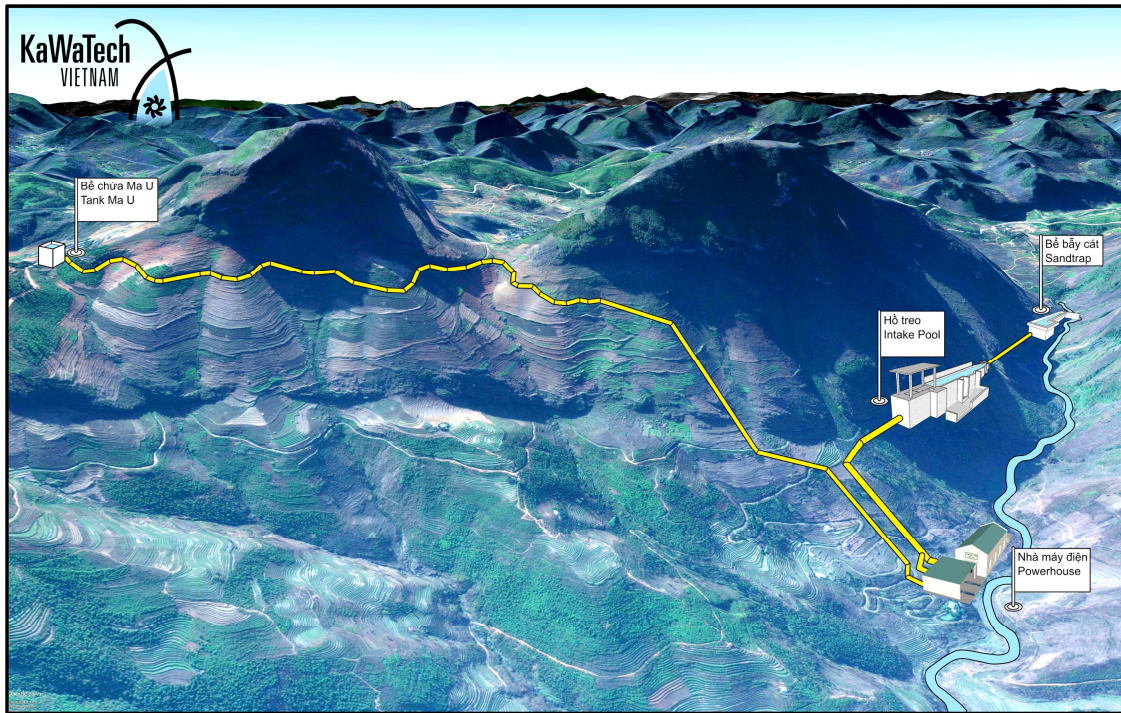


Fig. 1-9 Seo Ho water supply system that was planned and built within the KaWaTech and KaWaTech Solution project (modified after Oberle et al. 2017).

A small pilot treatment plant will be designed for permanent point-of-use operation in Dong Van City to provide high quality water for a public building, e.g. for the hospital.

In addition, KaWaTech Solution is dealing with an analysis of potential locations for a pilot implementation of decentralized photovoltaic-based pump systems (PVPS) as a sensible alternative to hydropower-driven pumping units. Due to the high radiation intensity in Vietnam, there is a high multiplication potential for PVPS, especially in extremely rural regions (KaWaTech 2018).

With the development and the pilot implementation of adapted technologies for the use of karst water, the KaWaTech projects aim to sustainably improve the water supply in poor and remote areas. However, detailed hydrogeological field investigations are the basis for adapted water supply strategies.

1.4 OBJECTIVES AND APPROACHES

The aim of this thesis is the contribution to a better understanding of subtropical karst systems and their functioning, particularly regarding the high variability due to dry and rainy seasons. Since many people are dependent on karst aquifers in subtropical and tropical regions, an exemplary and profound investigation of a very remote and complex karst area is presented in this thesis. This includes the development of a conceptual hydrogeological model for the project area by using a combination of hydrogeological methods, e.g. mapping activities, tracer tests and hydrochemical analyses. Based on the developed conceptual model, an evaluation of the water quality of the different water resources was conducted. In this context, the following research questions have arisen:

- Which factors influence water quality?
- Is there a correlation between hydrochemical water signatures and poor microbial water quality? Are there principal differences in the vulnerability of different water resources?
- What is the role of the underground karst conduit network in spring water quality?
- How does the change between dry and rainy season affect spring water quality?
- Do tapped springs display a better microbial water quality?

In the Dong Van area, the Seo Ho water supply system will be part of a sustainable and adapted karst water management strategy, so the characterization of the catchment area of the extracted water is another main aspect of this thesis. Therefore, the cave system located upstream of the Seo Ho water supply system was systematically studied with numerous tracer tests, whereby following questions were examined:

- What are the flow and transport characteristics of the cave system and how are they spatially distributed?
- Is a multiple pulse injection approach feasible to study the spatial resolution?
- What is the impact of dry and rainy seasons on these parameters?

The characterization of the cave system with its high variable flow and transport parameters indicated that the water quality at the receiving spring might also be subject to strong fluctuations. So, the next step was a detailed monitoring of different water quality parameters at the spring. A new, mobile pilot device was applied to observe faecal contamination patterns on-site and in almost real-time by measuring the enzymatic activity of *E. coli*. The main focus was on the following research questions:

- Is a monitoring combination of enzymatic activity and particle-size distribution an adequate tool to investigate faecal contamination dynamics?

- What is the relationship between the methods of enzymatic activity measurements and cultivation-based determinations of *E. coli*, as well as other water quality parameters (PSD, turbidity, electrical conductivity, water temperature)?
- How do precipitation events impact the different observed parameters? Which parameter combination seems to be suitable as an early warning system to protect the technical facilities from an increased abrasion risk, but also to prevent the supply of poor quality water?

By addressing these specific research questions, a profound understanding of the studied karst region could be developed, which is also important for the projected water supply system. Furthermore, based on the results presented in this thesis, water protection strategies can be developed in order to enable a sustainable use of the valuable karst water resources.

1.5 STRUCTURE OF THE THESIS

The structure of the present thesis is of a cumulative type, consisting of three studies (chapter 2, 3 and 4) that cover different aspects of karst hydrogeology exemplary for the Dong Van area at different scales (Fig. 1-10).

Chapter 2 presents results from mapping activities, artificial tracer tests, hydrochemical and microbiological analyses. It results in a hydrogeological, conceptual model for the entire Dong Van area. Based on this model, an evaluation of the microbial water quality and their influencing factors is addressed.

Chapter 3 considers the Ma Le cave system on a smaller scale. With several tracer tests, the karst system could be characterized for different hydrological conditions during dry and wet seasons, whereby a spatial resolution of flow and transport parameters could be obtained.

Since the water of the Ma Le system is used for the planned water supply system, the focus is further concentrated on the cave system outlet, the karst spring ML 4, in **chapter 4**. In this study a high-resolution spring monitoring is presented, whereby innovative methods were used to observe the microbiological water quality variations. The study aims to investigate the contamination patterns of the spring water and to find adequate real-time and on-site monitoring solutions for an early-warning system. Such a system is essential to protect both the technical facilities of the water supply system and people that use the water, from poor water quality.

In **chapter 5**, a summary and an evaluation of the major results and highlights are given to understand the meaning of the findings for the region. The site-specific conclusions are set to a regional scale and an outlook is given for further research questions. Chapter 3 has been accepted and chapter 4 has been published in peer-reviewed journals, whereas chapter 2 is currently under review.

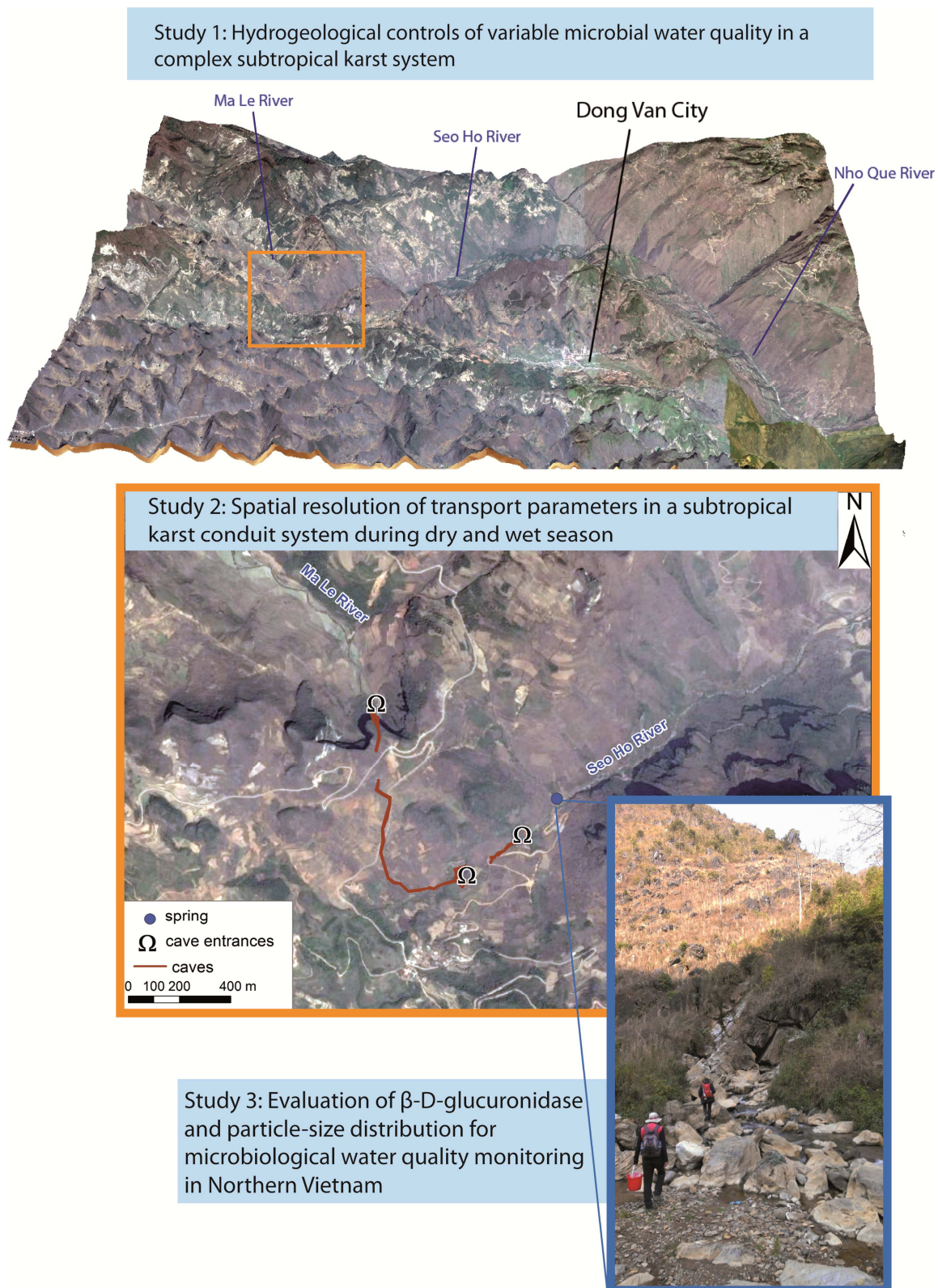


Fig. 1-10 Studies that were carried out on different scales in the Dong Van region (Satellite Image: Google Earth, photo: karst spring ML 4, where the monitoring was performed, March 2014).

CHAPTER 2

2 HYDROGEOLOGICAL CONTROLS OF VARIABLE MICROBIAL WATER QUALITY IN A COMPLEX SUBTROPICAL KARST SYSTEM IN NORTHERN VIETNAM

Reproduced from: Ender A, Goepfert N, Goldscheider N (2018) Hydrogeological controls of variable microbial water quality in a complex subtropical karst system in Northern Vietnam. Hydrogeology Journal, doi 10.1007/s10040-018-1783-5

Abstract

Karst aquifers are particularly vulnerable to bacterial contamination. Especially in developing countries, poor microbial water quality poses a threat to human health. In order to develop effective groundwater protection strategies, a profound understanding of the hydrogeological setting is crucial. The goal of this study was to elucidate the relationships between high spatio-temporal variability in microbial contamination and the hydrogeological conditions. Based on extensive field studies, including mapping, tracer tests and hydrochemical analyses, a conceptual hydrogeological model was developed for a remote and geologically complex karst area in Northern Vietnam called Dong Van. Four different physicochemical water types were identified; the most important ones correspond to the karstified Bac Son and the fractured Na Quan aquifer. Alongside comprehensive investigation of the local hydrogeology, water quality was evaluated by analysis for three types of fecal indicator bacteria (FIB): *Escherichia coli*, enterococci and thermotolerant coliforms. The major findings are: (1) Springs from the Bac Son formation displayed the highest microbial contamination, while (2) springs that are involved in a polje series with connections to sinking streams were distinctly more contaminated than springs with a

catchment area characterized by a more diffuse infiltration. (3) FIB concentrations are dependent on the season, with higher values under wet season conditions. Furthermore, (4) the type of spring capture also affects the water quality. Nevertheless, all studied springs were faecally impacted, along with several shallow wells within the confined karst aquifer. Based on these findings, effective protection strategies can be developed to improve groundwater quality.

2.1 INTRODUCTION

Some of the most spectacular subtropical karst landscapes are located in Vietnam, where 60,000 km² or 18% of the total area of the country is covered by karst (Tuyet 2001). Thick carbonate rocks with intercalations of terrigenous or siliceous units were formed from the Early Cambrian to Late Mesozoic (Tran et al. 2013; Van Nguyen et al. 2013). Numerous deformational events led to thickening and fragmentation of the different rock units (Tran et al. 2013). The most widespread formation in Northern Vietnam is the Bac Son formation (Fm.), which comprises mainly homogenous, massive to thick-bedded limestone. This formation is highly karstifiable, especially under the influence of subtropical climate conditions. The combination of rock composition, deformational events and exogenic processes led to an exceptional karst landscape, which was officially designated as a UNESCO Global Geopark in 2010. However, the high degree of karstification presents a significant challenge in terms of water management strategies. Within the karst areas, precipitation infiltrates rapidly and enters deep cave systems. Especially during the extended dry seasons, water scarcity exacerbates the living conditions of the local population. With the designation as a UNESCO Global Geopark, tourist numbers have strongly increased from 257,621 in 2011 to 511,819 in 2015 for the Ha Giang province (Statistical Yearbook, Ha Giang 2015).

Although there are no available statistical data for Dong Van City, it can be assumed that the relative increase in tourist numbers lies within a similar range. Due to the increase in tourism, the water demand in Dong Van City has also strongly increased. The local population and hotels obtain water from karst springs and, increasingly, from private and public wells, extracting water from the karst aquifer underneath Dong Van City; however, until now, there is no hydrogeological conceptual model for this area. Some general information about groundwater characteristics in northeastern Vietnam can be found in Nguyen et al. (2013); nevertheless, detailed information about the hydrogeological conditions in Dong Van City is not yet available. As already shown for other Vietnamese karst areas, the poor microbial water quality is a significant problem in subtropical karst regions and poses a threat for human health (Nguyet and Goldscheider 2006; Nguyet et al. 2016).

Due to karst characteristics such as rapid infiltration and low filtration potential, contaminants can easily reach the water table. Furthermore, turbulent flow regimes in conduits with high flow velocities result in a rapid transport of contaminants to springs (Ford and Williams 2007). The input paths and contamination sources are usually complex and range from agricultural activities to domestic wastewater due to inadequate or absent sewage systems, leaking sewer pipes or septic tanks. Therefore, an improvement of the water quality requires the development of groundwater protection strategies, based on both intensive water quality investigations and a comprehensive understanding of the hydrogeology using a realistic conceptual model.

This study presents results from intensive field investigations between 2014 and 2016 with a combination of different methods, including mapping activities, hydrochemical analysis, tracer tests and microbiological investigations. The hydrogeological conceptual model and the microbial water quality of the different water resources in the study area are both utilized to examine the following research questions: (1) Is it possible to group different water types based on hydrochemistry and to recognize geogenic as well as anthropogenic processes? (2) Is there a correlation between wastewater discharge in swallow holes and water quality deterioration at springs used for drinking water supply? (3) What is the influence of intensified precipitation during wet season conditions on spring water quality? (4) Can the water quality be improved through a tapping of the springs?

2.2 MATERIALS AND METHODS

2.2.1 *Study site*

Dong Van City is located in the northernmost province of Vietnam, Ha Giang (Fig. 2–1a). In 2016, 6856 people lived in Dong Van City (Report No. 470 of Dong Van People’s Committee, 15 November 2016), one of the most remote and poorest regions of the country.

However, with the designation as a UNESCO Global Geopark, “Dong Van Karst Plateau”, tourism has strongly increased and an increase in economic power has led to the fast growth of Dong Van City. The cultural diversity and the beautiful karst landscape attract many Vietnamese and international tourists. The massive limestone units of the Carboniferous-Permian Bac Son Formation are highly karstifiable, leading to peak clusters, intra-mountain depressions, large cave systems, deep river valleys and steep slopes (Tam and Batelaan 2011).

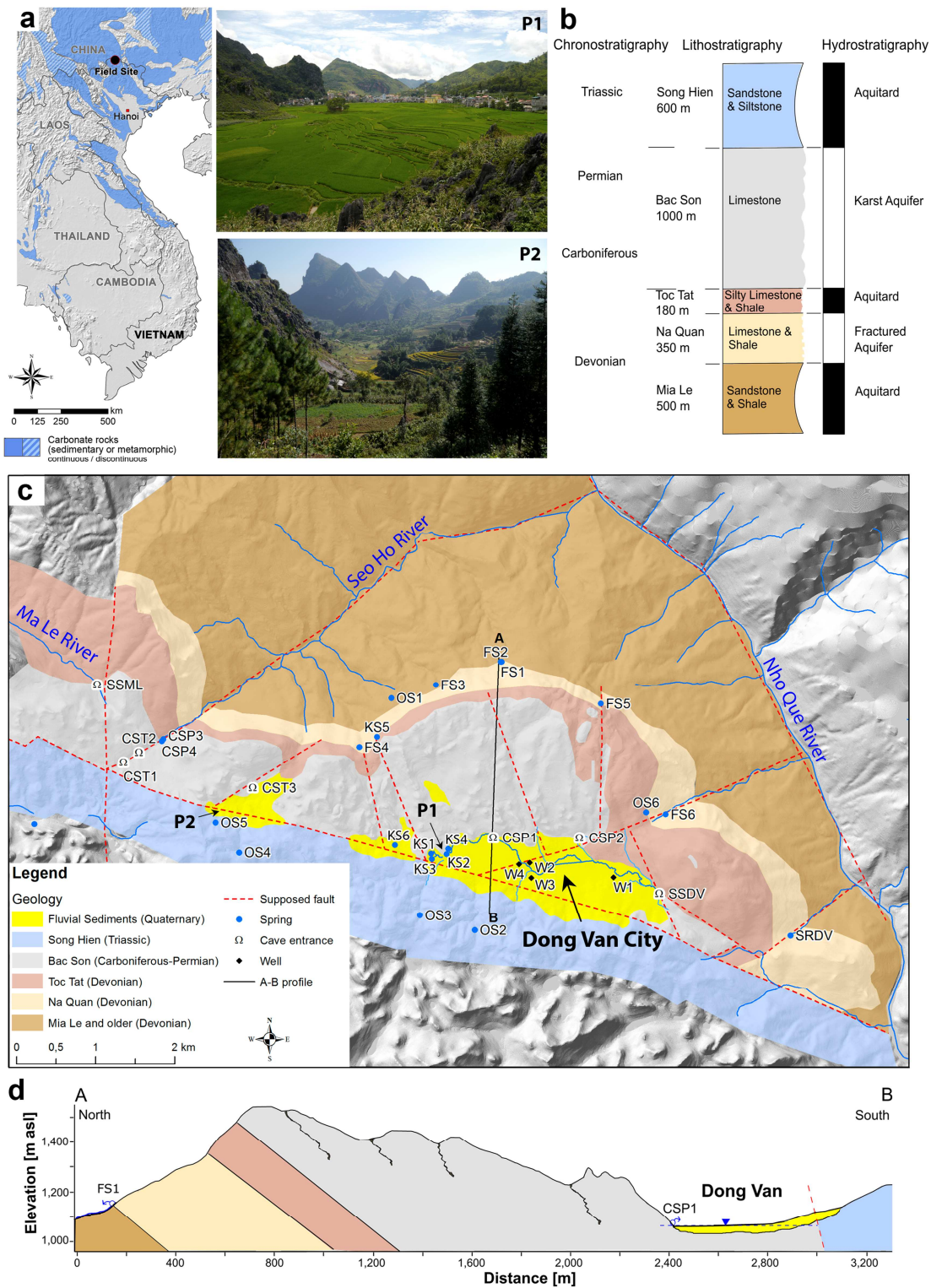


Fig. 2-1 **a** Location of the study site (close to the Chinese border) is shown on a section of the world karst aquifer map. The distribution of carbonate rocks in Vietnam and the adjacent countries is shown in blue (based on the WOKAM approach after Chen et al. 2017). **b** Lithostratigraphic and hydrostratigraphic profile. **c** Geological map of the Dong Van area (the digital elevation model

(DEM) in the background is from B Zindler, A Degen, H Stolpe, RUB Bochum, unpublished data, 2015. **d** Cross-section through the Dong Van Valley from North to South. The location of the photos is shown with labels P1 and P2. P1: Dong Van Valley (from W to E), P2: Sang Ma Sao Valley (from SW to NE)

The W–E oriented valley of Dong Van is at an elevation of around 1,060 m above sea level (masl), the highest peak of the mountain range north of Dong Van is 1,590 m asl, and the deep river valley of the Nho Que. River on the eastern side is at an elevation of 460 m asl (Fig. 2–1c,d). Based on previous mapping activities in the Dong Van Karst Plateau (DGMV 2000; Vietnam Institute of Geosciences and Mineral Resources (VIGMR), unpublished “Geological Map of Ha Giang, Scale 1:50,000”, 2016), a small-scale geological map was generated for the Dong Van area (Fig. 2–1c). The Devonian Formations are composed of carbonates, from shelf facies in the Middle Devonian to pelagic facies in the Upper Devonian (Lepvrier et al. 2011). The Toc Tat Fm., the Na Quan Fm., the Mia Le Fm., and older Devonian units (Son Cau Group, Si Ka Fm.) are represented; however, for simplification, the older Devonian units were summarized as “Mia Le and older” for this study, since the focus lies on the Middle Devonian to Lower Triassic units. Massive marine carbonates of Carboniferous and Permian ages conformably overlie the Upper Devonian formation and consist of limestone and siliceous limestone (Lepvrier et al. 2011). This Bac Son Fm. is strongly karstified with typical karst morphologies. The Lower Triassic formation (Song Hien Fm.) is dominated by terrigenous turbiditic sediments, partly mixed with marine carbonates (Lepvrier et al. 2011). Multiple deformational events under ductile, brittle-ductile and brittle strain conditions with repeated shearing, folding and faulting have led to a complex geological pattern (Tran et al. 2013). The subtropical monsoon climate with a dry season from November until April and a rainy season from May until October results in an intense karstification (Khang 1985; Tam and Batelaan 2011). For Dong Van, the mean annual precipitation was 1,335 mm in the period 2000–2012 (data provided by National Center of Water Resources Planning Measurements and Analysis and Investigation (NAWAPI), climate station Dong Van District, operated by Vietnam National Centre for Hydro-Meteorological Forecasting, (NCHMF) with highest rainfall in June (285 mm) and lowest in February (17 mm).

2.2.2 *Sampling campaigns*

Five sampling campaigns were conducted between 2014 and 2016 with two campaigns during dry seasons (February/March 2014, March/April 2015), two during wet seasons (July/August 2014, June/July 2016) and one under transient conditions (September/October

2015). Samples were taken at the springs, water caves, surface streams and wells (Fig. 2–1c; Table 2–1).

Table 2-1 Sampling points

Category	Abbreviation	Sampling points
sinking stream Dong Van	SSDV	SSDV
sinking stream resurgence Dong Van	SRDV	SRDV
sinking stream Ma Le	SSML	SSML
cave stream	CST	CST1, CST2, CST3
cave spring	CSP	CSP1, CSP2, CSP3, CSP4
karst spring	KS	KS1, KS2, KS3, KS4, KS5, KS6
well	W	W1, W2, W3, W4
fractured aquifer spring	FS	FS1, FS2, FS3, FS4, FS5, FS6
other springs	OS	OS1, OS2, OS3, OS4, OS5, OS6

In March 2015, a 48-h monitoring exercise with hourly sampling intervals was performed at one karst spring (KS2) to investigate short-term water-quality fluctuations. In July/August 2014, a cave spring (CSP1) was monitored for a time period of 24 days with daily sampling intervals to investigate the spring dynamics during rainy season.

i. Discharge measurements

Depending on the type of spring, different methods were applied to determine the discharge. Most of the springs allowed a direct discharge measurement with a bucket or beaker and a stopwatch. The discharge of larger springs, rivers and cave streams were measured with the salt-dilution method (Groves 2007). The discharge of spring KS2 during the 48-h monitoring was measured at a pipe with a portable ultrasound flow measuring device (UDM 200, SebaKMT, Baunach, Germany).

ii. Physicochemical parameters

A portable multi-parameter device (Multi 3430 IDS, WTW, Weilheim, Germany) was used to measure the pH (IDS SenTix 980). The probe was calibrated on a regular basis with standard buffer solutions. Electrical conductivity (EC) and temperature (T) were determined (TetraCon 325) as well as dissolved oxygen (DO) which was measured with galvanic DO sensor (Cellox 325). Turbidity was determined with a portable turbidity meter (Turb 355 IR, WTW).

Water samples for major ions analysis were filtered with cellulose acetate membrane filters (0.45 µm, 25 mm, Sartorius AG, Göttingen, Germany) and collected in high density polyethylene bottles (30 ml, Rixius AG, Mannheim Germany). Samples for cation analyses were stabilized with nitric acid, and all samples were stored in a fridge before they were

transported to Germany for analysis. Ca^{2+} and Mg^{2+} were analyzed with an atomic absorption spectrometer (3030(B), Perkin Elmer, Waltham, MA, USA). The cations K^+ and Na^+ and the anions SO_4^{2-} , NO_3^- and Cl^- were measured with ion chromatography (Dionex ICS-1100/Dionex ICS-2100, Thermo Fisher Scientific Inc., Waltham, MA, USA). An alkalinity test (111,109, Merck Millipore, Billerica, MA, USA) was used for the direct, on-site determination of HCO_3^- and CO_3^{2-} . Since the pH values were generally <8.2 , CO_3^{2-} was mainly negligible and total alkalinity could be considered to be equal to HCO_3^- . The calculation of the charge balance error was carried out with PHREEQC (Parkhurst and Appelo 1999). All analyses with a charge balance error $> 10\%$ were discarded.

The spring monitoring campaigns included measurements of the particle-size distribution (PSD). A mobile particle counter (Abakus mobile fluid classic, Klotz GmbH, Bad Liebenzell, Germany) was used to count particles at 32 different definable size classes in a range of 0.8 to 140 μm . Furthermore, at the spring KS2, colored dissolved organic matter (CDOM) was determined by using a filter fluorimeter (Trilogy, Turner Designs, San Jose, CA, USA). Samples were taken in 50-ml-brown glass bottles and were stored in a cooling box for maximum 24 h before analysis. Each sample was filled into the cuvette twice and each was measured three times. The mean value for the six measurements was calculated. Fluorescence intensity was transferred to CDOM concentration by using a calibration with quinine hemisulfate salt monohydrate (Sigma-Aldrich, Darmstadt, Germany) standards, since it has a maximum absorption wavelength of 350 nm and fluorescence wavelength of 450 nm, similar to many CDOM compounds. Its fluorescence intensity is highest in weak acids. Therefore, standard solutions were diluted in 0.05 M H_2SO_4 to concentrations in a range of 0.01–0.08 mg/L. Precipitation data were obtained from a meteorological station located in Dong Van (Hydro-Meteorological Forecasting Center, Ha Giang).

iii. Faecal bacteria analysis

The concept of fecal indicator bacteria (FIB) is widely used and accepted to assess water quality in terms of a potential presence of pathogens. The most important indicators are *Escherichia coli* (*E. coli*) and thermotolerant coliform bacteria (TTC), which is a coliform group that is able to ferment lactose at 44–45 °C, including the genus *Escherichia*, *Klebsiella*, *Enterobacter*, and *Citrobacter* (Foppen and Schijven 2006). However, only *E. coli* is unfailingly related to excreta of humans and warm-blooded animals. Other important FIB are enterococci (ENT), which are opportunistic pathogens and abundant in human and warm-blooded animal feces. They are commonly used for water quality assessment and are proposed by the US Environmental Protection Agency (2012) as a recreational water quality criterion. However, recent studies showed that in contrast to an ideal FIB, ENT may not be invariably of fecal origin, but might be endogenous in sediments and soils (Byappanahalli et al. 2012). For the enumeration of *E. coli* and TTC, Colilert-18

and Colisure (IDEXX Laboratories Inc., ME, USA) were used. For the first two sampling campaigns, Colilert was used. However, since an incubation time of 24 h was easier to realize with fieldwork, Colisure was used for the following sampling campaigns. Both methods are US EPA approved and were recommended for remote applications (Abramson et al. 2013). ENT were analyzed with Enterolert (IDEXX Laboratories Inc.), which is also US EPA approved. However, analyses for ENT were started at the second sampling campaign in July 2014, after the results of the first campaign indicated a high contamination with fecal bacteria. Test procedures were carried out following the manufacturer's instructions (IDEXX Laboratories 2011).

Water samples were incubated for 24 h at 35 ± 0.5 °C for *E. coli* and at 41 ± 0.5 °C for ENT determination, respectively. Results are given as most probable number (MPN) of colony forming units in 100 ml, based on the Quanti-Tray/2000 method. Without a dilution step, the upper detection limit (UDL) is 2420 MPN/100 ml.

iv. Statistical analysis

A principal component analysis (PCA) was carried out with OriginPro 9.1 using all samples collected during the five sampling campaigns that had a complete analysis and a charge balance error < 10% (n = 108). Samples taken during monitoring at specific springs were not considered. Despite the small variability in chemical composition in carbonate systems, the PCA categorizes the natural tracers by using a projection of variables. Multiple axes are reduced into two axes (PC or factors), whereby PC1 explains most of the variance of the data, followed by PC2 which is uncorrelated with PC1. Each observation can be located on a scatterplot along the new axes (PC1 and PC2) which describe the most important information about the variation in the dataset (Bertrand et al. 2015; Helsel and Hirsch 2002). The maximum number of extracted factors is determined by the Kaiser Criterion, which considers only factors with eigenvalues greater than 1 (Jiang et al. 2009). Prior to the extraction of the factors a Kaiser-Meyer-Olkin (KMO) test was performed to assess the suitability of the data for factor analysis (Kaiser and Rice 1974).

v. Tracer tests

Artificial tracer tests are a valuable tool to investigate the origin, movement and destination of groundwater (Goldscheider et al. 2008). In this study, five tracer tests were conducted with the fluorescent dyes uranine ([518–47-8], AppliChem GmbH, Darmstadt, Germany) and amidorhodamine G (Amido G, [5873–16-5], ORCO Organic Dyes and Pigments, RI, USA). A field fluorometer GGUNFL30 (Albillia Co, Neuchâtel, Switzerland, Schnegg 2002) was used for monitoring the tracer breakthrough curves (BTCs). Additionally, water samples were analyzed with a mobile filter fluorometer (Trilogy, Turner Designs, San Jose,

CA, USA) in the field or in Germany with a spectrofluorometer (LS55, Perkin Elmer, Waltham, MA, USA) following standard procedure (Käss 2004). During one tracer test, only charcoal bags were applied for a qualitative prediction about a connection between a sinking stream and a remote spring. BTCs were analytically modeled with a conventional one-dimensional Advection-Dispersion-Model (ADM) by using the software CXTfit (Toride et al. 1999).

2.3 RESULTS AND DISCUSSION

2.3.1 Tracer tests

The major findings of the tracer tests, conducted at five different locations (

Fig. 2-2 **a** Injection and major sampling points for the tracer tests conducted in Dong Van and the identified connections (arrows), and **b** the observed breakthrough curves (DEM: B Zindler, A Degen, H Stolpe, RUB Bochum, unpublished data, 2015): 1a, 1b, 2a, 2b, 3) are:

- There is a connection between the Ma Le valley and the Seo Ho valley. The tracer test revealed that the Ma Le River remerges at springs CSP3 and CSP4 to form the Seo Ho River, whose water will be used by the projected water supply system.
- A cave stream (CST3), located in the Sang Ma Sao polje (Fig. 2–1, P2), is connected to the Seo Ho River. The inflow takes place a few meters upstream of the water extraction for the future water supply system, leading to the inclusion of the Sang Ma Sao valley in the catchment area.
- A series of connected poljes causes a groundwater flow from the Quan Xin Ngai Valley (Fig. 2–2, No. 2) in the west to the Nho Que. River in the east. Within the Dong Van polje (Fig. 2–1, P1), water from several springs are mixed with a substantial amount of wastewater. This water mixture enters the stream sink (SSDV), remerges at the stream resurgence SRDV and finally reaches the Nho Que. River.

The flow and transport parameters for these tracer tests are shown in Table 2–2.

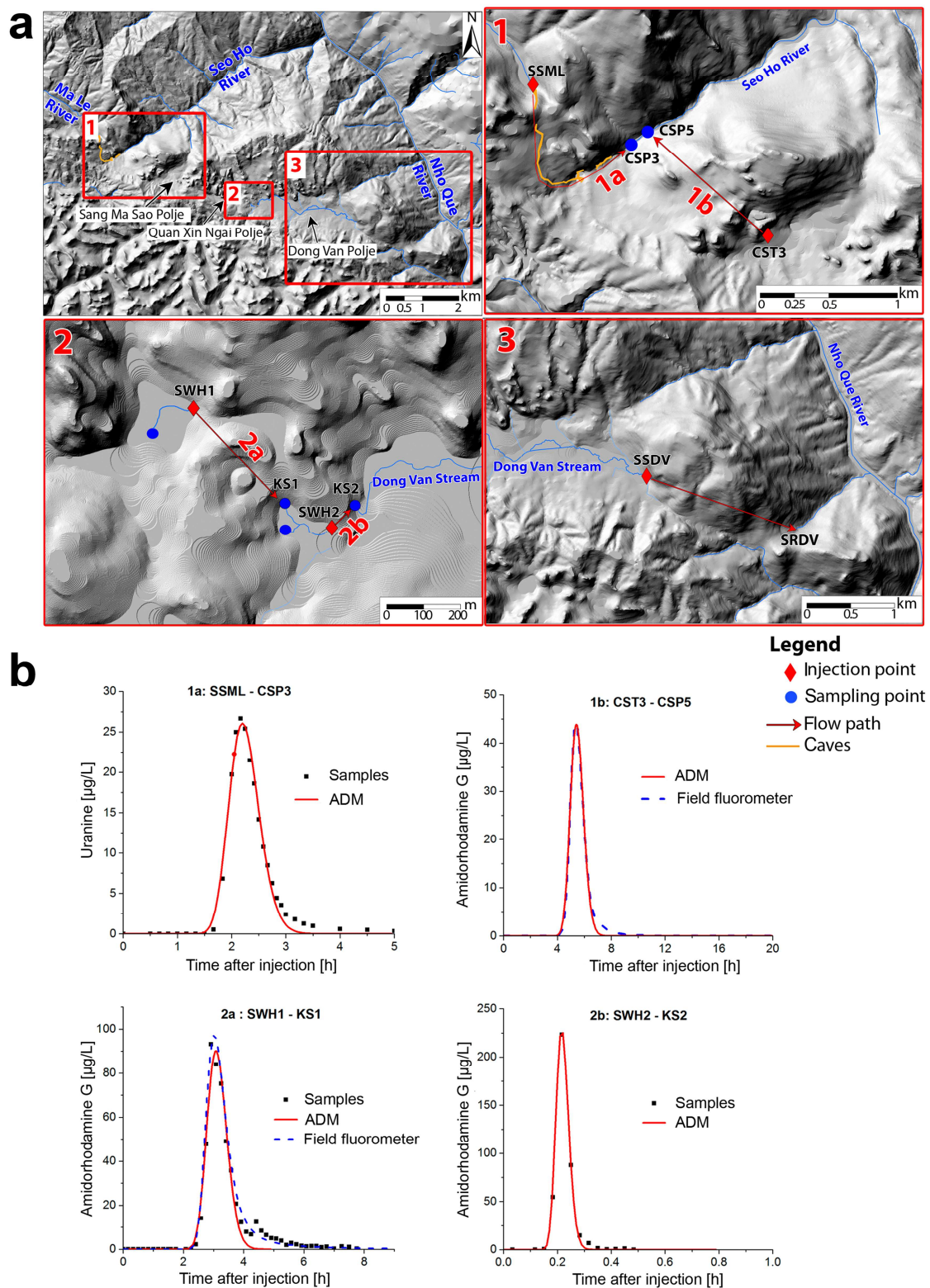


Fig. 2-2 **a** Injection and major sampling points for the tracer tests conducted in Dong Van and the identified connections (arrows), and **b** the observed breakthrough curves (DEM: B Zindler, A Degen, H Stolpe, RUB Bochum, unpublished data, 2015)

Table 2-2 Flow and transport parameters for the tracer tests conducted in Dong Van and shown in Fig. 2-2. Parameters are given for the major springs

Parameter	Symbol	Units	Tracer test			
			1a	1b	2a	2b
Injection point	IP	–	SSML	CST3	SWH1	SWH2
Sampling point with BTC	SP	–	CSP3 ^a	CSP5	KS1	KS2
Tracer	–	–	Uranine	Amido G	Amido G	Amido G
Injected mass	M	[g]	50	50	20	10
Spring discharge	Q	[L/s]	664	ND	62.6	182
Linear distance	x	[m]	1,492	1,229	322	120
Peak time	t_p	[h]	2.17	5.4	2.92	0.22
Peak velocity	v_p	[m/h]	688	228	110	545
Mean flow velocity (ADM)	v_{mean}	[m/h]	663	219	101	546
Dispersivity (ADM)	α	[m]	11.55	5.09	1.83	0.70
Recovery rate	R	[%]	92	ND	95	85

ND not determined, ADM advection-dispersion model, BTC breakthrough curve

^a Since the courses of the Ma Le caves (SSML–CSP3) are known, the real distance is used for calculations (Ender et al. (2018b), where SSML =ML1 and CSP3=ML4)

2.3.2 Physicochemical characterization

The mapping activities and the physicochemical investigations revealed that the springs can be categorized into four groups corresponding to the hydrostratigraphic units. Their physicochemical characters are influenced by the mineralogical composition of the geological units, residence time and potential anthropogenic input by agricultural activities or sewage infiltration.

The KMO test revealed an overall measure of sampling adequacy of 0.67, which justifies the application of a PCA. The PCA enables the identification of preferential correlations between the nine physical and chemical variables that were used for this study (Table 2-3). Two factors were extracted (Table 2-4).

The two main discriminative axes F1 and F2 explain 72.19% of the variance within the data set. Figure 2-3a exhibits the distribution of 108 observations from 28 different sampling points that are listed separately in Suppl. Table 1 of the supplementary material (SM). The variables indicate a preferential correlation between EC, HCO_3^- and Ca^{2+} , which represent the first axis. Along this axis, a weaker but significant correlation was found between Ca^{2+} and SO_4^{2-} and between Ca^{2+} and NO_3^- .

Table 2-3 Correlation matrix of the physicochemical parameters included in the PCA

	EC	Ca ²⁺	Mg ²⁺	HCO ₃ ⁻	K ⁺	Na ⁺	Cl ⁻	SO ₄ ²⁻	NO ₃ ⁻
EC	1.000								
Ca ²⁺	0.937*	1.000							
Mg ²⁺	0.310*	0.144	1.000						
HCO ₃ ⁻	0.964*	0.956*	0.360*	1.000					
K ⁺	-0.036	-0.094	0.201	-0.019	1.000				
Na ⁺	-0.007	-0.080	0.447*	0.054	0.411***	1.000			
Cl ⁻	0.357*	0.294**	0.633*	0.424**	0.558*	0.726*	1.000		
SO ₄ ²⁻	0.419**	0.508*	-0.114	0.409***	-0.027	-0.309*	0.095	1.000	
NO ₃ ⁻	0.640*	0.694*	0.146	0.627*	-0.066	-0.207	0.231	0.499*	1.000

p-values: * <0.001, ** <0.005, ***<0.01

Table 2-4 Factor loadings of the variables

Variables	Factor 1	Factor 2
EC	0.471	-0.067
Ca ²⁺	0.467	-0.147
Mg ²⁺	0.201	0.397
HCO ₃ ⁻	0.479	-0.028
K ⁺	0.034	0.413
Na ⁺	0.040	0.554
Cl ⁻	0.266	0.494
SO ₄ ²⁻	0.270	-0.254
NO ₃ ⁻	0.380	-0.173
% of variance	44.43	27.76

Since Ca²⁺ and HCO₃⁻ are the major ions of those karst waters, they contribute strongly to the EC. With increasing residence time, more carbonate can be dissolved, leading to an increase in EC. Observations from the Ma Le System or from the group “Others” are more characterized by superficial waters and are anti-correlated with EC, Ca²⁺ and HCO₃⁻. They have short or even lacking residence times, resulting in a low content of dissolved solids and therefore low EC. For this reason, factor 1 was assumed to be indicative for carbonate water-rock interaction.

The second axis is characterized by a preferential correlation between K⁺, Na⁺ and Cl⁻ and to a lesser extent Mg²⁺. In particular, samples from the Dong Van sinking stream (SSDV) and the stream resurgence (SRDV) are projected along this second axis. Samples from the Na Quan and Toc Tat group have negative values for factor 2, indicating lower Mg²⁺, K⁺, Na⁺ and Cl⁻ concentrations. The PCA resulted in a more transient passage between the formations than a clear separation. The preferential correlation of K⁺, Na⁺ and Cl⁻ can be associated with anthropogenic activities. Since the study area is dominated by limestone,

the sources of Na^+ , K^+ and Cl^- likely include agricultural fertilizers, and domestic and industrial effluents (Jiang et al. 2009). Magnesium is also projected on this axis, but is attributed to dolomite and is usually seen as a residence time tracer in carbonate reservoirs (Batiot et al. 2003; Emblanch et al. 1998), which disagrees with this correlation; however, this unexpected behaviour can be explained with knowledge of the sampling sites and their connections. The samples SSDV within the right upper quarter (Fig. 2–3a) are from the sinking Dong Van stream, which receives water mainly from the karst springs. Therefore, the water might be in contact with dolomite or experience partly high residence times, which might result in a higher Mg^{2+} content than for samples of other formations. Simultaneously, sewage from households and from agriculture enter the stream, leading to higher K^+ , Na^+ and Cl^- concentrations and, therefore, to an apparent correlation of these variables. This phenomenon also concerns samples from SRDV, because as the tracer test (No. 3) revealed, SSDV is directly connected to the resurgence SRDV; therefore, factor 2 is assumed to be indicative for anthropogenic contamination.

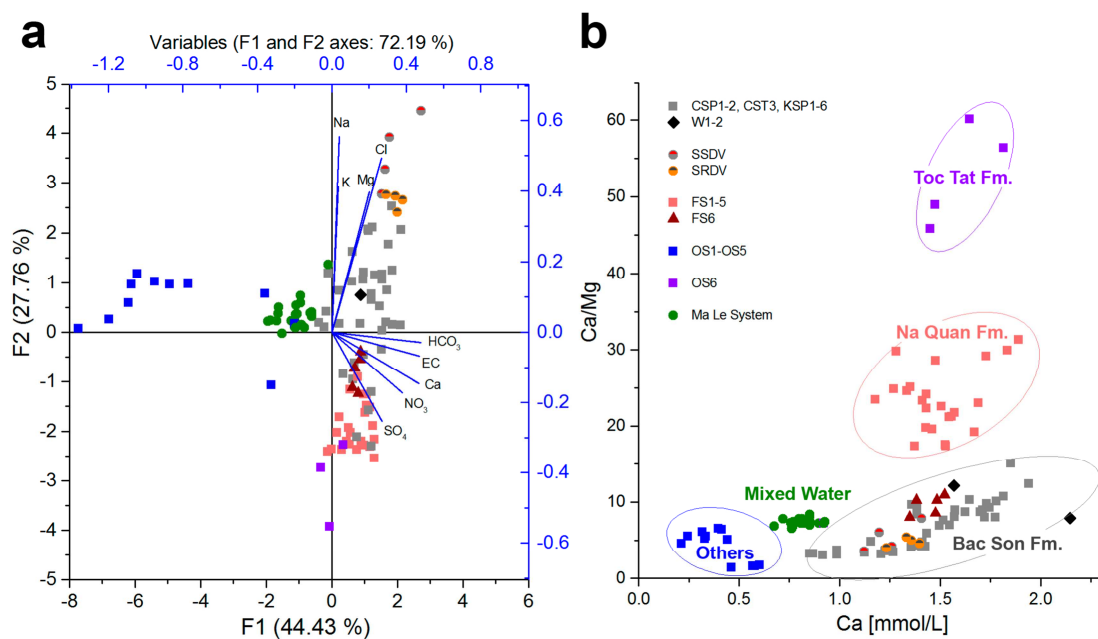


Fig. 2-3 **a** Principal component analysis (PCA) of the samples ($n = 108$) taken in the Dong Van area. The variables are shown with blue lines and the individual observation in colored points, depending on the different sampling points. One outlier (W2) was excluded from the PCA. **b** Hydrochemical groups according to the $\text{Ca}^{2+}/\text{Mg}^{2+}$ molar ratio versus Ca^{2+} . The blue group “Others” include observations from springs of the Song Hien Fm. and the Mia Le Fm. The group “Mixed Water” includes the samples of the Ma Le cave system (SSML, CST1, CST2, CSP3, CSP4), since the Ma Le River drains a catchment area where all the geological units are represented

The $\text{Ca}^{2+}/\text{Mg}^{2+}$ ratio distinctly illustrates the hydrochemical difference of the four identified groups (Fig. 2–3b). While Ca^{2+} concentrations are quite similar, a decrease of the $\text{Ca}^{2+}/\text{Mg}^{2+}$ ratio can be observed from Toc Tat over Na Quan to Bac Son Fm. The group “Others” includes springs of the Song Hien and Mia Le Fm., which were defined as aquitards; however, a limited shallow groundwater movement is possible due to the weathered surface zone. These springs are characterized by little mineralization due to the lower content of carbonates and the probable shorter residence time. The water samples from the Ma Le system can be ascribed to a mixed water group, since in the catchment area of the Ma Le River all described geological units are represented.

A lower Ca/Mg ratio at similar Ca concentrations could be indicative for higher dolomite content within the carbonate units, leading to the assumption that dolomite is more common in the Bac Son Fm. and barely represented within the Toc Tat Fm.

Furthermore, if Mg^{2+} is seen as an indicator for residence times in carbonate reservoirs, variations can be observed within the group of the Bac Son Fm. Samples from karst springs that are directly connected to swallow holes are characterized by higher influences of surface water, leading to higher $\text{Ca}^{2+}/\text{Mg}^{2+}$ ratios (e.g. KS1 and KS2). In contrast, samples from springs with larger recharge areas and longer residence times showed higher Mg^{2+} concentrations and therefore, lower $\text{Ca}^{2+}/\text{Mg}^{2+}$ ratios (CSP1 and CSP2).

Samples of the sinking stream resurgence (SRDV) and the spring FS6 (highlighted in Fig. 2–3a, b), which are located within the Na Quan Fm., clearly exhibited a hydrochemical signature of the Bac Son Fm. as shown by a lower $\text{Ca}^{2+}/\text{Mg}^{2+}$ ratio. Since the spring receives water from the sinking stream (SSDV), which drains the water from several karst springs, the hydrochemical character is clearly dominated by the Bac Son water type. For the spring FS6, no profound information is available, but since the spring is located within a fault zone, a hydraulic connection to the karst aquifer cannot be excluded.

2.3.3 Hydrogeological conceptual model

Figures 2–4 and 2–5 exhibit the conceptual model for the Dong Van karst aquifer. The Bac Son Fm., which outcrops north and west to Dong Van (Fig. 2–1c) is the most important aquifer in the region and Dong Van City is largely dependent on this water.

The autogenic recharge area of the karst springs in and the aquifer below Dong Van include the mountainous area north and northwest of Dong Van (Fig. 2–5). The latter could be shown by the conducted tracer tests, which revealed the polje series with a water flow direction from northwest to southeast to the Nho Que. River. The watershed might be

between the Sang Ma Sao Valley and the Quan Xin Ngai Valley, because the tracer test (Fig. 2–2, No. 1b) indicated the westward drainage from the Sang Ma Sao Valley to the Seo Ho River.

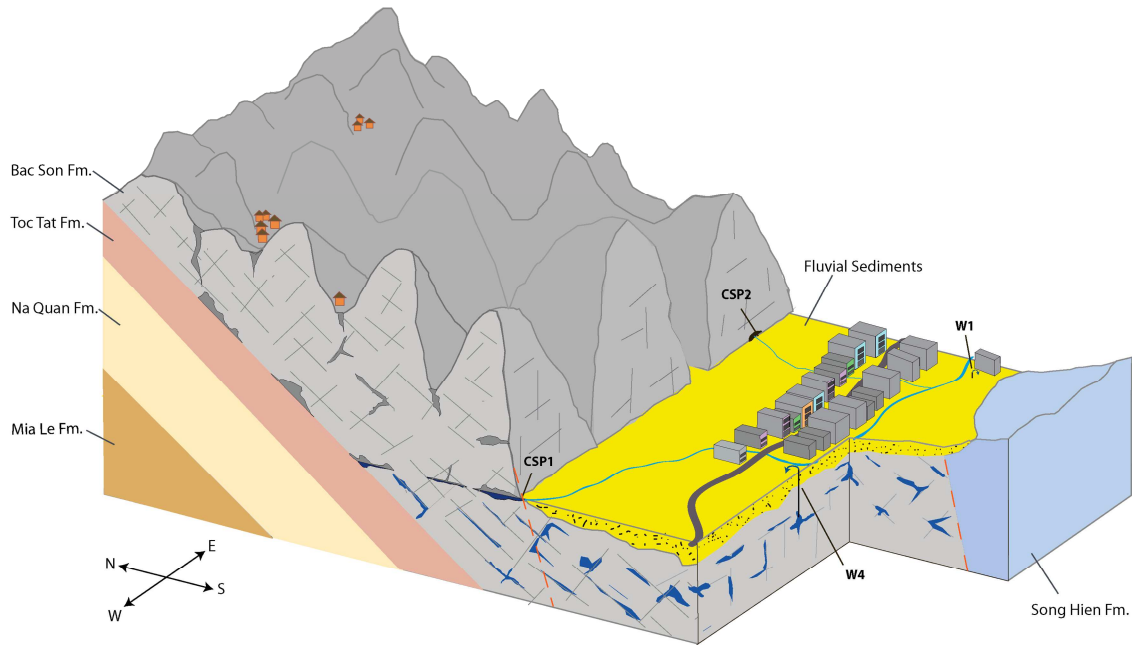


Fig. 2-4 Schematic model of the Dong Van polje. The recharge area of the karst aquifer lies, at least partly, in the northern mountainous region. Water from the cave and corresponding spring CSP1 is used for the water supply system of Dong Van. Additionally, groundwater is extracted by private (W1, W4) and public wells. Colors correspond to the geological map (Fig. 2–1c)

The springs with the largest discharge are associated with the Bac Son Fm. (CSP1, CSP2, KS1–4, Suppl. Table 1 in SM. One exception is the Dong Van sinking stream resurgence (SRDV), at the eastern side of Dong Van, which is located within the fractured Na Quan Fm. Generally, springs associated with this geological unit exhibit rather small discharge (<5 L/s); however, the spring discharge of SRDV ranged between 32 and 230 L/s, due to the fault zone and the direct connection to SSDV.

The karst springs are mainly located at the margin of the poljes, which are elongated, flat-floored, closed depressions, surrounded by highly karstified limestone with karstic drainage. The spring water is usually canalized in a stream, flowing to one or more karst sinks (SSDV). The weathered material from the surrounding highlands was deposited on the plain and sealed the underlying limestone (shown in yellow in Figs. 2–1c and 2–4 and hatched in yellow in Fig. 2–5) leading to confined conditions. Poljes were usually developed close to

the local water table (Ford and Williams 2007), which is evidenced in the study area by the presence of artesian springs in a polje (KS6).

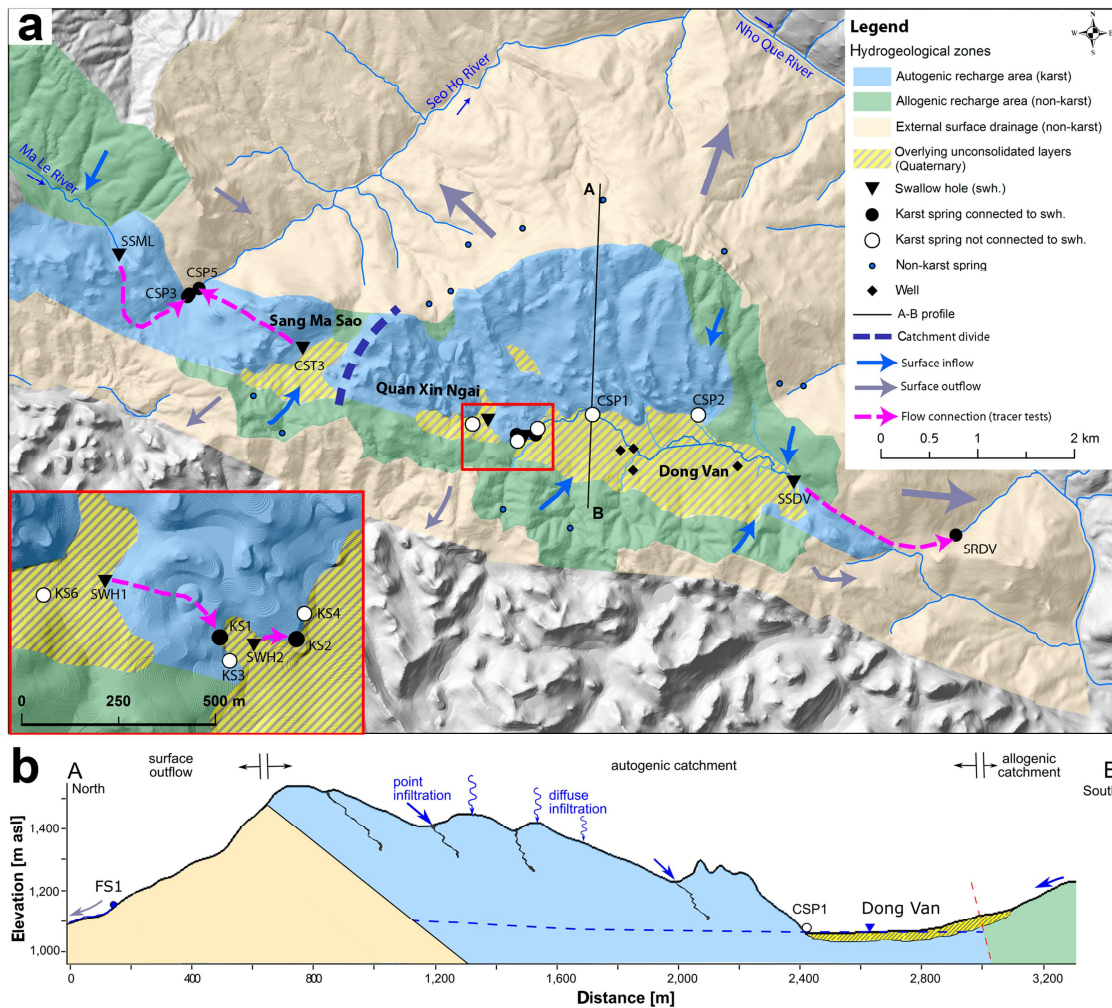


Fig. 2-5 **a** Hydrogeological map of the Dong Van region. The different hydrogeological zones are related to the Bac Son karst aquifer. The less important fractured Na Quan aquifer is not considered in this figure. Geological information can be found in Fig. 2-1 (DEM in the background: B Zindler, A Degen, H Stolpe, RUB Bochum, unpublished data, 2015). **b** North-south cross-section through the Dong Van Valley

The Toc Tat Fm. acts as aquitard due to its high clay content; however, in some sections, limestone layers can be present that allow a spatially restricted groundwater movement (e.g. spring OS6). The Na Quan Fm. is less important for the region, but on a local scale, the Na Quan springs are essential for the smaller mountainous villages on the northern slope, that are completely dependent on these springs. The discharge of the Na Quan springs is significantly smaller than that of the karst springs, but generally more constant.

The dip of the bedding is directed to the southwest (Fig. 2–1d), but groundwater apparently flows partially via vertical fractures in the northern direction. The Na Quan Fm. was defined as a fractured aquifer (Fig. 2–1b), although karstification processes can take place, but to a much lower extent than within the thick and massive limestone of the Bac Son Fm. The underlying Mia Le Fm. limits the groundwater flow, although one spring can be allocated to this formation (OS1).

South of Dong Van, a normal fault zone led to direct contact between the Bac Son Fm. and the younger Song Hien Fm., which confines the karstic aquifer. Some small springs were found within the Triassic unit (OS2–5); however, groundwater only circulates in the weathered zone close to the surface and is captured in small ditches. The development of small bog areas is common in the small tributary valleys.

In the northwestern side of the study area, the Ma Le River drains a large (30 km²) surface catchment area. The river sinks to a cave system (SSML) at the boundary between the Toc Tat and Bac Son Fm., flows through a cave system and reemerges at the springs CSP3 and CSP4 to form the Seo Ho River. Detailed information about the Ma Le cave system can be found in Ender et al. (2018b, 2017). The Seo Ho River is the receiving stream for the springs at the northwestern slope and flows to the Nho Que. River at the border to China and, therefore, to the regional base level.

With private and public wells (e.g. W1–W4) groundwater is extracted from the aquifer below Dong Van City. Although, the groundwater is generally well protected by the overlying layers of fluvial sediments (Fig. 2–4), the water extraction is seen to be problematic. There is no knowledge about residence times, recharge rates and groundwater ages; furthermore, there is no control of water extraction rates or even knowledge of the exact number of private wells. Ford and Williams (2007) have already emphasized that karst water resources are often exploited without any evaluation of the resource until problems of depletion emerge; therefore, investigations of the water resources below Dong Van City should be carried out.

2.3.4 *Microbiological water quality*

i. Sampling campaigns

A total of 122 samples were analyzed for *E. coli* and TTC, and 94 for ENT. The results are listed in Suppl. Table 2 of the SM and are depicted in Fig. 2–6, where *E. coli* and ENT concentrations are shown for three different seasons (dry, rainy and transient season).

Furthermore, the relationships between FIB, aquifer type and sampling point are illustrated in Fig. 2–6; in addition, Fig. 2–7 illustrates descriptive statistics.

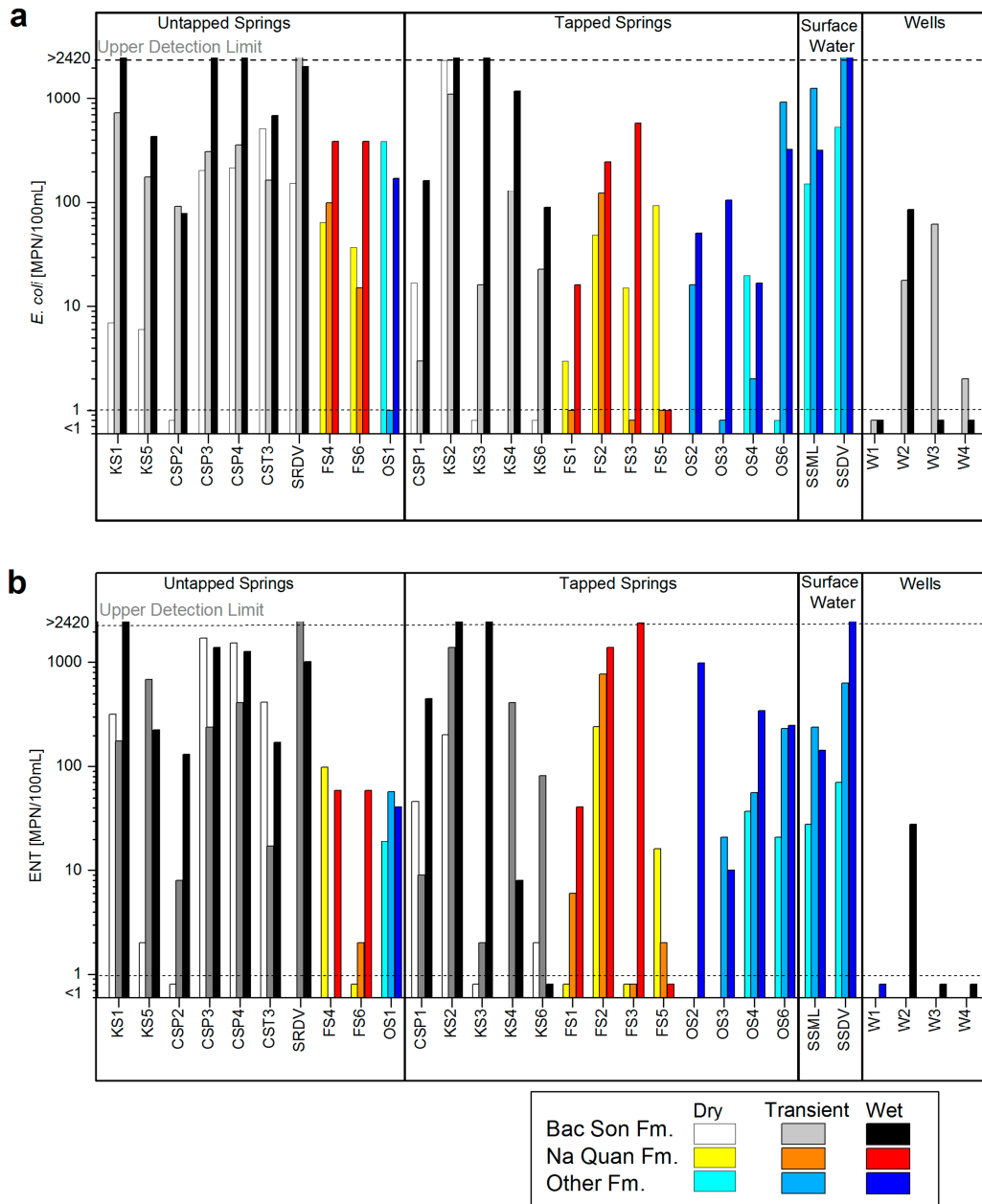


Fig. 2-6 Concentrations of **a** *Escherichia coli* (*E. coli*) and **b** enterococci (ENT), dependent on hydrogeology, seasons and the type of sampling points. Considered values are from dry and transient season 2015, and rainy season 2016. The group “Other Fm.” includes samples from surface streams and the spring from the Toc Tat Fm. (OS6)

In 46% of all water samples, >100 MPN/100 ml *E. coli* were detected and in 12%, >2420 MPN/100 ml (>UDL) were detected. These results illustrate the extremely high

contamination level, especially with reference the legal limit of 0 cfu/100 ml for TTC, *E. coli* and ENT according to the WHO (2008). Generally, the pollution with *E. coli* was higher during wet season (Fig. 2–7a), as already shown by other researchers, e.g. Kapembo et al. (2016). Stronger precipitation events lead to more surface runoff that flushes contaminants from the surface to swallow holes and to the water table, while, on the other hand, reduced spring discharges during dry season could also lead to a lower dilution of contaminants, as observed for the stream resurgence SRDV during transient conditions. The combination of large amounts of sewage due to very high tourist numbers in Dong Van and lower discharge rates at the end of rainy season resulted in high concentrations of FIB at the sinking stream SSDV and the stream resurgence SRDV.

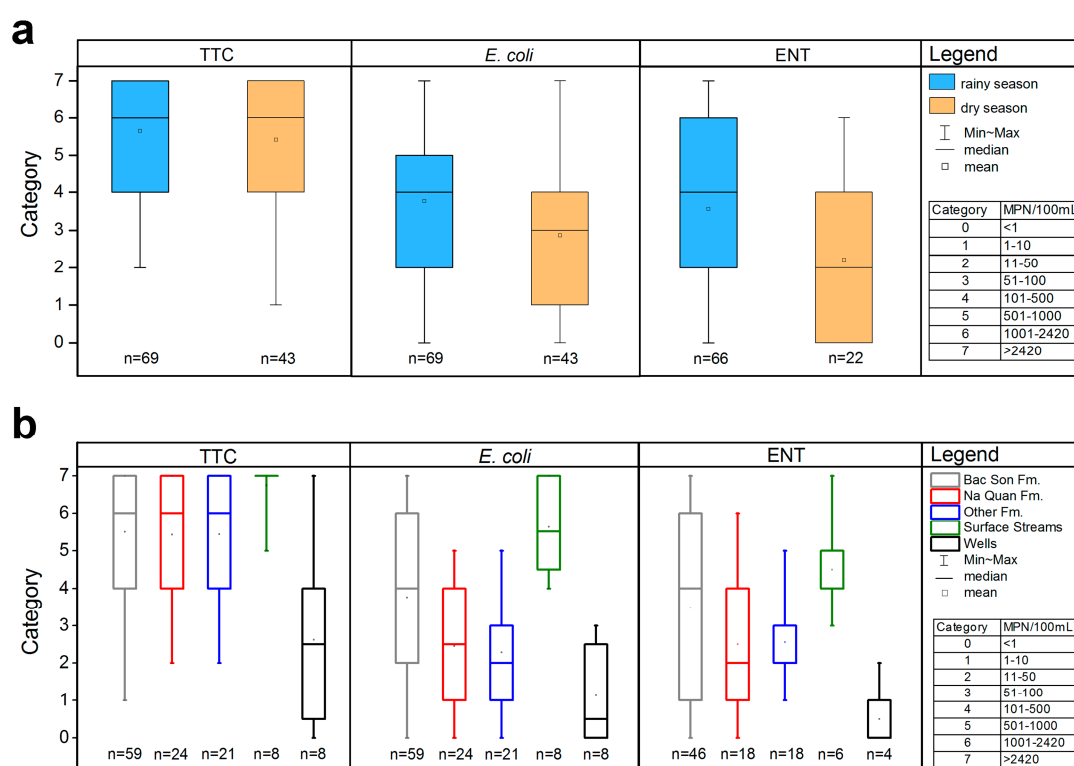


Fig. 2-7 Categories for fecal indicator bacteria depending on **a** hydrological conditions and **b** on aquifer type. The group “wet season” contains analysis from three campaigns (July 2014, September 2015 and June 2016) and the group “dry season” from two campaigns (February 2014, March 2015). Samples from wells are not considered within the comparison of seasons

The analyses of ENT generally confirm the results from the *E. coli* investigations; however, some springs of the Bac Son Fm. showed highest ENT concentrations for the dry season, while *E. coli* concentrations were highest during wet season. This might be explained by the differences in persistence of the two FIB within the environment; furthermore, ENT may

not be solely of fecal origin, but may be endogenous in sediments and soils (Byappanahalli et al. 2012).

Due to a high variety of potential contaminant sources in the catchment areas of surface waters, they showed highest concentrations of FIB (Fig. 2–7b). Besides, rivers are often used as natural waste water systems, leading to extremely high bacteria loads (e.g. *E. coli* in SSDV: 31,060 MPN/100 ml; September 2015, Suppl. Table 2 of the SM).

In contrast, spring waters are generally better protected by the aquifer properties against pollution than surface waters, but a high degree of karstification leads to a higher vulnerability of groundwater. For this reason, the springs of the Bac Son Fm. are most strongly contaminated with fecal bacteria, but as Fig. 2–7b illustrated, they also exhibited the highest variation in contamination levels ranging between uncontaminated and extremely contaminated with *E. coli* and ENT. Samples from shallow wells did not show *E. coli* and ENT concentrations as high as the springs of the Bac Son Fm., due to protective overlying layers. Four water samples met the water quality standard with <1 MPN/100 ml for *E. coli* and 3 samples for ENT; however, *E. coli* concentrations of 161 and 62 MPN/100 ml for the wells W2 and W3 are alarming, since the groundwater should be well protected due to the confined conditions. This indicates that the construction of wells led to hydraulic connections between the valuable karst groundwater and surface water and/or that leakages of septic tanks polluted the groundwater. Springs of the Na Quan Fm. are less impacted than those of the Bac Son Fm., probably caused by more diffuse than point infiltration via swallow holes. Diffuse infiltration also takes place in granular aquifers, where the contamination level of springs was found to be relatively moderate. An attachment of bacteria to the immobile aquifer media might be another reason for the relatively low contamination levels (Mahler et al. 2000).

The type of the spring or sampling point also plays an essential role in spring water quality. Untapped springs are most exposed to a contaminant input in the vicinity of the springs and are often used as drinking-water troughs for animals. However, tapped springs can also be prone to contamination, especially if the spring water is directly captured in a storage tank, as is the case for the springs KS3, FS1, FS2, FS5, OS3 and OS6. Local residents are often not aware of the contamination risk and might bring contaminants to the spring reservoir. In this case, the water quality problem might not be caused by a contaminant input within the recharge area, but within the tapping of the spring; additionally, sufficient purification and maintenance of the storage tanks may be lacking.

ii. Monitoring

The water quality monitoring at the cave spring CSP1 with daily measurements of Q, T, EC, DO, turbidity and PSD (Fig. 2–8) for a time period of 24 days revealed a relatively good water quality. The eight water samples that were analyzed for *E. coli*, ranged between 4 and 32 MPN/100 ml.

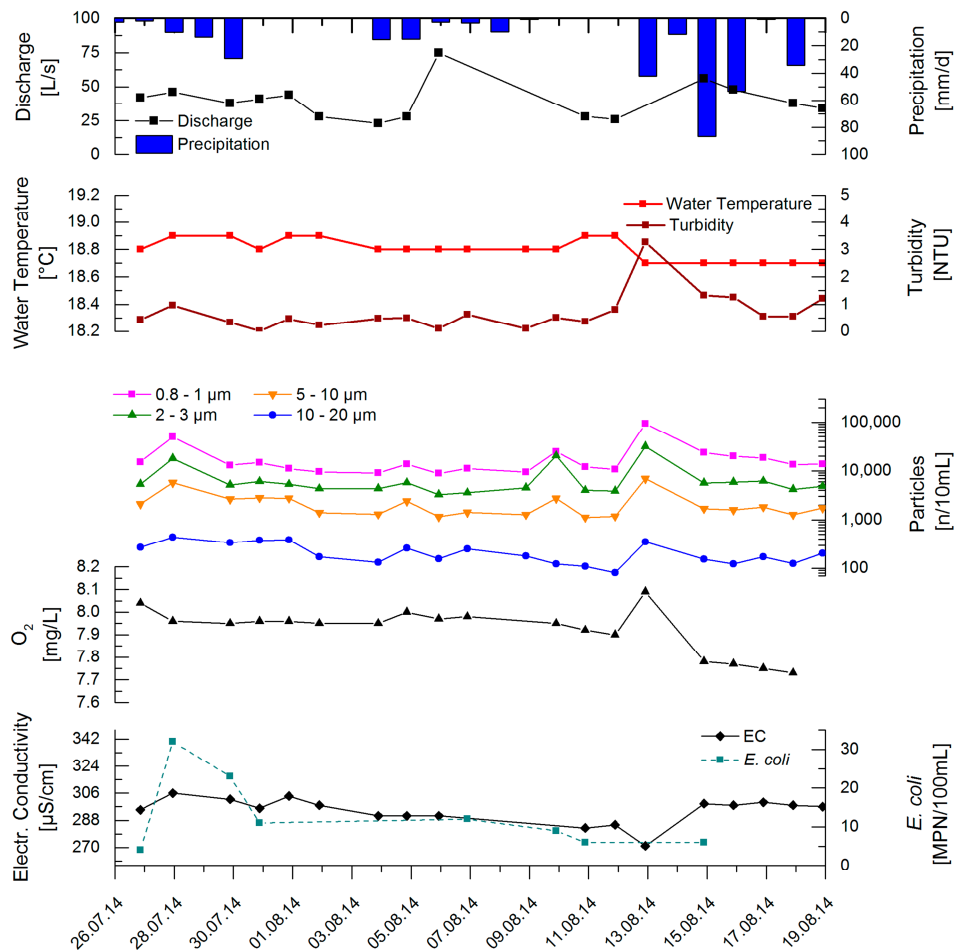


Fig. 2-8 Monitoring at the spring CSP1 for a time period of 24 days with daily measurements. In total, eight samples were taken for the analysis for *Escherichia coli* (*E. coli*)

Although several precipitation events occurred, the physicochemical parameters did not show a strong response to those events. An exception to this observation was the precipitation event on 13 August 2014, which caused an increase in turbidity, particles and oxygen concentrations, as well as a decrease in electrical conductivity, although the precipitation intensity was apparently lower compared to the previous events. The climate station is located southeast of Dong Van, meaning a difference in elevation of around 300–

400 m between the recharge area of the spring and the climate station. The high spatial variability of precipitation in this area, in particular during thunderstorms, might cause uncertainties concerning the exact precipitation intensity within the mountainous area. However, the intensity of the physicochemical response was found to be rather small, although discharge ranged from 23 to 75 L/s. These small variations could be explained by a larger catchment area with more diffuse groundwater recharge and without a direct connection between the spring and a sinking stream. Furthermore, from speleological investigations, it is known that the spring drains a cave with a pond (Ho Tien Chung, Vietnam Institute of Geosciences and Mineral Resources, personal communication, 2015), which could act as a buffer and could explain the rather small reaction to precipitation events.

In contrast, the monitoring of the karst spring KS2 showed very strong fluctuations in *E. coli* (Fig. 2–9).

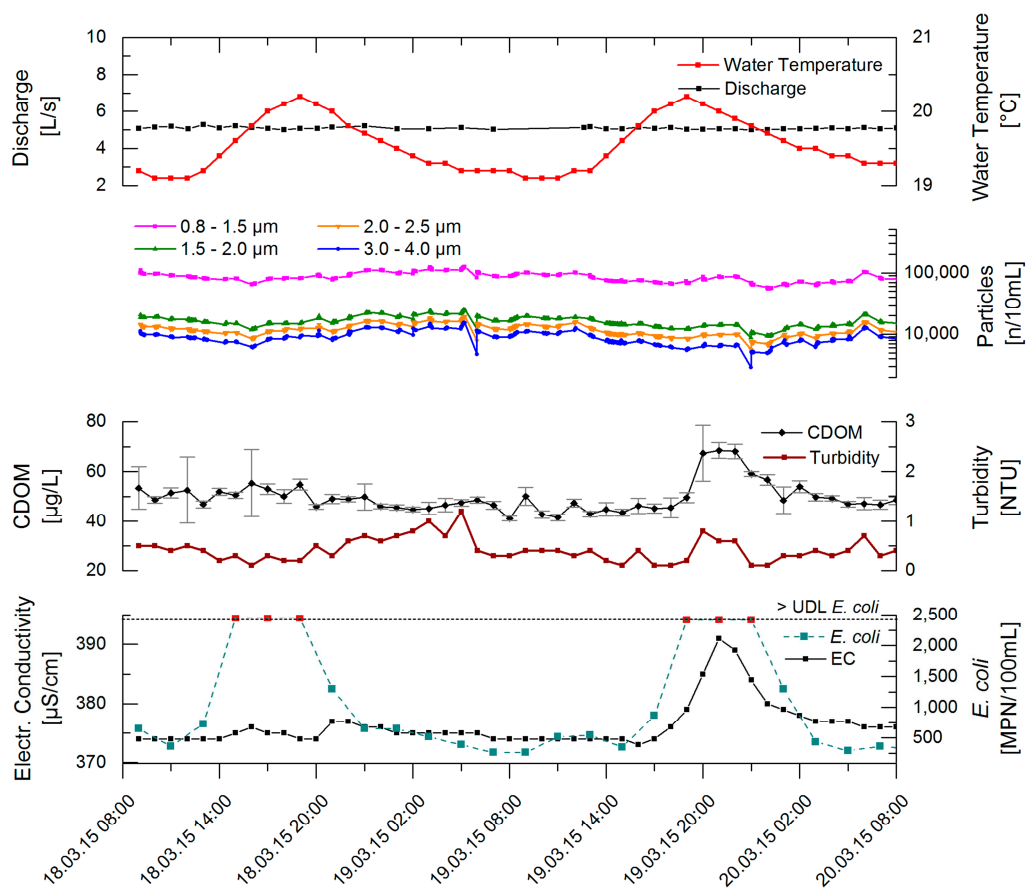


Fig. 2-9 Forty-eight-hour monitoring at the spring KS2 for the evaluation of short-term water quality dynamics. Although no precipitation event occurred, daily contamination events could be identified with *E. coli* levels of >2,420 MPN/100 ml (>UDL)

Although the monitoring was carried out during dry season where the spring discharge was constant (5.0 ± 0.2 L/s), two contamination events could be observed with $>2,420$ MPN/100 ml *E. coli*. The simultaneous daily fluctuations of water temperature ($19.1\text{--}20.2$ °C) indicated that a general increase of *E. coli* is associated with anthropogenic activities that take place during daytime. Since the spring is part of the polje series, it is directly connected to sinking surface streams that are strongly influenced by air temperature. The second *E. coli* peak was strongly correlated with an increase of EC and CDOM, but without an influence on discharge, turbidity or particle concentrations. Hence, it can be assumed that a direct inlet of sewage into the swallow hole caused the water quality deterioration at the spring.

Karst springs that are directly connected to swallow holes are extremely vulnerable to a high input of fecal bacteria, especially if the recharge area is characterized by agricultural activities. Furthermore, swallow holes are often used as natural sewage system by settlements, which cause a direct input of feces. In this study, the springs KS1, KS2, CSP3, CSP4 and the Dong Van stream resurgence SRDV are directly affected by a sinking stream (Fig. 2–10).

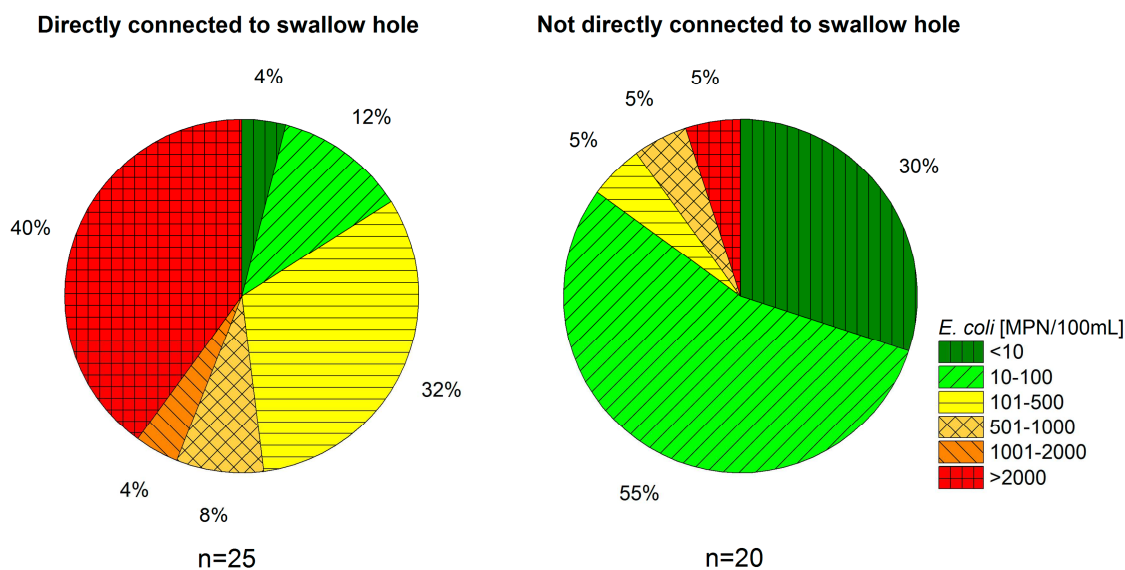


Fig. 2-10 Comparison of contamination levels of 45 samples (n) collected at springs with and without a direct connection to a swallow hole: five springs are known to be directly connected to a swallow hole (KS1, KS2, CSP3, CSP4 and SRDV), and four springs are assumed to have no direct connection to a swallow hole (CSP1, CSP2, KS3 and KS6)

Karst springs that are not directly associated with specific swallow holes show a better water quality in general. Larger mountainous and more pristine catchment areas of the karst springs CSP1 and CSP2 result in relatively moderate *E. coli* concentrations (<165 and < 91MPN/100 ml), even during wet season.

In general, the concentrations of FIB are far too high and result in an increased risk of water-related diseases such as gastrointestinal, typhoid, cholera and other diarrhoeal diseases (Kapembo et al. 2016). Although several springs are not used for drinking water, they were used for personal hygiene, bathing and irrigation; nevertheless, even in recreational waters, such high concentrations of FIB pose a threat for human health (Prüss 1998; Stallard et al. 2016; Vogel et al. 2017).

An alternative water supply will be realized soon, where water from the Seo Ho River will be pumped to the Ma U pass and distributed to the villages and to Dong Van, without additional energy demand (Oberle et al. 2017). This project will lead to an ease of the water quantity problem, but the challenge of a good water quality, at least for now, will remain.

2.4 CONCLUSIONS

This study revealed that all springs in the Dong Van area were faecally impacted and even shallow wells in Dong Van exhibited a partial deterioration of the microbial water quality. But to develop adapted groundwater protection strategies, a profound hydrogeological understanding is necessary. Especially in geological complex areas, where the delineation of the spring catchment areas is difficult, detailed investigations are essential to evaluate the reasons and factors of microbial water quality deterioration. Two aquifers are important for the region: the Bac Son karst aquifer and the fractured Na Quan aquifer, which are separated by the Toc Tat Fm., in which groundwater flow is limited. Table 2–5 summarizes the main characteristics of the four identified water types.

General conclusions are:

- The PCA revealed that 72% of the physicochemical variance can be described by two factors: factor 1 is indicative for water-rock interaction and factor 2 can be associated with anthropogenic influences.
- A relation between hydrochemical properties and microbial contamination could be found, since samples with the hydrochemical signature of the Bac Son type tendentially showed highest FIB values.

- Microbial water quality varied by season. During the dry season, most of the water samples showed *E. coli* concentrations between 51 and 100 MPN/100 ml, while they ranged between 101 and 500 MPN/100 ml during the wet season. But due to a smaller dilution during dry season, water quality was poor throughout.
- Spring waters that are captured with storage tanks were found to be prone to contamination, since people might unknowingly pollute the water reservoir. Furthermore, maintenance and purification of the tanks were insufficient or even lacking.

Table 2-5 Main characteristics of the different aquifer types

Characteristic	Geological unit			
	Bac Son Fm.	Na Quan Fm.	Toc Tat Fm.	Others (Mia Le and Song Hien Fm.)
<i>General characteristics</i>				
Media type	Karst Aquifer	Fractured aquifer	Aquitard	Aquitard
Groundwater flow	Within matrix, fractures and conduits	Mainly along vertical fractures and along faults	Limited within thin limestone beds, along faults	Limited within weathered zone, close to the surface
<i>Water characteristics</i>				
Ca/Mg molar ratio	3 - 15	17 - 31	46 - 60	1 - 7
Ca [mmol/L]	0.9 - 2.1	1.2 - 1.9	1.5 - 1.8	0.2 - 0.6
Median <i>E. coli</i> category / concentrations [MPN/100mL]	6 / 1001-2420	2.5 / 20 - 75	ND.	2 / 11 - 50
Median ENT category / concentrations [MPN/100mL]	4 / 101 - 500	2 / 11 - 50	ND.	3 / 51 - 100

The concentrations of *Escherichia coli* (*E. coli*) and enterococci (ENT) for the Toc Tat spring (OS6) were included in the group "Others" for this analysis. Definition of FIB categories can be found in Fig. 2-7
ND not determined

For the karstified Bac Son aquifer, which is the most important one for water supply, the following major conclusions could be made:

- The development of the sub-surface karst conduit network played an essential role in terms of water quality. For springs with a direct connection to a sinking stream, 84% of the samples were contaminated with >100 MPN/100 ml *E. coli*. In contrast, only 15% of the samples from karst springs that are not directly connected to active swallow holes showed *E. coli* values >100 MPN/100 ml.

- Contamination events of springs with direct connections to swallow holes are not always associated with precipitation events. They can be caused by discharge of wastewater from households and agriculture. In Dong Van, springs that are involved in the polje series are especially affected, since the closed depressions are extensively used for agriculture. The tracer tests indicated that contaminants can be transported with high velocities ($v_p = 110\text{--}545$ m/h) without a high potential of retention ($R = 85\text{--}95\%$). Therefore, an increasing deterioration of water quality could be observed from west to east.
- Karst springs at the northern rim of the Dong Van polje are less affected due to a mountainous and more pristine spring catchment area. Springs from the Na Quan aquifer are less contaminated due to a more diffuse infiltration.
- Water extracted by wells in Dong Van partially met the WHO drinking water regulations concerning FIB; however, some samples exhibited distinct fecal contamination. It can be assumed that in some cases the protective confining layers were perforated by an inexpert construction of wells, which resulted in a hydraulic connection between the aquifer and surface waters. This assumption is supported by the high concentrations of K^+ , Na^+ and Cl^- , which are associated with domestic and industrial effluents.

The obtained information delivers a valuable base for groundwater protection strategies, which should be aimed at reducing the contaminant input. This study revealed that one major problem is associated with an insufficient waste water system, leading to a displacement of the water quality problem, since contaminants are transported from one polje to the next, until they reach the Nho Que River. However, other villages at a lower elevation might be dependent on this water; thus, a holistic approach is necessary, including groundwater protection, water purification and waste water treatment, but also awareness-raising activities for the local population.

2.5 ACKNOWLEDGEMENTS

We want to thank the Vietnam Institute for Geosciences and Mineral Resources (VIGMR, Hanoi), Ha Giang People Committee and Dong Van People Committee for their support during the field work. Special thanks for the support from Ho Tien Chung, Doan The Anh, Tran Diep Anh, Lai Quang Tuan and Do Van Thang from VIGMR. Also, we want to thank the whole KaWaTech project team and the students that were involved (Matthias Hofer, Tobias Zaege, Christian Weippert, Nguyen Tra My, Luisa Röckel, Rainer Schumacher and Marian Bechtel) as well as the KIT laboratory team (Daniela Blank, Christine Buschhaus

and Christine Roske-Stegemann) for their support. Finally, we gratefully acknowledge Arica Beisaw for the language support.

Funding Information We gratefully acknowledge the financial support of the German Federal Ministry of Education and Research (BMBF) [grant number 02WCL1291A].

CHAPTER 3

3 SPATIAL RESOLUTION OF TRANSPORT PARAMETERS IN A SUBTROPICAL KARST CONDUIT SYSTEM DURING DRY AND WET SEASONS

Reproduced from: Ender A, Goepfert N, Goldscheider N (2018) Spatial resolution of transport parameters in a subtropical karst conduit system during dry and wet seasons. Hydrogeology Journal, doi 10.1007/s10040-018-1746-x

Abstract

Karst aquifers are characterized by a high degree of hydrologic variability and spatial heterogeneity of transport parameters. Tracer tests allow the quantification of these parameters, but conventional point-to-point experiments fail to capture spatiotemporal variations of flow and transport. The goal of this study was to elucidate the spatial distribution of transport parameters in a karst conduit system at different flow conditions. Therefore, six tracer tests were conducted in an active and accessible cave system in Vietnam during dry and wet seasons. Injections and monitoring were done at five sites along the flow system: a swallow hole, two sites inside the cave, and two springs draining the system. Breakthrough curves (BTCs) were modeled with CXTFIT software using the one-dimensional advection-dispersion model and the two-region nonequilibrium model. In order to obtain transport parameters in the individual sections of the system, a multi-pulse injection approach was used, which was realized by using the BTCs from one section as input functions for the next section. Major findings include: (1) In the entire system, mean flow velocities increase from 183 to 1,043 m/h with increasing discharge, while (2) the proportion of immobile fluid regions decrease; (3) the lowest dispersivity was found at

intermediate discharge; (4) in the individual cave sections, flow velocities decrease along the flow direction, related to decreasing gradients, while (5) dispersivity is highest in the middle section of the cave. The obtained results provide a valuable basis for the development of an adapted water management strategy for a projected water-supply system.

3.1 INTRODUCTION

Karst aquifers are important for the freshwater supply in many regions of the world, with roughly 20–25% of the world's population largely or entirely dependent on karst groundwater (Ford and Williams 2007). In Southeast Asia, around 215,000 km² or 10% of the mainland is covered by karst areas (Mouret 2004) and, therefore, karst aquifers constitute an important freshwater resource. In particular, they are characterized by anisotropy and heterogeneity (Stevanovic 2015), exacerbating the investigation of the water resources and, hence, the development of adapted and sustainable karst water management strategies. High flow velocities under partly turbulent flow conditions within the conduit network lead to a rapid transport of contaminants and, therefore, render the groundwater highly vulnerable to contamination. In Northern Vietnam, strong precipitation events during the rainy season intensify this problem, but extended dry seasons also pose a challenge to deal with. To ensure a continuous freshwater supply and a sustainable use of these valuable water resources, a profound understanding of these systems is crucial.

Artificial tracer tests are valuable tools to study the nature of karst systems because they can deliver clear information about hydraulic connections, spring catchment areas, transit time distributions and linear flow velocities (Atkinson et al. 1973; Brown et al. 1969; Goldscheider et al. 2008). Furthermore, relevant transport parameters can be determined by the quantitative analysis and modeling of breakthrough curves (Barberá et al. 2017; Hauns et al. 2001; Morales et al. 2007).

Tracer tests in active cave systems can be used to investigate transport mechanisms and to reveal the influence of cave structures or conduit configurations on parameters such as mean flow velocity and dispersion. However, few tracer experiments have been performed in active caves where both injection points and sampling points were within the cave system, to obtain more detailed information about internal structures—for example, Lauber et al. (2014) studied an active karst conduit network, and obtained spatially and temporally resolved information on conduit flow in the Blue Spring system (Blaubeuren, Germany). The flow velocities between the sampling points could be determined by using peak transit times, but dispersion coefficients were only calculated between the injection point and the sampling points. Recently, Dewaide et al. (2016) presented modeling results of tracer tests in the cave system of Han-sur-Lesse in South Belgium, whereby they obtained a spatial

discretization of transport parameters by using the OTIS model (Runkel 1998; Runkel and Broshears 1991). This model is based on a two-region nonequilibrium (2RNE) approach to consider mobile and immobile flow regions and the influence of transient storage on the observed breakthrough curves. They assumed that the recovery rate amounts to 100% at each sampling site and that no bypaths, lateral inflows, or outflows occur; however, caves are known to be very dynamic and, in most cases, this assumption leads to oversimplification of the system. There remains a gap in knowledge regarding the spatial resolution of transport parameters for systems with bypaths, lateral inflows and outflows.

To improve the understanding of spatial variations of flow and transport parameters within a karst conduit system, tracer tests were conducted in a cave system in Northern Vietnam. At this study site, there is one main stream, entering and flowing through the cave system; however, bypaths, lateral inflows and outflows cannot be excluded. Therefore, the following four major research questions were examined: (1) what are the flow and transport characteristics of the cave system? (2) how are flow velocities and transport parameters spatially distributed within the individual sections in the vadose and phreatic zone? (3) what is the influence of flow conditions (rainy and dry seasons) on these parameters? and (4) is a multiple pulse injection approach feasible to obtain spatial discretization?

3.2 MATERIALS AND METHODS

3.2.1 *Study Site*

The study area is located in the northernmost district of Vietnam, called Dong Van, with the identically named capital city (Fig. 3–1). It is one of the poorest and most remote areas of the country and lies at the northern rim of the Dong Van Karst Plateau. This site was designated as a UNESCO Global Geopark in 2010, leading to the attraction of an increasing number of tourists. Massive limestone formations, mainly of Carboniferous and Permian ages, form an impressive karst landscape. The so-called Bac Son Formation (Fig. 3–1) has undergone several phases of regional tectonic deformation (Tran et al. 2013) and is characterized by dissected topography due to peak cluster, intra-mountain blind depressions, deep river valleys and steep slopes (Tam and Batelaan 2011). The Dong Van District and the neighboring Meo Vac District are facing increasing problems in terms of water supply and water quality.

With the extended dry seasons, groundwater recharge is mainly limited to 4–5 months in the summer (Van Nguyen et al. 2013). For the period 2000–1012, the mean annual precipitation in Dong Van amounts to 1,335 mm/year with the highest rainfall in June (285 mm) and

lowest in February—(17 mm, data provided by National Center of Water Resources Planning and Investigation (NAWAPI), climate station Dong Van District, operated by Vietnam National Centre for Hydro-Meteorological Forecasting, (NCHMF)).

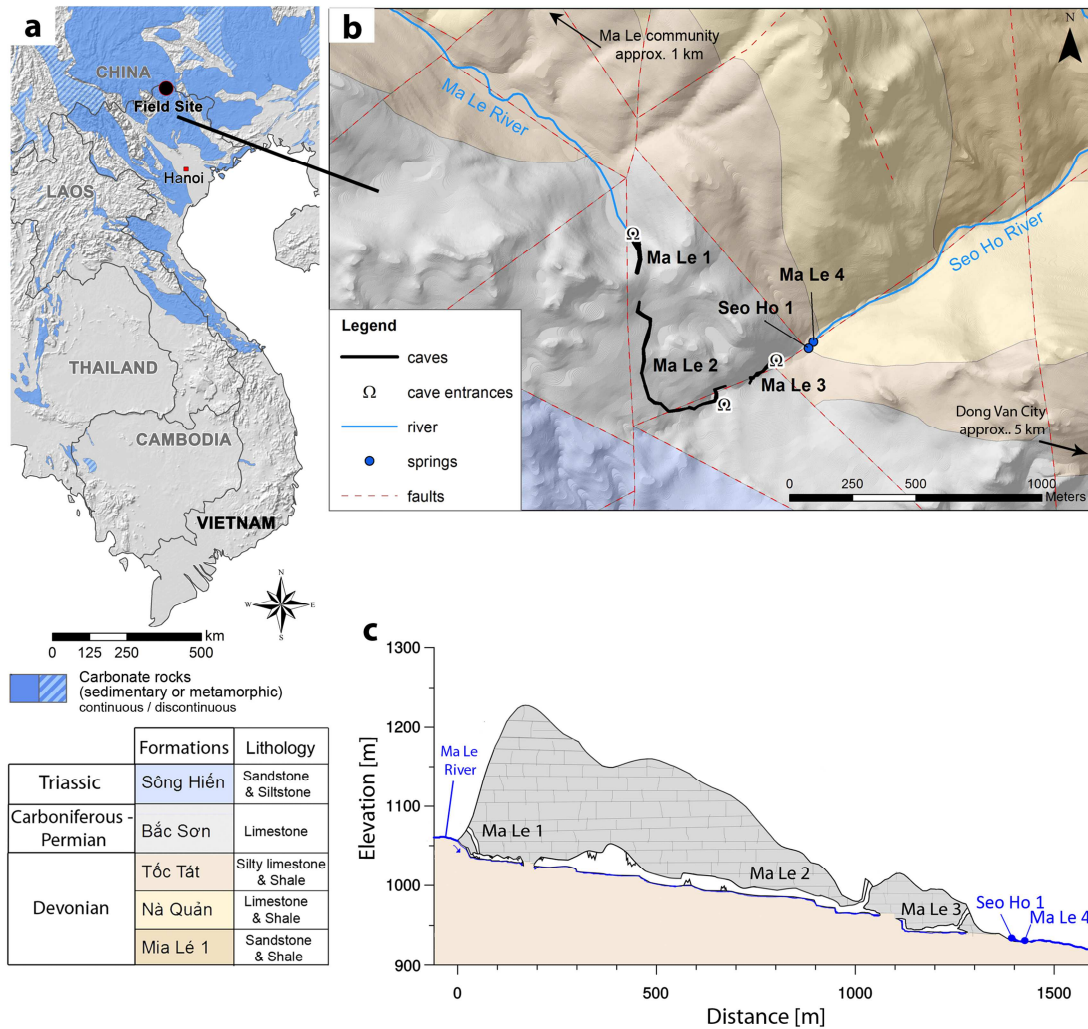


Fig. 3-1 **a** Study area in Northern Vietnam near the Chinese border. The overview map is a section of the world karst aquifer map that exhibits the distribution of carbonate rocks (blue) in Vietnam (Chen et al. 2017). **b** The Ma Le cave system (D Lagrou, SPEKUL, unpublished report, 2005), shown on the 1:50,000 geological map (Vietnam Institute of Geosciences and Mineral Resources, unpublished data, 2017) with a digital elevation model in the background (B. Zindler, A. Degen, H. Stolpe, RUB Bochum, unpublished data, 2015). **c** Cross section, following the course of the caves. The course of the caves is not to scale, but is, however, in the range of measured dimensions

Due to the high infiltration rates of the strongly karstified limestone, surface water resources are scarce. Additionally, great depth to the water table in deep cave systems prohibits access to groundwater for the population (Van Nguyen et al. 2013). Northwest of Dong Van lies the Ma Le Valley (Fig. 3–1), located in the nonkarstified Devonian units of the Mia Le Formation, which are composed of schists interbedded with sandstone, siltstone, calcareous shales and limestone lenses.

The surface stream sinks into a cave system at the boundary to the Carboniferous-Permian Bac Son Formation. Large sections of the cave system were explored and mapped by the Belgian caving club SPEKUL, but there are phreatic zones in between that are not accessible without cave diving. The hydraulic gradient of the three cave sections Ma Le 1–3 (ML 1–3) decrease along the flow direction from 11% (ML 1) over 5% (ML 2) to 2% (ML 3) (D. Lagrou, SPEKUL, unpublished report, 2005; and D. Lagrou, SPEKUL, personal communication, 2017). The caves have separate entrance chambers facilitating access (Fig. 3-1b,c). Within approximately 1 km linear distance from the sinking stream, there are two springs, Ma Le 4 (ML 4) and Seo Ho 1 (SH 1), forming the Seo Ho River that flows into the receiving stream, the Nho Que River. The two separate cave entrances (ML 2 and ML 3) enable in-cave tracer tests and allow for a finer spatial resolution of parameters. It is planned to use the water from this cave system for the water supply of the small mountainous villages and Dong Van City. For the development of an adapted karst-water-management strategy, a hydrogeological understanding of the system is essential, including parameters such as the variability of discharge, flow and transport parameters, in addition to the chemical composition of groundwater and surface water, water quality and suspended load (Ender et al. 2017).

3.2.2 *Tracer Tests*

In total, six tracer tests (Table 3–1 and Suppl. Figure 1 of the supplementary material (SM)) were performed in this cave system to investigate the influences of rainy and dry seasons on flow and transport parameters and to study the structure of the cave system. Four tracer tests were conducted with an injection mass of 50 g uranine (Fluorescein Sodium, CAS: 518–47–8) into the sinking stream of the Ma Le Valley (Injection point (IP) ML 1 in Suppl. Figure 1 of the SM). One tracer test was conducted during the dry season on 25 February 2014 (test No. 1), when discharge at ML 4 was low (72 L/s). During the rainy season, two tracer tests were performed, on 28 July 2014 and on 3 October 2015 (test Nos. 4 and 2, respectively), where the sampling points coincided with those of the test during the dry season. The fourth tracer test, with IP ML 1 as the injection point, was performed to gain more information

about flow and transport parameters under high flow conditions (16 August 2014, test No. 6), where samples were only taken at ML 4.

Table 3-1 Tracer tests conducted in the Ma Le cave system.

No.	Date	Season	Injection point	Injection mass of uranine [g]	Sampling points	Spring discharge [L/s]
1	25.02.2014	Dry	ML 1	50	ML 2, ML 3, ML 4, SH 1	72
2	03.10.2015	Wet	ML 1	50	ML 2, ML 3, ML 4, SH 1	664
3	29.09.2015	Wet	ML 2	10	ML 3, ML 4, SH 1	690
4	28.07.2014	Wet	ML 1	50	ML 2, ML 3, ML 4, SH 1	785
5	26.09.2015	Wet	ML 3	5	ML 4, SH 1	856
6	16.08.2014	Wet	ML 1	50	ML 4	1,296

Note: Spring discharge is the discharge of ML 4.

To investigate individual cave sections, one tracer test was conducted with a tracer injection in ML 3 (26 September 2015, test No. 5) and another one with an injection in ML 2 (29 September 2015, test No. 3). Discharge measurements were made on the day of the tracer test via the salt dilution method. The accuracy of this method is within maximum $\pm 10\%$ (Richardson et al. 2017), since it is constrained by the requirement of a complete mixture of salt throughout the traced stream. However, in the authors' experience, uncertainties of the salt dilution method are usually in a range of $\pm 2\%$. Nevertheless, for the calculation of uncertainties of recovery rates, a $\pm 10\%$ uncertainty of discharge rates was applied (Tables 3-3 and 3-4). Discharge rates were assumed to be constant due to the short duration of tracer tests (less than 12 h) during the rainy season. During the dry season, the discharge generally does not exhibit strong fluctuations, except after precipitation events; therefore, throughout the duration of the tracer tests (55 h), discharge can be assumed as constant.

In general, samples from the tracer tests were transported to Germany and analyzed in the laboratory using the spectrofluorometer LS55 from Perkin Elmer following standard procedures (Käss 2004). Samples from August 2014 were analyzed in Dong Van using the portable laboratory fluorometer (Trilogy, Turner Design). A field fluorometer GGUN-FL30 (Schnegg 2002) was installed in ML 3 on the 3rd of October 2015. All three fluorometers were calibrated using water from the ML 4 sampling point. The time intervals for sampling were smaller during the rainy season (1–10 min) than during the dry season (15–30 min) and were adjusted to 30 and 60 min after the main breakthrough. From the BTCs three different flow velocities can be obtained (Table 3-2). The mean flow velocity cannot be directly extracted from the BTC, but it is calculated by using an analytical model.

Table 3-2 Different flow velocities that can be yielded by tracer tests (Käss 2004).

Flow velocity	Time	Concentration
maximum flow velocity v_{\max}	first detection time t_1	detection limit
peak flow velocity v_p	time of peak concentration t_p	maximal concentration c_{\max}
mean flow velocity v_m	mean residence time t_m	NA

NA not applicable

3.2.3 Modelling of the results

The transport of conservative tracers can be described by the one-dimensional (1D) advection-dispersion equation (Bear 1979) as follows:

$$\frac{\partial C}{\partial t} = D \frac{\partial^2 C}{\partial x^2} - v_m \frac{\partial C}{\partial x} \quad (3.1)$$

with C = concentration, t = time, D = longitudinal dispersion coefficient, x = distance along flow direction, and v_m = mean flow velocity.

For the analytical modeling of the observed breakthrough curves (BTCs), the software CXTFIT (Toride et al. 1999) was used. Two 1D analytical models were applied: the conventional advection-dispersion model (ADM), and the two-region nonequilibrium model (2RNE). The simplification by using a 1D model can be justified, since flow through a karst conduit can be ascribed as a 1D process and thus advection is also 1D (Goepfert and Goldscheider 2008). Some BTCs from tracer tests in karst aquifers show a distinct tailing due to immobile fluid regions, which cannot be reproduced by the ADM. The 2RNE model was developed to describe the solute exchange between mobile and immobile fluid regions as first-order mass transfer process (Toride et al. 1993). For simplification, only the dimensionless form is given (modified after Field and Pinsky 2000 and Toride et al. 1993):

$$\beta \frac{\partial C_1}{\partial T} = \frac{1}{Pe} \frac{\partial^2 C_1}{\partial Z^2} - \frac{\partial C_1}{\partial Z} - \omega(C_1 - C_2) \quad (3.2)$$

$$(1 - \beta) \frac{\partial C_2}{\partial T} = \omega(C_1 - C_2) \quad (3.3)$$

Equations 3.2 and 3.3 include additional parameters with subscripts referring to mobile (1) or immobile (2) fluid regions. C represents the dimensionless solute concentration and T and Z dimensionless time and space variables, respectively. The Peclet number, Pe , is defined by the model parameters mean flow velocity (v_m) and dispersion coefficient (D):

$$Pe = \frac{x v_m}{D} = \frac{x}{\alpha} \quad (3.4)$$

where x is the flow distance and α the dispersivity. The dimensionless partitioning coefficient β ($0 \leq \beta \leq 1$) indicates the proportion of mobile water, while the mass transfer coefficient ω (>0) describes the exchange rate between the fluid regions. This model was successfully applied to the simulation of BTCs from tracer tests in karst systems (Barberá et al. 2017; Birk et al. 2005; Field and Pinsky 2000; Geyer et al. 2007; Goeppert and Goldscheider 2008; Lauber et al. 2014).

The fitting procedure is based on a nonlinear least square method (Tang et al. 2010; Toride et al. 1999; van Genuchten et al. 2012). The ADM considers two fitting parameters, advection (expressed as mean flow velocity v_m) and dispersion (expressed as longitudinal dispersion coefficient D), while the 2RNE includes additionally β and ω . For both models, ADM and 2RNE, tracer mass was included in the fitting procedure. All parameters were calculated with real flow distances, since the course of the cave stream is essentially known. The distance for the phreatic zones between the single cave sections and for the section ML 3–ML 4, where no cave plans are available, were assumed to be linear.

Two different input scenarios were used:

1. Pulse injection (Dirac input of tracer)
2. Multi pulses injection (MPI = multiple pulse input)

The Dirac input was used to investigate flow and transport parameters from the injection point, in this case at the stream sink (IP ML 1 in Suppl- Figure 1 of the SM), to the individual sampling point. In contrast, the MPI approach was applied to gain more information about specific cave segments between the sampling points. The input function is realized by a series of successive applications of constant solute pulses (Toride et al. 1995), which correspond to the BTCs observed inside the cave system. This enables an investigation of transport parameters between ML 2 and ML 3, for instance, without a real tracer injection in ML 2. The flow chart (Fig. 3–2) exhibits the straight forward procedure of the MPI approach by using the example of the section ML 3–ML 4.

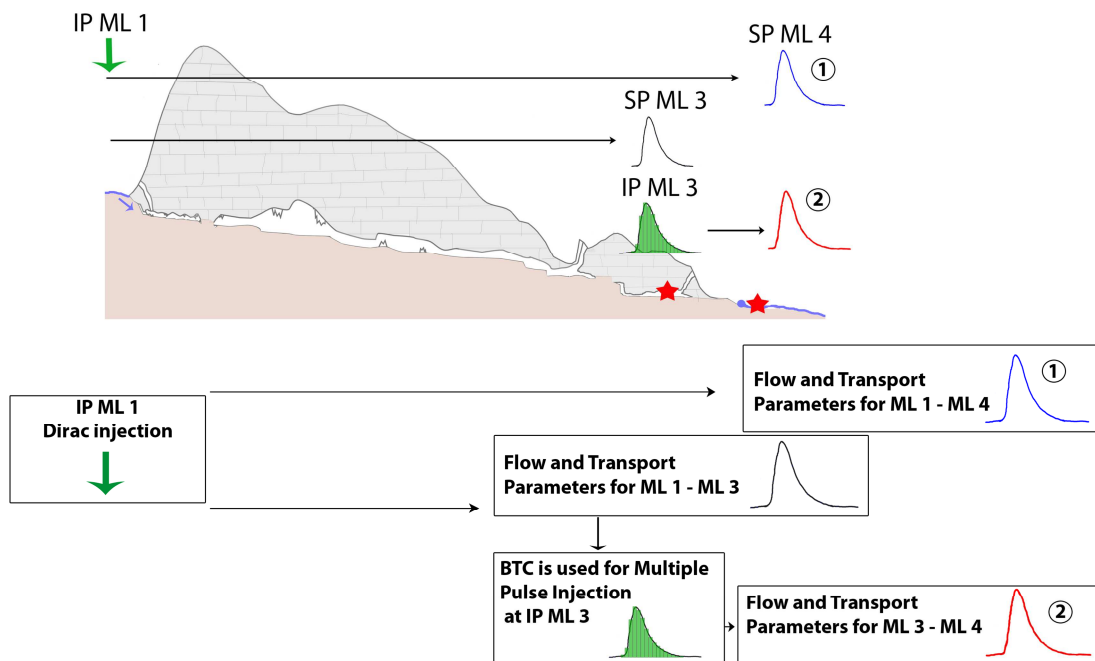


Fig. 3-2 Flow chart illustrating the procedure of the multiple pulse injection application, exemplified with the section ML 3–ML 4 and marked with the circled numbers 1 and 2. Cross section follows the course of the caves (Fig. 3–1b).

The starting time of the multiple pulse injection (t_0) corresponds to the first detection time of the BTC (t_1), which is used as the input function. While this pragmatic procedure delivers robust model parameters by using the ADM, it does not work for the 2RNE, which results in high uncertainties. Therefore, the MPI approach was modified by using the 2RNE modelled concentrations of the input functions. Although, there are some deviations within the modelled and observed input BTCs, this procedure delivers a good approximation of the transport parameters without such high uncertainties. With the 2RNE model, at least four different parameters were fitted at the same time, so the results are less robust than those from the ADM (Goepfert and Goldscheider 2008; Lauber et al. 2014; van Genuchten et al. 2012). Therefore, concerning the MPI approach, the figures focus on the results obtained by the ADM; however, the results from 2RNE are additionally shown in the tables and are discussed.

For the quality evaluation of the modelling results, the coefficient of determination (R^2), the root mean square error (RMSE) as well as a modified Nash-Sutcliffe efficiency ($E_{j=1}$) were computed for each BTC simulation. The calculation of $E_{j=1}$, based on Luhmann et al. (2012), delivers values between 1.0 (perfect fit) and $-\infty$.

3.3 RESULTS

3.3.1 Variability of flow parameters

In total, four BTCs were obtained for the main outlet of the cave system, ML 4, as shown in Fig. 3–3. During high flow conditions ($Q = 1,296 \text{ L/s}$), the first tracer detection took place within 1 h, resulting in a maximum flow velocity of $1,492 \text{ m/h}$. With the exception of the BTC on 3 October 2015, all BTC showed similar maximum tracer concentrations. The discharge ranged between 72 and $1,296 \text{ L/s}$, illustrating the high variability of this system.

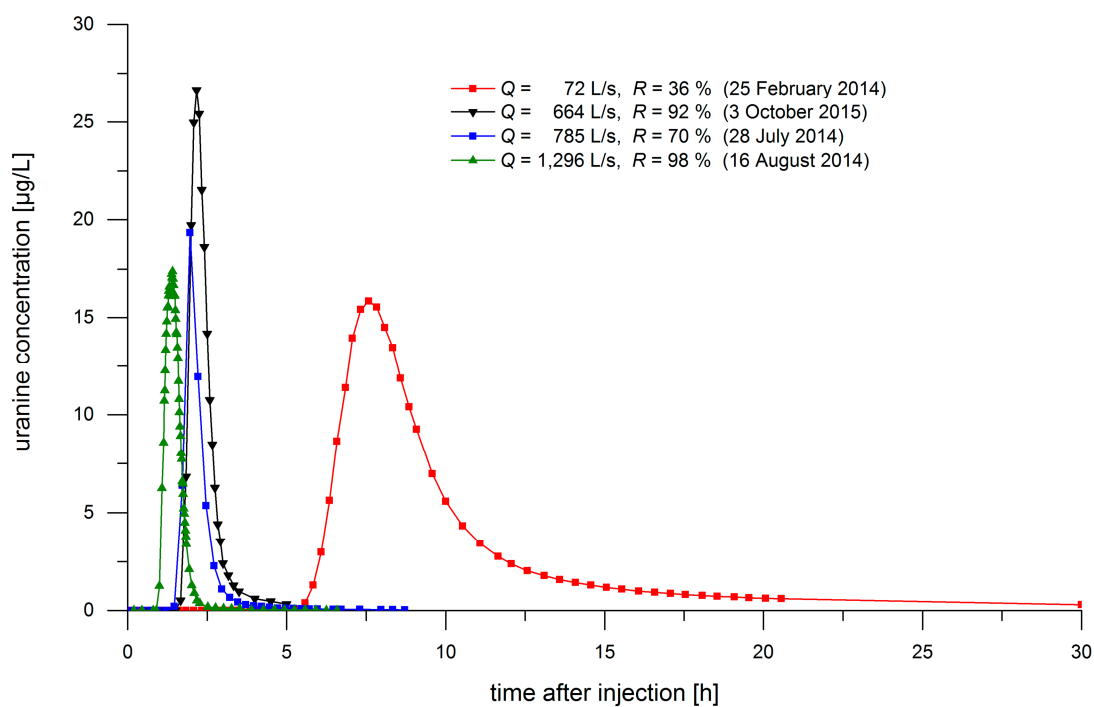


Fig. 3-3 Breakthrough curves observed at the spring ML 4 under different hydrologic conditions. Discharge (Q) and recovery rate (R) were determined for the spring ML 4

Consequently, flow and transport parameters are affected by the variation in discharge (Fig. 3–4). By applying an ADM, mean flow velocities for the complete cave section (ML 1–ML 4, distance $1,492 \text{ m}$) were between 183 m/h during the dry season (25 February 2014) and $1,043 \text{ m/h}$ during the rainy season (16 August 2014). With increasing discharge, an increasing recovery rate was observed between 36% ($Q = 72 \text{ L/s}$) and 98% ($Q = 1,296 \text{ L/s}$, Tables 3–3 and 3–4).

Dispersivity first decreased from 19 to 10 m with increasing discharge, but increased again to 21 m for higher discharge rates. The conditions of the tracer test on 28 July 2014

(785 L/s) and 3 October 2015 (664 L/s) were quite similar, leading to similar mean flow velocities (724 m/h and 663 m/h) and dispersivities (10 and 12 m). Yet, the maximum concentration on 3 October (26.65 $\mu\text{g/L}$) exceeded the one on 28 July (19.33 $\mu\text{g/L}$).

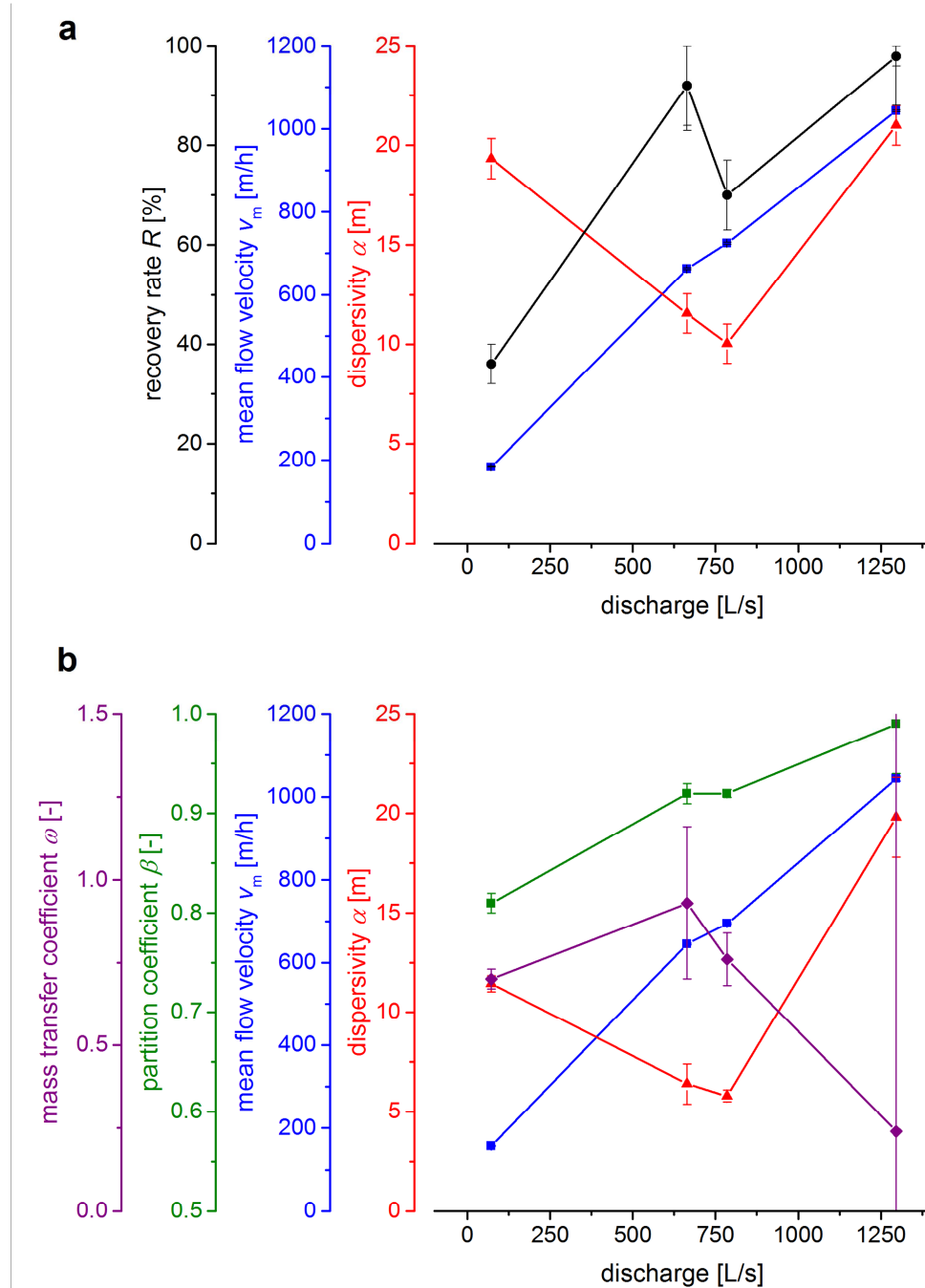


Fig. 3-4 Variation of flow and transport parameters for the complete cave system (ML 1–ML 4) dependent on the spring discharge (ML 4), modelled with **a** ADM and **b** 2RNE

The 2RNE delivered slightly lower values for mean flow velocities and dispersivities, but the behavior with increasing discharge is similar to the ADM. Additionally, the 2RNE revealed an increase of the partition coefficient β from 0.81 to 0.99 with increasing discharge. The mass transfer coefficient ω first increased and decreased again with increasing discharge, but exhibited high uncertainties.

The BTCs of ML 4 (Fig. 3-3) and the flow and transport parameters (Fig. 3-4) exhibit strong seasonal variability. To investigate the differences in flow and transport parameters in more detail, the BTCs of each sampling site within the cave system are shown in Fig. 3-5 for both dry and wet season.

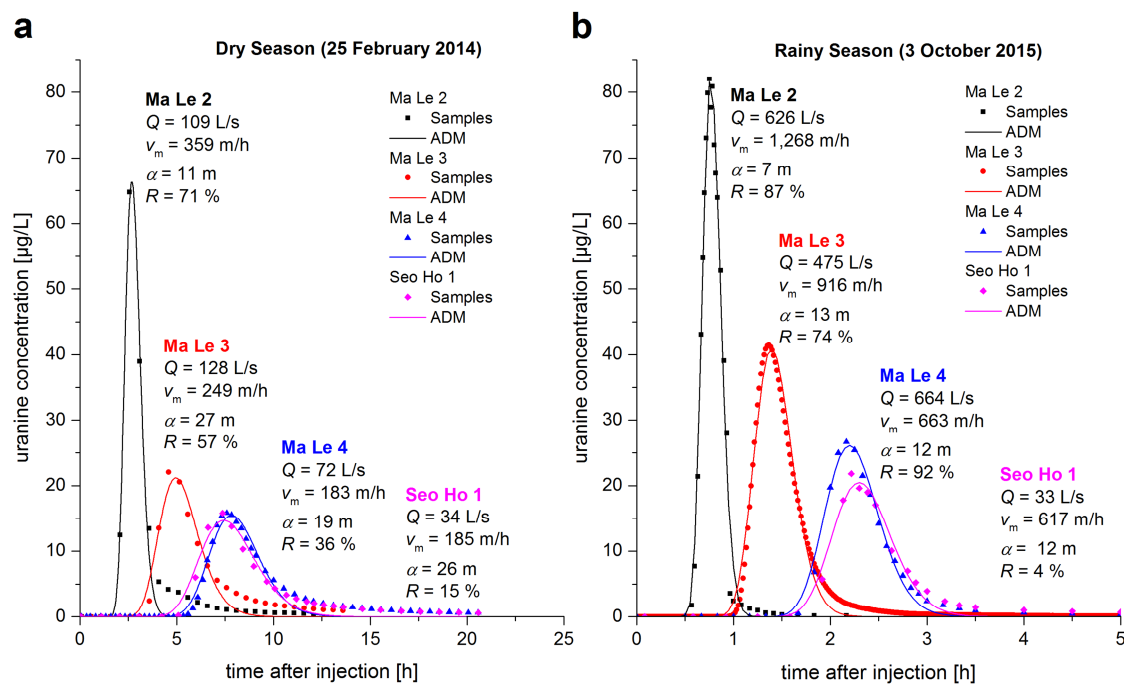


Fig. 3-5 Breakthrough curves, modelled with the advection-dispersion model, for each sampling site within the cave system for both **a** dry and **b** wet season (Q discharge, v_m mean flow velocity, α dispersivity, R recovery rate). The Dirac input function was applied. Note the different scales of the time axes

The BTCs for the second tracer test during rainy season (28 July 2014) are exhibited in Suppl. Figure 2 of the SM. Table 3–3 and 3–4 list all parameters for the ADM and 2RNE with the corresponding uncertainties.

Table 3-3 Flow and transport parameters for the sampling sites within the cave system and the karst springs by using a Dirac injection in ML 1, for tracer tests from February, July and August 2014.

	Term	Units	Dry Season (25 February 2014)				Rainy Season (28 July 2014)				Rainy Season (16 August 2014)
			50 g uranine in ML 1 ($Q = 120$ L/s)				50 g uranine in ML 1 ($Q = 463$ L/s)				50 g uranine in ML 1 (Q ND)
Injection			ML 1–ML 2	ML 1–ML 3	ML 1–ML 4	ML 1–SH 1	ML 1–ML 2	ML 1–ML 3	ML 1–ML 4	ML 1–SH 1	ML 1–ML 4
<i>Parameters</i>											
Distance	x	[m]	992	1,314	1,492	1,454	992	1,314	1,492	1,454	1,492
Discharge	Q	[L/s]	109 ± 11	128 ± 13	72 ± 7	34 ± 3	ND	ND	785 ± 79	37 ± 4	1,296 ± 130
Tracer recovery	R	[%]	71 ± 7	57 ± 6	36 ± 4	15 ± 2	ND	ND	70 ± 7	4 ± 1	98 ± 10
Maximum concentration	c_{max}	[µg/L]	64.75	22.08	15.83	15.79	67.06	30.56	19.33	12.4	17.39
Peak time	t_p	[h]	2.57	4.58	7.58	7.37	0.72	1.22	1.97	1.97	1.42
Peak velocity	v_p	[m/h]	386	287	197	197	1,378	1,077	757	738	1,066
<i>ADM approach</i>											
Mean flow velocity	v_m	[m/h]	359 ± 2	249 ± 3	183 ± 1	185 ± 2	1,350 ± 2	1,009 ± 4	724 ± 3	650 ± 4	1,043 ± 2
Dispersion	D	[m ² /h]	3,802 ± 292	6,653 ± 761	3,538 ± 227	4,848 ± 578	8,603 ± 272	12,240 ± 689	7,258 ± 502	12,280 ± 1,366	21,900 ± 454
Dispersivity	α	[m]	11 ± 1	27 ± 3	19 ± 1	26 ± 3	6.4 ± 0.2	12 ± 1	10 ± 1	19 ± 2	21 ± 1
Root mean square error	RMSE	[-]	2.16	1.62	0.92	1.22	0.95	1.12	0.61	0.41	0.47
Coeff. of determination	R^2	[-]	0.980	0.939	0.964	0.939	0.997	0.983	0.981	0.990	0.995
Nash-Sutcliffe efficiency	$E_{j=1}$	[-]	0.82	0.71	0.82	0.72	0.96	0.88	0.86	0.90	0.95
<i>2RNE approach</i>											
Mean flow velocity	v_m	[m/h]	297 ± 5	211 ± 3	157 ± 1	160 ± 3	1,332 ± 1	971 ± 4	695 ± 2	607 ± 3	1,044 ± 6
Dispersion	D	[m ² /h]	2,643 ± 98	2,825 ± 147	1,795 ± 56	2,102 ± 117	5,893 ± 236	6,499 ± 434	4,024 ± 184	5,303 ± 1,277	20,680 ± 1,727
Dispersivity	α	[m]	9 ± 1	14 ± 1	11.4 ± 0.4	13 ± 1	4.4 ± 0.2	6.7 ± 0.5	5.8 ± 0.3	9 ± 2	20 ± 2
Partition coeff.	β	[-]	0.82 ± 0.01	0.78 ± 0.01	0.81 ± 0.01	0.81 ± 0.01	0.950 ± 0.004	0.91 ± 0.01	0.916 ± 0.004	0.909 ± 0.005	0.99 ± 0.05
Mass transfer coeff.	ω	[-]	0.34 ± 0.01	0.71 ± 0.04	0.70 ± 0.03	0.64 ± 0.04	0.72 ± 0.11	0.81 ± 0.11	0.76 ± 0.08	0.43 ± 0.04	0.24 ± 2.50
Mean flow velocity (mobile prop.)	v_m/β	[m/h]	362	271	194	198	1,402	1,067	755	667	1,055
Root Mean Square Error	RMSE	[-]	0.44	0.37	0.23	0.28	0.10	0.36	0.11	0.06	0.40
Coeff. of determination	R^2	[-]	0.999	0.997	0.998	0.997	1.000	0.998	0.999	1.000	0.996
Nash-Sutcliffe efficiency	$E_{j=1}$	[-]	0.97	0.94	0.96	0.94	0.99	0.96	0.97	0.98	0.95

Mean flow velocities and dispersion were obtained with the ADM and the 2RNE approach, while the partition coefficient and mass transfer coefficient were additionally yielded with the 2RNE approach. Dispersivity was calculated ($\alpha = D/v_m$). The standard deviation (\pm STD) for the fitted parameters were given by CXTFIT, while the uncertainty of discharge measurements was assumed to be maximal ± 10 %, based on Richardson et al. (2017). Table 3–4 provides further data on the parameters yielded by the tracer tests from September and October 2015. *ND* not determined; *prop.* proportion; *coeff.* coefficient

Table 3-4 Flow and transport parameters for the sampling sites within the cave system and the karst springs by using a Dirac injection in ML 1, for tracer tests from September and October 2015

Injection Sections	Term	Units	Rainy Season (26 September 2015)		Rainy Season (29 September 2015)			Rainy Season (3 October 2015)			
			5 g uranine in ML 3 ($Q = 849$ L/s)		10 g uranine in ML 2 ($Q = 905$ L/s)		50 g uranine in ML 1 ($Q = 564$ L/s)				
			ML 3–ML 4	ML 3–SH 1	ML 2–ML 3	ML 2–ML 4	ML 2–SH 1	ML 1–ML 2	ML 1–ML 3	ML 1–ML 4	ML 1–SH 1
<i>Parameters</i>											
Distance	x	[m]	178	140	322	500	462	992	1,314	1,492	1,454
Discharge	Q	[L/s]	856 ± 86	34 ± 3	902 ± 90	690 ± 69	33 ± 3	626 ± 63	475 ± 48	664 ± 66	33 ± 3
Tracer recovery	R	[%]	85 ± 9	5 ± 1	105 ± 11	82 ± 8	4 ± 1	87 ± 9	74 ± 7	92 ± 9	4 ± 1
Maximum concentration	c_{\max}	[$\mu\text{g/L}$]	5.27	5.39	10.28	5.82	4.16	82.04	41.46	26.65	21.81
Peak time	t_p	[h]	0.60	0.72	0.50	1.15	1.33	0.75	1.37	2.17	2.22
Peak velocity	v_p	[m/h]	297	194	644	435	347	1,323	959	688	655
<i>ADM approach</i>											
Mean flow velocity	v_m	[m/h]	285 ± 2	181 ± 1	598 ± 5	408 ± 2	309 ± 2	$1,268 \pm 4$	916 ± 1	663 ± 2	617 ± 4
Dispersion	D	[m^2/h]	645 ± 38	400 ± 28	$5,106 \pm 335$	$2,427 \pm 172$	$2,515 \pm 150$	$9,404 \pm 451$	$11,700 \pm 204$	$7,656 \pm 486$	$7,552 \pm 755$
Dispersionity	α	[m]	2.3 ± 0.2	2.2 ± 0.2	9 ± 1	6.0 ± 0.5	8 ± 1	7.4 ± 0.4	12.8 ± 0.2	12 ± 1	12 ± 1
Root mean square error	RMSE	[-]	0.23	0.27	0.52	0.32	0.16	3.31	1.13	1.19	1.29
Coeff. of determination	R^2	[-]	0.984	0.978	0.984	0.982	0.991	0.991	0.987	0.986	0.976
Nash-Sutcliffe efficiency	$E_{j=1}$	[-]	0.90	0.86	0.88	0.90	0.92	0.92	0.89	0.88	0.85
<i>2RNE approach</i>											
Mean flow velocity	v_m	[m/h]	269 ± 6	175 ± 2	571 ± 4	364 ± 22	284 ± 12	$1,236 \pm 3$	889 ± 1	645 ± 2	584 ± 10
Dispersion	D	[m^2/h]	434 ± 44	166 ± 49	$1,531 \pm 304$	$1,718 \pm 209$	$1,899 \pm 140$	$3,859 \pm$	$5,179 \pm 160$	$4,115 \pm 453$	$4,104 \pm 525$
Dispersionity	α	[m]	1.6 ± 0.2	1.0 ± 0.3	3 ± 1	5 ± 1	7 ± 1	3 ± 1	8.8 ± 0.2	6 ± 1	7 ± 1
Partition coeff.	β	[-]	0.91 ± 0.02	0.86 ± 0.03	0.77 ± 0.02	0.87 ± 0.05	0.90 ± 0.03	0.86 ± 0.05	0.889 ± 0.002	0.92 ± 0.01	0.91 ± 0.01
Mass transfer coeff.	ω	[-]	0.47 ± 0.15	1.38 ± 0.63	2.12 ± 0.35	0.39 ± 0.10	0.28 ± 0.06	2.92 ± 1.43	1.36 ± 0.07	0.93 ± 0.23	0.62 ± 0.17
Mean flow velocity (mobile prop.)	v_m/β	[m/h]	296	203	742	418	316	1,437	999	701	642
Root Mean Square Error	RMSE	[-]	0.16	0.17	0.19	0.24	0.10	1.42	0.32	0.41	0.66
Coeff. of determination	R^2	[-]	0.993	0.992	0.998	0.991	0.997	0.998	0.999	0.998	0.995
Nash-Sutcliffe efficiency	$E_{j=1}$	[-]	0.94	0.91	0.96	0.93	0.96	0.97	0.96	0.96	0.94

Mean flow velocities and dispersion were obtained with the ADM and the 2RNE approach, while the partition coefficient and mass transfer coefficient were additionally yielded with the 2RNE approach. Dispersionity was calculated ($\alpha = D/v_m$). The standard deviation (\pm STD) for the fitted parameters were given by CXTFIT, while the uncertainty of discharge measurements was assumed to be maximal ± 10 %, based on Richardson et al. (2017). *ND* not determined; *prop.* proportion; *coeff.* coefficient

The following results can be summarized:

- During the rainy season, the discharge at the springs (ML 4 + SH 1) increased by 78 and 24% compared to the discharge of the sinking stream at ML 1 for July 2014 and October 2015, respectively (Tables 3–3 and 3–4). Thus, there might be an inflow within the cave system, whose contribution decreases or is even absent during the dry season, while in contrast, the springs in February 2014 exhibited a slightly smaller discharge ($Q = 106$ L/s) than the sinking stream ($Q = 120$ L/s). Although, the difference was within the uncertainty range of discharge measurement, there could be water and tracer losses along the flow path.
- The tracer recovery rate at the outlet, the karst springs ML 4 and SH 1, was higher in the rainy season (74–98%) compared to the dry season (51%). Parallel flow paths might be partly active, since recovery rate was found to be higher at the springs than in ML 2 and ML 3. These parallel flow paths might not be active during the dry season, where the recovery rate decreased with increasing flow distance.
- A tracer injection in ML 2 resulted in a complete tracer recovery at ML 3; however, slightly lower recovery rates were found at the springs (86%).
- Depending on hydrological conditions, there have to be water gains and losses along the flow path.
- Mean flow velocities were positively correlated with discharge and were found to be increased by a factor of approximately 4 during the rainy season compared to dry season.
- Dispersivity first decreased and then increased again with increasing discharge. During the dry season, dispersivity is smallest in the ML 1–ML 2 section and highest in the sections ML 1–ML 3 and ML 1–SH 1. During the rainy season, section ML 1–SH 1 exhibited the highest dispersivity, followed by the section ML 1–ML 3.
- The BTCs of the dry season showed a stronger tailing that could not be reproduced by the ADM, but rather with the 2RNE. The partition coefficient increased with increasing discharge, indicating that immobile fluid regions decreased from 19 to 1%, while during the dry season, the smallest β was found for section ML 1–ML 3, an increase of β with increasing flow path could be observed during rainy season. The mass transfer coefficient was fraught with high uncertainties. With increasing discharge, ω first increased and decreased again. During the dry season, ω was the smallest in the ML 1–ML 2 section, while during the rainy season, the smallest ω was found for ML 1–SH 1.

3.3.2 Spatial resolution by using the multiple pulse injection approach

In order to better understand the transport parameters of the individual cave sections, an MPI approach was applied by using one BTC as an input function for the subsequent downstream cave section. Fig. 3-2 illustrates the procedure of the approach used to obtain the modelled BTCs shown in Fig. 3-6.

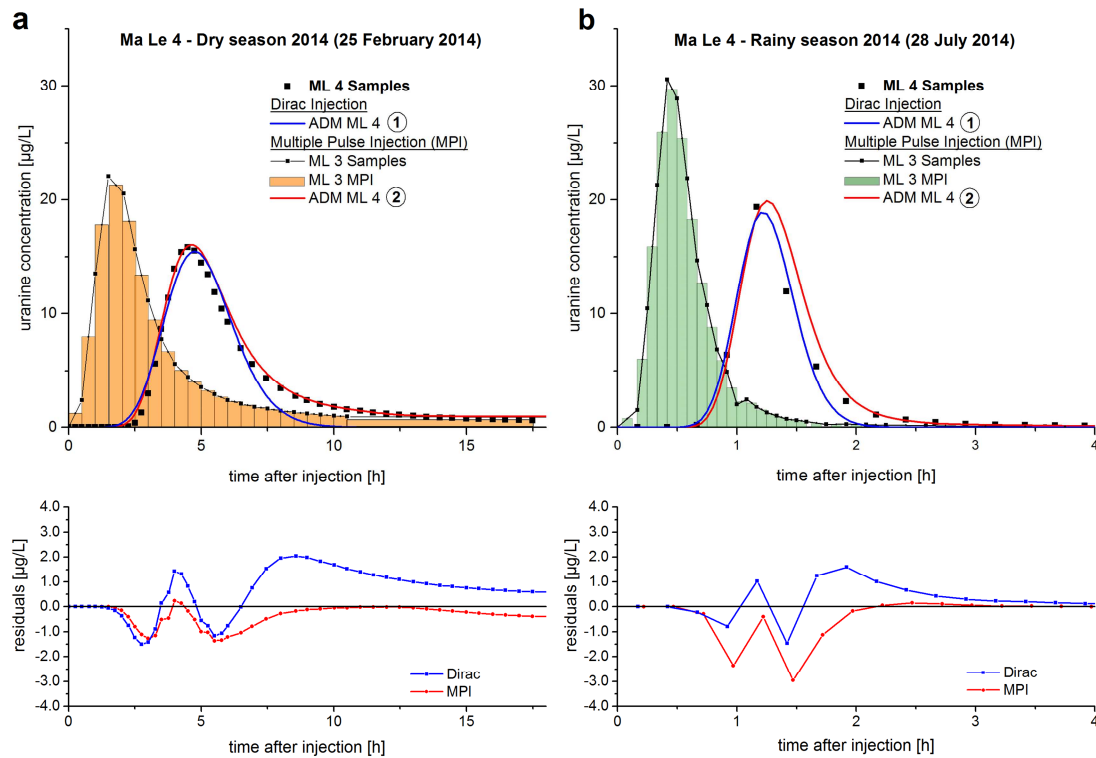


Fig. 3-6 For ML 3, a multiple pulse injection (MPI) was applied to model the BTC in ML 4 (number 2), for **a** dry season 2014, and **b** rainy season 2014. For comparison, the ADM, modelled with a Dirac injection in ML 1, is also shown (number 1; note, numbers 1 and 2 refer to Fig. 3-2). In the descending branch, the MPI approach resulted in a better fitting of the tailing that is indicated by smaller residuals

Especially for the dry season, where the tailing was much more pronounced, the ADM was able to display the complete BTC when an MPI approach was applied (Fig. 3-6); however, concentrations were slightly overestimated, which became more obvious when examining the residuals. This resulted in an R^2 of 0.985 for the ML 4 ADM (Fig. 3-6a, number 2), which was better than using the Dirac injection approach with an injection in ML1 ($R^2 = 0.964$, Fig. 3-6a, number 1). The decreasing limb of the BTC was fitted by an ADM, which indicates that the tailing did not originate in the section ML 3–ML 4, but rather in ML 2–ML 3 and was, therefore, already considered within the input function. This effect was smaller for the rainy season, where the tailing was not as pronounced (MPI: $R^2 = 0.968$

(Fig. 3–6b, number 2) Dirac: $R^2 = 0.981$ (Fig. 3–6b, number 1)). Flow and transport parameters for all cave sections and all tracer tests are given in Tables 3–5 and 3–6.

The tailing can be fitted better with the 2RNE, resulting in significant higher R^2 , $E_{j=1}$, and smaller RMSE. Although, dispersivity is smaller by using the 2RNE than by applying the ADM, the highest dispersivities were found for the section ML 2–ML 3. For low discharge rates, the section ML 2–ML 3 exhibited the smallest β (0.31), but for higher discharge rates this section had the highest values compared to the subsequent sections. While the mass transfer coefficient ω was higher during the wet season than during the dry season, the section ML 2–ML 3 exhibited always the highest ω .

Table 3-5 Flow and transport parameters for the tracer tests in February and July 2014 for the individual cave sections by using the multiple pulse injection approach and the ADM as well as the 2RNE

Term	Units	Dry Season (25 February 2014)				Rainy Season (28 July 2014)			
		DIRAC		MPI		DIRAC		MPI	
		ML 1–ML 2	ML 2–ML 3	ML 3–ML 4	ML 3–SH 1	ML 1–ML 2	ML 2–ML 3	ML 3–ML 4	ML 3–SH 1
Parameters									
x	[m]	992	322	178	140	992	322	178	140
Q	[L/s]	109 ± 11	128 ± 13	72 ± 7	34 ± 3	ND	ND	785 ± 79	37 ± 4
R	[%]	71 ± 7	57 ± 6	36 ± 4	15 ± 2	ND	ND	70 ± 7	4 ± 1
c_{\max}	[µg/L]	64.75	22.08	15.83	15.79	67.06	30.59	19.33	12.40
t_p	[h]	2.57	2.50	4.50	4.29	0.72	0.58	1.17	1.17
v_p	[m/h]	386	129	40	33	1,378	555	152	120
ADM (observed input function)									
v_m	[m/h]	359 ± 2	132 ± 9	76 ± 1	74 ± 2	1,350 ± 2	621 ± 5	246 ± 4	154 ± 2
D	[m ² /h]	3,802 ± 292	10,570 ± 1,567	690 ± 64	806 ± 110	8,603 ± 272	9,756 ± 491	1,388 ± 195	1,588 ± 144
α	[m]	11 ± 1	80 ± 16	9 ± 1	11 ± 2	6.4 ± 0.2	16 ± 1	6 ± 1	10 ± 1
RMSE	[-]	2.16	2.12	0.64	0.58	0.95	0.87	0.80	0.30
R^2	[-]	0.980	0.900	0.985	0.986	0.997	0.989	0.968	0.995
$E_{j=1}$	[-]	0.82	0.72	0.89	0.90	0.96	0.89	0.84	0.91
2RNE (with 2RNE modelled input function)									
v_m	[m/h]	297 ± 5	48 ± 4	44 ± 3	35 ± 4	1,332 ± 1	569 ± 5	152 ± 11	129 ± 2
D	[m ² /h]	2,643 ± 98	1,133 ± 107	212 ± 22	194 ± 32	5,893 ± 236	4,534 ± 431	442 ± 57	678 ± 81
α	[m]	9 ± 1	24 ± 4	5 ± 1	5 ± 1	4.4 ± 0.2	8 ± 1	3 ± 1	5 ± 1
β	[-]	0.82 ± 0.01	0.31 ± 0.02	0.61 ± 0.04	0.53 ± 0.06	0.950 ± 0.004	0.82 ± 0.01	0.58 ± 0.04	0.79 ± 0.01
ω	[-]	0.34 ± 0.01	0.38 ± 0.02	0.14 ± 0.01	0.13 ± 0.01	0.72 ± 0.11	0.52 ± 0.08	0.21 ± 0.01	0.20 ± 0.02
v_m/β	[m/h]	362	155	72	66	1,402	694	262	163
RMSE	[-]	0.44	0.36	0.20	0.22	0.10	0.35	0.21	0.07
R^2	[-]	0.999	0.997	0.998	0.998	1.000	0.998	0.998	1.000
$E_{j=1}$	[-]	0.97	0.95	0.96	0.95	0.99	0.97	0.94	0.98

The symbols are explained in Table 3–3 and Table 3–4. ND not determined

Table 3-6 Flow and transport parameters for the tracer tests in September and October 2015 for the individual cave sections by using the multiple pulse injection approach and the ADM as well as the 2RNE

Term	Units	Rainy Season (29 September 2015)			Rainy Season (3 October 2015)			
		DIRAC	MPI		DIRAC	MPI		
		ML 2–ML 3	ML 3–ML 4	ML 3–SH 1	ML 1–ML 2	ML 2–ML 3	ML 3–ML 4	ML 3–SH 1
Parameters								
x	[m]	322	178	140	992	322	178	140
Q	[L/s]	902 ± 90	690 ± 69	33 ± 3	626 ± 63	475 ± 48	664 ± 66	33 ± 3
R	[%]	105 ± 11	82 ± 8	4 ± 1	87 ± 9	74 ± 7	92 ± 9	4 ± 1
c_{max}	[µg/L]	10.28	5.82	4.26	82.04	41.46	26.65	21.82
t_p	[h]	0.5	0.85	1.03	0.75	0.83	1.27	1.32
v_p	[m/h]	644	209	136	1,323	388	140	106
ADM (observed input function)								
v_m	[m/h]	598 ± 5	279 ± 6	154 ± 3	1,268 ± 4	525 ± 1	225 ± 6	150 ± 9
D	[m ² /h]	5,106 ± 335	1,983 ± 260	1,079 ± 117	9,404 ± 451	7,456 ± 43	1,500 ± 291	1,852 ± 479
α	[m]	9 ± 1	7 ± 1	7 ± 1	7.4 ± 0.4	14.2 ± 0.1	7 ± 1	12 ± 4
RMSE	[-]	0.52	0.57	0.33	3.31	0.34	2.55	3.40
R^2	[-]	0.984	0.939	0.962	0.991	0.995	0.931	0.825
$E_{j=1}$	[-]	0.88	0.84	0.85	0.92	0.93	0.75	0.65
2RNE (with 2RNE modelled input function)								
v_m	[m/h]	571 ± 4	236 ± 13	142 ± 3	1,236 ± 3	561.4 ± 0.5	152 ± 7	70 ± 7
D	[m ² /h]	1,531 ± 304	631 ± 133	573 ± 55	3,859 ± 1,740	2,932 ± 96	462 ± 41	161 ± 34
α	[m]	3 ± 1	3 ± 1	4.0 ± 0.5	3 ± 1	5.2 ± 0.2	3.0 ± 0.4	2 ± 1
β	[-]	0.77 ± 0.02	0.81 ± 0.04	0.87 ± 0.02	0.86 ± 0.05	0.772 ± 0.004	0.68 ± 0.03	0.44 ± 0.04
ω	[-]	2.12 ± 0.35	0.26 ± 0.08	0.23 ± 0.07	2.92 ± 1.43	1.03 ± 0.03	0.20 ± 0.01	0.42 ± 0.03
v_m/β	[m/h]	742	291	163	1,437	729	224	159
RMSE	[-]	0.19	0.26	0.09	1.42	0.15	0.34	0.61
R^2	[-]	0.998	0.989	0.998	0.998	0.999	0.999	0.995
$E_{j=1}$	[-]	0.96	0.92	0.96	0.97	0.96	0.97	0.94

The symbols are explained in Table 3–3 and Table 3–4. *ND* not determined

The flow and transport parameters obtained by using the ADM are illustrated in Fig. 3–7.

With increasing distance from the sinking stream, the mean flow velocity decreased due to a decreasing gradient in flow direction and, presumably, an increasing flow cross-sectional area. Dispersivity is highest in section ML 2–ML 3, whereas section ML 3–SH 1 displays similar values during the wet season. Regarding the segments of the cave system, dispersivity generally decreased with increasing discharge, except for segment ML 2–ML 3. Similar to the results from the complete system (ML 1–ML 4, Fig. 3–4), dispersivity first decreased with increasing discharge and then increased again at higher discharge rates.

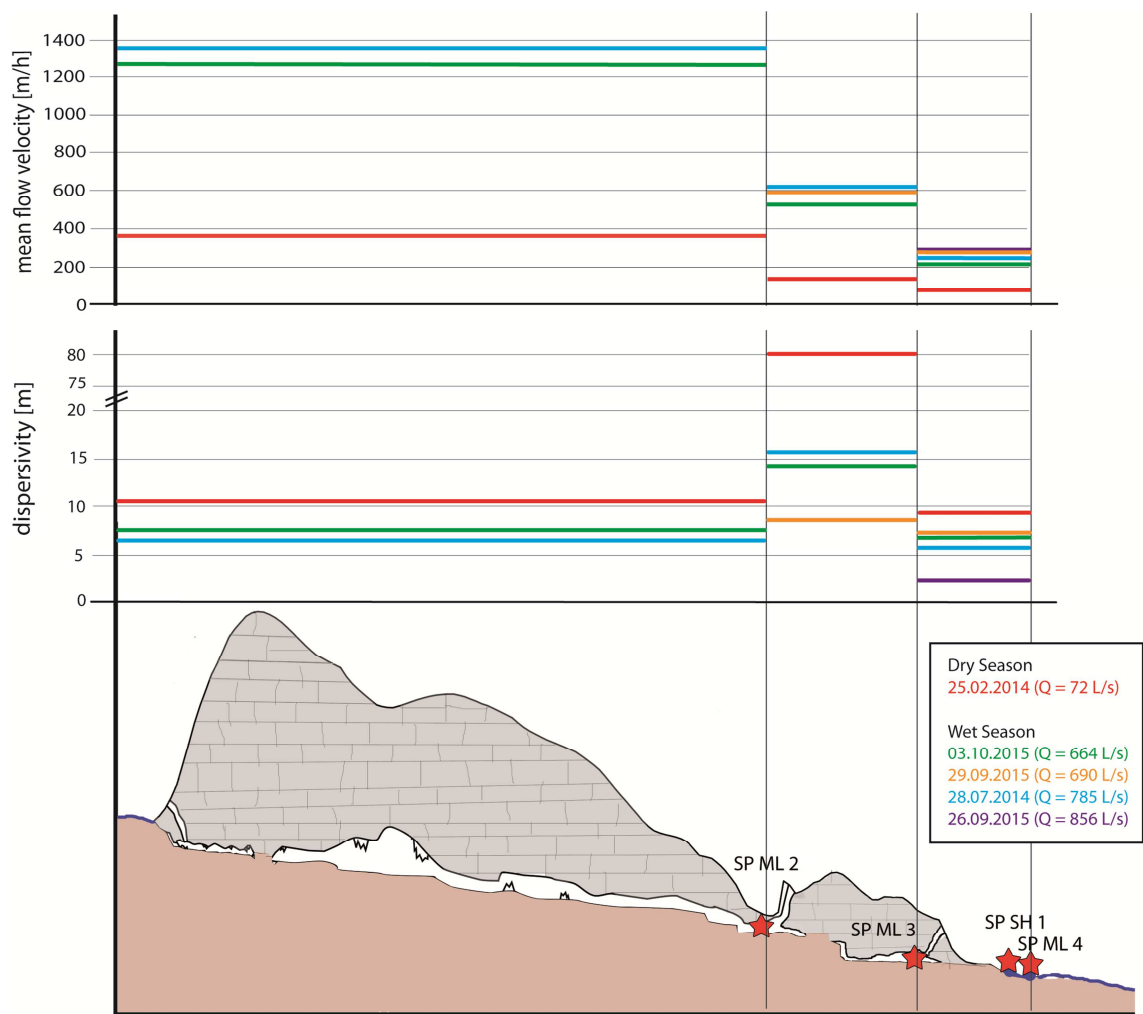


Fig. 3-7 Spatial resolution of flow and transport parameters within the cave system. Mean flow velocity (v_m) and dispersivity (α) are calculated with an ADM and a Dirac input for the first segment and a MPI input function for all subsequent segments. The parallel flow path ML 3–SH 1 is not considered in this figure, but exhibits lower mean flow velocities and higher dispersivity than ML 3–ML 4 (Table 3–5 and Table 3–6). Cross section follows the course of the caves (Fig. 3-1b).

3.4 DISCUSSION

3.4.1 Variability of flow parameters

The spatial distribution of sampling points allowed for the investigation of the internal structure of the cave system. The findings of the tracer tests and the discharge

measurements indicated that the Ma Le cave system is a highly dynamic system, with additional in- and outflows and partly active bypaths.

The total recovery rate at both springs decreased with decreasing discharge, whereby the spring SH 1 is characterized by a very constant discharge independent of flow conditions. However, recovery rates increased from 4% during the rainy season to 15% during the dry season, since the relative contribution of SH 1 to the total discharge of both springs increased with decreasing total runoff; therefore, it is highly probable that SH 1 is fed by a conduit of limited dimensions that diverts from the main flow path somewhere between ML 3 and ML 4. An explanation for lower recovery rates at the springs during the dry season might be another unknown (ground) spring, located in the riverbed of the Seo Ho. If the discharge capacity of the spring is limited, the relevance of this spring would increase with decreasing total discharge of the system; furthermore, the lower recovery rates during low flow conditions could be explained by retention of tracer in pools, siphons and immobile fluid regions. Part of the solute tracer was restituted from immobile to mobile fluid regions, causing a pronounced tailing (Dewaide et al. 2016).

Recovery rates, along with flow and transport parameters, exhibited a dependence on discharge, as shown in Fig. 3–4. Dispersivity first decreased with increasing discharge, but increased again for higher discharge rates. At small discharge rates, the cave streambed is not completely filled, so the higher dispersivity may be explained by redirections within the cave streambed and a higher relative influence of friction forces (Massei et al. 2006). With increasing discharge rates, the effect becomes less important and the water is canalized within the conduit, leading to a smaller dispersivity. The high dispersivity at very high discharge rates could be caused by a higher water pressure to pores and fractures, a stronger interaction with conduit walls, as well as by activation of higher elevated flow paths.

The mean flow velocities appear to be smaller by using the 2RNE than by using the ADM. Since the ADM is not able to describe the tailing of the BTC, only the fast flow components are considered. In contrast, the 2RNE accounts for both the fast and slow flow components. The mean flow velocity of the mobile fluid region, obtained by dividing the mean flow velocity by β , was even slightly higher than yielded by the ADM (Tables 3–3, 3–4, 3–5 and 3–6). The higher dispersivity values of the ADM might be caused by immobile fluid regions that are not considered by the ADM, but that were compensated by higher dispersivity values. The difference between the dispersivity obtained by the ADM and 2RNE decreased with increasing β and discharge. This led to the assumption that the contribution of immobile fluid regions decreased with increasing discharge as already assumed by Barberá et al. (2017); although unfortunately, ω contained high uncertainties.

3.4.2 *Multiple-pulse-injection approach*

The MPI approach is suggested to be a valuable tool to obtain more information about the spatial variation of transport parameters within cave systems. It clearly revealed that the highest dispersivities were found in the sections ML 2–ML 3 and ML 3–SH 1, most likely controlled by the cave structure. Particularly, macrodispersivity is formation-specific and not only scale dependent, as shown by Zech et al. (2015). During the dry season, the high dispersivity in the section ML 2–ML 3 yielded by the ADM could be partly explained by pools and siphons and a larger phreatic passage, thus by a higher content of immobile fluid regions. The 2RNE supported this assumption, since the fraction of mobile water only amounted to 31%; however, during the rainy season the proportion of immobile fluid regions was smallest in this section (highest β), while dispersivity was still the highest. So, the high dispersivity values of the ADM are not only caused by the compensation of immobile fluid regions, but might be caused by slower flow components due to friction forces (Massei et al. 2006). At the same time, ω indicated a higher exchange rate between mobile and immobile fluid regions in the section ML 2–ML 3, meaning more of the initial tracer mass in the mobile fluid region had time to equilibrate with tracer mass in the immobile fluid region (Field and Pinsky 2000). This led to the assumption that sections with small proportions of immobile fluid zones but high dispersivity show higher exchange rate between mobile and immobile fluid regions. With increasing discharge and flow velocities, the contribution of immobile fluid regions was generally reduced in the cave sections, leading to lower dispersivity values when using an ADM and higher β values with the 2RNE. The high dispersivity in the section ML 3–SH 1 can be explained by the smaller dimensions of this section and by the interaction with the conduit walls. This interaction likely enhances the inhomogeneity of the velocity profile and leads to smaller mean flow velocities and a higher dispersion, as described in Hauns et al. (2001).

In general, the MPI approach revealed a progressive decrease of mean flow velocities along the flow path. This observation was already shown by Worthington (2009) and is also described in Lauber et al. (2014). It is caused by a decreasing gradient, which is most likely associated with an increase in the extent of phreatic zones. Within the phreatic zones, the area of flow cross-section is increased, leading to a further reduction of flow velocities.

The comparison of flow and transport parameters obtained by a Dirac and an MPI injection, as a function of discharge, supported the suitability of the approach, since the Dirac injection produced no outliers compared to the MPI values (Suppl. Figure 3 of the SM). However, the comparison revealed that dispersivity obtained from the Dirac injection appears low compared to the values yielded by the MPI approach. This could be explained by the identified bypaths from ML 1 and ML 2 to the springs that are partly active. The MPI

approach assumes a tracer injection in ML 3, but if bypaths from ML 1 are active, an additional tracer input takes place from the real tracer injection in ML 1. Such a confluence of tributaries might increase dispersion (Hauns et al. 2001) and can lead to an apparent enhanced dispersivity for the section ML 3–ML 4 by using the MPI approach. In such a case, the yielded parameters consider the studied section, as well as the bypath, and consequently differ from a Dirac injection.

To obtain clear evidence of the applicability of the MPI approach, a combined tracer test should be performed with a Dirac injection in ML 1 for the MPI approach in ML 2 and ML 3, and simultaneous Dirac injections in ML 2 and ML 3 with different tracers. However, tracers with equal transport behavior should be used, which is challenging.

3.5 CONCLUSIONS

Six tracer tests were performed in a cave system in Northern Vietnam to characterize flow and transport parameters under highly variable flow conditions that are influenced by extended dry and wet seasons. A multiple-pulse-injection approach enabled a spatial resolution of flow and transport parameters and led to a better understanding of the active karst system that can be concluded as followed:

- Flow and transport parameters are subject to strong variability depending on hydrological conditions. The mean flow velocity for the whole cave system (ML 1–ML 4) increased from 183 to 1,043 m/h with increasing discharge (72–1,296 L/s), whereby recovery rate increased from 36% to 98%. Dispersivity first decreased from 19 m to 10 m and increased again to 21 m with increasing discharge.
- With increasing discharge the impact of immobile fluid regions, expressed by the partition coefficient β , on flow and transport parameters decreased.
- The cave system consists not only of a sinking stream that enters the cave system and reemerges at the springs. Instead, the system is composed of further contributions, which vary in quantity depending on the hydrological conditions.
- There is not only one cave stream, but also smaller parallel flow paths. Such a bypath likely runs from ML 1 and ML 2 to the springs, whereby other flow paths could be activated depending on discharge rates.
- There is no indication that bypaths constrain the application of the MPI approach. However, it has to be considered that yielded transport parameters are influenced by potential bypaths.

- By using the multiple pulse input approach, a spatial resolution could be achieved not only for flow velocities, but also for transport parameters.
- While the combination of the MPI approach and the ADM delivered reliable parameters, an adjustment was necessary to combine the MPI with the 2RNE. For the injection function the concentrations, modeled with the 2RNE were used instead of the observed concentrations.
- It could be clearly shown that the sections ML 2–ML 3 and ML 3–SH 1 are characterized by the highest dispersivity, which leads to the generation of hypotheses concerning the structure of the system.

In the section ML 2–ML 3, the high dispersivity resulted from the ADM, can partly be explained by a higher proportion of immobile fluid regions due to pools, siphons and a larger extent of phreatic zones, as shown by a smaller β . The high dispersivity for ML 3–SH 1 might be caused by the smaller conduit dimension and the enhanced interaction with the conduit wall.

Generally, in-cave tracer tests were validated again as a powerful tool to investigate karst aquifers. The MPI approach enables a more detailed insight into the spatial resolution of transport parameters within the conduit system. This study revealed that karstic systems are highly dynamic and cannot be considered as static systems. Such high variabilities in flow and transport parameters impose a particularly big challenge for the usage of karst water resources in terms of technical requirements, but also in terms of water quality.

ACKNOWLEDGEMENT

We gratefully acknowledge the financial support of the German Federal Ministry of Education and Research (BMBF) [grant number 02WCL1291A]. We want to thank Ha Giang Peoples Committee, Dong Van Peoples Committee as well as the Vietnam Institute of Geosciences and Mineral Resources (Hanoi) for their support during fieldwork. Special thanks are given to the whole sampling team, especially to Arno Hartmann, Marian Bechtel, Philipp Holz, Alexandra Roth, Christian Weippert and Tobias Zaege and to the colleagues from VIGMR. Furthermore, we thank the cavers from the Belgian SPEKUL club, particularly David Lagrou, for their support during the tracer tests and the provision of cave maps and Nguyet Vu Thi Minh, for borrowing the field fluorimeter. We thank Arica Beisaw for proofreading and the associate editor, Prof. Luhmann, as well as the three anonymous reviewers for their valuable comments.

CHAPTER 4

4 EVALUATION OF β -D-GLUCURONIDASE AND PARTICLE-SIZE DISTRIBUTION FOR MICROBIOLOGICAL WATER QUALITY MONITORING IN NORTHERN VIETNAM

Reproduced from: Ender A, Goeppert N, Grimmeisen F, Goldscheider N (2017) Evaluation of β -D-glucuronidase and particle-size distribution for microbiological water quality monitoring in Northern Vietnam. Science of The Total Environment 580: 996-1006, doi 10.1016/j.scitotenv.2016.12.054

Abstract

In many karst regions in developing countries, the populations often suffer from poor microbial water quality and are frequently exposed to bacterial pathogens. The high variability of water quality requires rapid assays, but the conventional cultivation-based analysis of fecal indicator bacteria, such as *Escherichia coli* (*E. coli*), is very time-consuming. In this respect, the measurement of the enzymatic activity of *E. coli* could prove to be a valuable tool for water quality monitoring. A mobile automated prototype device was used for the investigation of β -D-glucuronidase (GLUC) activity at a remote karst spring, connected to a sinking surface stream, in Northern Vietnam. To assess the relationship between GLUC activity, discharge dynamics and contamination patterns, multiple hydrological, hydrochemical, physicochemical and microbiological parameters, including discharge, turbidity, particle-size distributions, and *E. coli*, were measured with high temporal resolution during ten days of on-site monitoring. A complex contamination pattern due to anthropogenic and agricultural activities led to high *E. coli* concentrations (270 to >24,200 MPN/100 ml) and a GLUC activity between 3.1 and 102.2 mMFU/100 ml. A strong daily fluctuation pattern of GLUC activity and particle concentrations within small

size classes (<10 μm) could be observed, as demonstrated by autocorrelations. A Spearman's rank correlation analysis resulted in correlation coefficients of $r_s = 0.56$ for *E. coli* and GLUC activity and $r_s = 0.54$ for GLUC activity and the concentration of 2–3 μm particles. On an event scale, correlations were found to be higher ($r_s = 0.69$ and 0.87 , respectively). GLUC activity and *E. coli* displayed a general contamination pattern, but with significant differences in detail, which may be explained by interferences of e. g. viable but non-culturable cells. Although further evaluations are recommended, GLUC activity is a promising, complementary parameter for on-site and near real-time water quality monitoring.

4.1 INTRODUCTION

One of the main concerns in setting health-based targets for microbial safety of water is fecal contamination originating from humans or animals, which can be a source of pathogenic bacteria, viruses, protozoa, and helminths (WHO 2008). In developing countries, where wastewater treatment is often insufficient or entirely absent, many individuals are exposed to pathogens leading to the widespread occurrence of waterborne diseases (Montgomery and Elimelech 2007). Especially in karst areas, microbial contaminants can easily reach the groundwater surface due to rapid infiltration via sinking surface streams, swallow holes, or thin soils. Furthermore, the lack of granular texture, turbulent flow regimes in conduit systems, and short residence times, in addition to rapid hydraulic and hydrochemical responses to rainfall events, lead to a high vulnerability of groundwater (Ford and Williams 1989; Goepfert and Goldscheider 2008; Pronk et al. 2007; White 1988).

The common hygienic-bacteriological evaluation of raw water is based on fecal indicator bacteria (FIB), such as total coliforms (TC), fecal coliforms (FC), *Escherichia coli* (*E. coli*), and intestinal enterococci (Ferguson et al. 2012; Servais et al. 2005). As microbial water quality often varies quickly over a wide range, and short-term peaks in pathogen concentrations may substantially increase the risk of disease outbreaks, there is a pressing need for rapid assays that enable near real-time quantification of FIB, particularly *E. coli* (Fiksdal and Tryland 2008; WHO 2008). However, standard culture-based techniques for the detection and enumeration of TC and FC require between 18 and 72 h, depending on the incubation time (Wildeboer et al. 2010), a time frame in which many individuals could be exposed to pathogens.

Enzyme assays are seen as a promising alternative to culture-based FIB assays (Heery et al. 2016), because they provide results in 1 h or less and are simple to perform (Fiksdal and Tryland 2008; Noble and Weisberg 2005). Roughly 97 % of *E. coli* strains demonstrate β -

D-glucuronidase (GLUC) activity, while the enzyme is absent in almost all other coliform bacteria (Kilian and Bülow 1979; Wildeboer et al. 2010). Further, while a small number of non-coliform micro-organisms may exhibit activity of this enzyme, interference by these micro-organisms becomes negligible in heavily polluted systems (Caruso et al. 2002). Therefore, GLUC activity is thought to be a specific biomarker for *E. coli* detection in microbiological water quality control (Rompré et al. 2002; Togo et al. 2006; Wildeboer et al. 2010; Wutor et al. 2007). The assay is based on bacterial hydrolysis of the added substrate 4-methylumbelliferyl- β -D-glucuronide (MUG) and fluorescence detection of the enzymatic reaction product 4-methylumbelliferone (MU) (Garcia-Armisen et al. 2005; Koschelnic et al. 2015).

In the last two decades, there has been an increasing interest in determining direct GLUC activity in order to evaluate microbial water quality (Farnleitner et al. 2002; Fiksdal et al. 1994; Fiksdal and Tryland 2008; Servais et al. 2005). However, all measurements of GLUC activity in previously published studies were conducted in specialized laboratories. Recently, automated devices, such as the Coliminder[®] (VWM, Austria), have been developed to measure enzymatic activity in water by fluorescence photometry on-site (Heery et al. 2016; Koschelnic et al. 2015; Stadler et al. 2016). A first automated long-term monitoring of enzymatic activity was presented by Ryzinska-Paier et al. (2014), who tested an automated device (Coliguard, mbOnline, Austria). While most studies focused on the correlation between GLUC activity and *E. coli* or fecal coliforms (Fiksdal et al. 1994; Heery et al. 2016; Servais et al. 2005; Wildeboer et al. 2010), bulk parameters including turbidity, spectral absorption coefficient at 254 nm (SAC254), conductivity and water temperature were also considered. Pronounced correlations were obtained between GLUC activity with SAC254, GLUC activity and turbidity and GLUC activity and discharge, along with lower, but still significant, correlation levels for GLUC activity and *E. coli*.

Stadler et al. (2016) recently tested two ColiMinder instruments in a hydrological open air laboratory to evaluate the reliability of measurements and compared it to measurements of two BACTcontrol (formerly Coliguard) devices, based on similar technology (Ryzinska-Paier et al. 2014). They monitored GLUC activity dynamics in a stream for one year and assessed time series data by correlation. An essential outcome of the study was that GLUC activity was not a useful proxy for *E. coli*, but they concluded that further field experiments and detailed monitoring, with a specific focus on diurnal GLUC activity fluctuations, were required. To date, on-line monitoring of enzymatic activity has been bound to well-established monitoring stations. However, in developing countries or in cases of natural disaster, required infrastructure is often insufficient or even absent. Therefore, in this study, a mobile prototype of ColiMinder was tested to investigate microbiological contamination patterns at an extremely remote karst spring in Northern Vietnam.

In the future, the water from the karst spring tested here, which is connected to a sinking surface stream, will be used as a water supply system for mountainous villages, underlining the importance of the investigation of water quality and the influences from the surface catchment area. Withal, suspended particles are important, since Abia et al. (2016) postulated that the risk of an infection due to *E. coli* increases approximately 10-fold if there is a river sediment disturbance, because bacteria tend to adhere to particles (Dussart-Baptista et al. 2003; Pronk et al. 2006; Schillinger and Gannon 1985) and are more persistent within the aquatic environment than free-floating bacteria. Due to their attachment to a mobile solid phase, they can be transported and are influenced by processes of sedimentation and remobilization (Mahler et al. 2000). In karst systems, a rainfall event can lead to a pressure pulse and, consequently, to a primary turbidity signal, caused by the remobilization of sediments from the karst aquifer itself (autochthonous turbidity). A secondary turbidity signal can occur with the arrival of turbid storm-derived water from outside the karst aquifer, e. g. from the surface catchment area that enters the swallow hole (allochthonous turbidity). This second turbidity signal is more likely associated with fecal contamination (Goldscheider et al. 2010). However, turbidity itself is a bulk parameter without any information about origin or nature. Detection of particle-size distribution (PSD) delivers more detailed information and is a valuable tool to specify the type of turbidity and to identify particle size classes that are related to microbial contamination, as shown in Pronk et al. (2007).

This study aims to determine the applicability of automated rapid on-site GLUC activity measurements by using a ColiMinder in an extremely remote, poor area, without public power supply, similar, for example, to the case of water quality monitoring during disaster management. Furthermore, PSD is evaluated as a complementary parameter to GLUC activity, to specify the type of contamination events and to assess the potential of this parameter combination for early warning systems.

The main research questions are: (i) are there daily fluctuations in GLUC activity and PSD caused by agricultural land use in the recharge area? (ii) how does GLUC activity react to hydrological events, such as rain fall, in comparison to PSD and other parameters? (iii) what is the relationship between GLUC activity and cultivation-based determinations of *E. coli*, as well as other water quality parameters (PSD, turbidity, electrical conductivity, water temperature)? and (iiii) what information can be obtained by using GLUC activity and culture-based methods and can they be used as complementary methods to indicate fecal contamination?

4.2 MATERIALS AND METHODS

4.2.1 Site selection and sampling campaign

The field site is located in Northern Vietnam, close to the Chinese border. The area was designated as a UNESCO Geopark in 2010, which has led to a strong increase in tourism and, consequently, in water demand. To meet this challenge, water from a remote karst spring will be captured to supply mountainous villages and the commune of Dong Van.

The recharge area of the karst spring predominantly consists of non-karstifiable rocks (clayish siltstone, marlaceous shale), and is drained by the Ma Le River (Fig. 4-1).

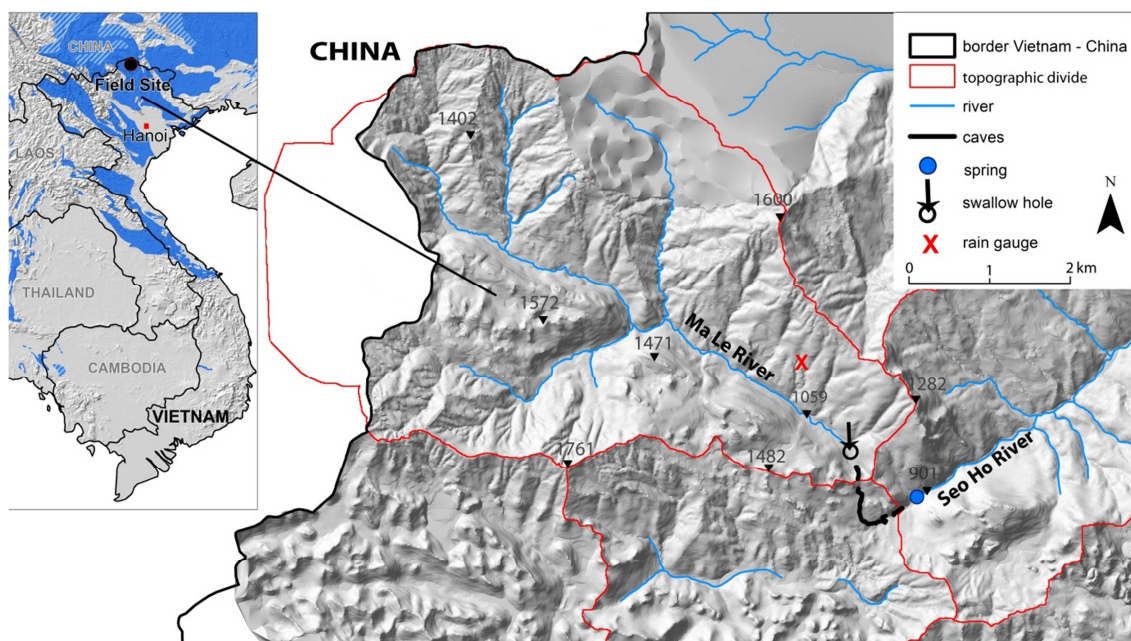


Fig. 4-1 Study area in Northern Vietnam near the Chinese border. The blue color on the overview map (left) exhibits the distribution of carbonate rocks in Vietnam (Chen et al. 2017). The Ma Le Valley is drained by the Ma Le River, which enters an underground cave system and emerges at the spring to form the Seo Ho River. A water quality monitoring program was performed at the Seo Ho spring. Grey numbers indicate the elevation in meters above sea level (modified after Zindler et al. 2015).

At the southeastern end of the Ma Le Valley, the river sinks into the karst aquifer, flows through a cave system and re-emerges at the karst spring to form the Seo Ho River. The non-karstic recharge area is characterized by agricultural land uses, including mainly rice

and corn cultivation. Furthermore, the area serves as grazing land for small herds of cattle, goats, and water buffaloes, whose dung is applied to the fields in the spring as manure. Manure application is most likely one of the main sources of fecal contamination and, generally, surface streams in the area are strongly burdened by contaminants.

Animal feces are not the only source of contamination: there are mountainous villages in the recharge area that are not connected to any wastewater system, leading to the entrance of untreated sewage from households and stables into the environment.

For field experiments, the monitoring equipment was installed at the karst spring and measurements were conducted for a period of ten days (September 27–October 7, 2015) at the end of the rainy season, when higher fecal contaminations are generally expected (Kostyla et al. 2015). GLUC activity and particle concentrations were analyzed together with hydrological, physicochemical, and microbiological parameters.

4.2.2 *Sensor measurements*

i. Enzymatic activity of β -D-glucuronidase

β -D-glucuronidase (GLUC) activity measurements were done with the mobile instrument, ColiMinder (VWM GmbH, Vienna, Austria), which was powered by 12 V car batteries. Detailed technical information about the device can be found in Koschelnik et al. (2015). One measurement is based on an increase in fluorescence intensity, resulting from the activity of GLUC and, hence, the accumulation of the highly fluorescent reaction product 4-Methylumbelliferone (MU).

Briefly, for each measurement, one fresh unfiltered water sample of 6.5 ml volume is pumped into the measurement chamber, where it is mixed with defined buffer and the fluorogenic substrate solution (CM.EC QuickDetect Reagents, VWM GmbH). Since maximal GLUC activity can be observed at 44 °C (George et al. 2000), the solution is preheated to a constant temperature of 44.0 ± 0.1 °C, before the measurement process is started automatically. The rate of enzymatic reaction is determined in volts per second. Results of GLUC activity measurements are expressed in “Modified Fishman Units” (MFU), following the standard Sigma Quality Control Test Procedure (Sigma-Aldrich 1998). One MFU of enzymatic activity of GLUC from *E. coli* liberates 1.0 μ g of phenolphthalein from phenolphthalein-glucuronide per hour at pH 6.8 at 37 °C. For calibration, commercial enzyme standards (G7396-25KU, type IX-A β -D-glucuronidase from *E. coli*, from Sigma-Aldrich) were measured in duplicates with full cleaning steps between measurements. According to manufacturer's information, a double polynomial

approximation algorithm was used to convert the changes in fluorescence intensity to corresponding enzyme activity. After the calibration procedure, a linear relationship is derived between the rate of enzymatic activity as mMFU/100 ml and the β -D-glucuronidase standards.

The influence of a sample's optical density on the fluorescence intensity is deducted by calibrations of ColiMinder with a set of turbidity standards: 2, 20, 40 and 60 NTU (Fluka Turbidity 4000NTU Calibration Standard - Polymer Bead TURB4000P-1 L) and a resulting data correction algorithm (patent: PCT/AT2014/050036). All calibration steps were performed by VWM, following Koschelnik et al. (2015).

Each measurement includes an automatic cleaning procedure, using the cleaning agents CMQuick Clean I and DanKlorix, which was diluted to a concentration of 0.5% sodium hypochlorite. The substrate CM.EC QuickDetect Reagent A (VWM) was stored at ca. -12 °C and an amount for approximately 30 measurements was filled up in the ColiMinder and refilled after complete consumption. The same procedure was followed for the buffer CM.EC QuickDetect Reagent B (VWM), but a fridge (ca. 7 °C) was used for storage. For transport, the substrate and the buffer were stored in a Styrofoam box with thermal packs to keep the temperature as low as possible. Once a day, a measurement with double distilled water was conducted, to correct GLUC activity measurements for any offset.

ii. Particle-size distribution (PSD)

PSD was determined with a portable particle counter (Abakus mobil fluid, Klotz GmbH, Bad Liebenzell, Germany), which counts suspended particles of 16 different definable size classes in a range of 0.9 to 150 μm .

Water samples were taken manually every hour to measure PSD directly, to avoid sedimentation and aggregation. Each measurement was started with a rinsing cycle, where 10ml sample water ran through the device. To improve replicate reproducibility, 5 measurements of 10 ml were performed for the same sample to calculate the mean concentration for the different size classes. In this study, small particle size classes were considered, namely particle concentrations of the size classes $1 \leq x < 2 \mu\text{m}$ (1–2 μm), $2 \leq x < 3 \mu\text{m}$ (2–3 μm) and $5 \leq x < 10 \mu\text{m}$ (5–10 μm), since pathogenic bacteria are in the range of ca. 1–3 μm (Goeppert and Goldscheider 2011; McKinney 2004; Reshes et al. 2008). Furthermore, small particles have a higher mobility and can be transported through the whole aquifer.

iii. Fecal bacteria analysis

For the conventional determination of *E. coli* Colisure® (IDEXX Laboratories Inc., USA) was used, which allows for the simultaneous determination of the total thermotolerant coliforms (TTC). TTC is a coliform group, including bacteria, that is able to ferment lactose at 44–45 °C, namely of the genus *Escherichia*, *Klebsiella*, *Enterobacter*, and *Citrobacter*, whereby only *E. coli* is considered to be exclusively of fecal origin (Foppen and Schijven 2006). Colisure, which is approved by the U.S. EPA, is based on the Most-Probable-Number method and enables a high temporal flexibility, because definitive results are obtained after 24 h, but can be read up to 48 h. Furthermore, no media preparation, no glassware cleaning, and no colony counting are required. The manufacturer's instructions (www.idexx.com/water/products/colisure.html) were followed, including incubation at 35 ± 0.5 °C. Briefly, aliquots of 10 ml of the original water sample, that were taken every 4 h in HDPE bottles (2-D0-0030-25, 30 ml, Rixius) and stored in a cooling box for maximum 24 h, were diluted with sterile deionized water in 100 ml sterile bottles (WV120SBAF-200, vessels w/antifoam, IDEXX). Due to the dilution, the upper detection limit was set to 24,200 MPN/100 ml.

During one rain event, grab samples were taken every 30 min to enhance the temporal resolution. In total, 65 grab samples were analyzed.

Colisure is based on the same bacterial hydrolysis as the measurement of GLUC activity. However, Colisure enables the selective growth of *E. coli* by using a defined substrate and an incubation time of 24–48 h. Therefore, it is widely used as a proxy for determinations with standard methods like the multiple-tube fermentation technique or the membrane filter technique (Rompré et al. 2002). In the following, any mention of *E. coli* concentration was determined using Colisure.

iv. Hydrological and hydrochemical measurements

Precipitation was collected with a rain gauge (Onset HOBO O-RG3-M, ecoTech, Germany), located in the recharge area (Fig. 4-1). A miniCTD-Diver and BaroDiver (Eigenbrodt, Germany) recorded the water level and air pressure to calculate discharge, applying salt dilution discharge measurements for calibration. A portable multi-parameter meter (Multi 3430 IDS, WTW) was used to measure electrical conductivity and temperature with a TetraCon® 925 and turbidity by using Viso-Turb*900-P.

4.2.3 Correlation analysis

Statistical Analysis was performed using PAST software (Version 3.11). Autocorrelations, cross-correlations, as well as Spearman's rank correlation analysis, were applied to investigate the dependency between the different time series.

A linear interpolation was used to obtain equidistant hourly time steps for GLUC activity. Furthermore, the datasets used for the correlation analysis were trend-corrected.

Autocorrelation function was used as a visual tool to investigate the amplitude of pre-existing periodicities in the time series. It is used to characterize the linear dependence of successive values over a time period, by applying the following equation:

$$r_k = \frac{\sum_{i=1}^{n-k} (x_i - \bar{x})(x_{i+k} - \bar{x})}{\sum_{i=1}^n (x_i - \bar{x})^2} \quad (4.1)$$

Eq. (4.1) estimates the correlation r_k between pairs of measurements (x_i, x_{i+k}) , collected k sampling events apart, so that k is the temporal lag corresponding to an integer multiple of the smallest measurement interval. The index i represents the value at time i and \bar{x} is the arithmetic mean of the time series (Chatfield 2004; EPA 2009).

To compare two time series that may have a temporal dependency, the cross-correlation function (CCF) is most appropriate (Davis 2002), whereas two different equidistant time series (x, y) can be investigated for a time lag with the following equation (Davis and Sampson 1986):

$$r_k = \frac{\sum_{i=1}^{n-k} (x_i - \bar{x})(y_{i+k} - \bar{y})}{\sqrt{(\sum_{i=1}^n (x_i - \bar{x})^2)(\sum_{i=1}^n (y_i - \bar{y})^2)}} \quad (4.2)$$

The data set x is shifted by k against the data set y ; the variables i , \bar{x} and \bar{y} have the same meaning than described for AC.

The Spearman's rank correlation (r_s) was computed to determine the nonparametric correlation based on a rank transformed method by using the following equation (Press et al. 1992):

$$r_s = \frac{\sum_{i=1}^n (R_i - \bar{R})(S_i - \bar{S})}{\sqrt{\sum_{i=1}^n (R_i - \bar{R})^2} \sqrt{\sum_{i=1}^n (S_i - \bar{S})^2}} \quad (4.3)$$

The data of two variables x_i and y_i are ranked independently among themselves to R_i and S_i . If there are identical values within one data set, called ties, the mean of the ranks was calculated.

4.3 RESULTS & DISCUSSION

4.3.1 Time series

The monitoring took place from September 27 to October 7, 2015, during a relatively constant period with respect to hydrological conditions. The discharge of the Ma Le River continuously decreased from 911 to 568 Ls⁻¹ (Fig. 4-2) and only three small rainfall events appeared on September 27 (1.6 mm/5 h), October 1st (6.6 mm/2 h), and October 3rd (6 mm/4 h).

i. Turbidity and particle-size distribution

In Fig. 4-2, turbidity and PSD are shown next to each other to illustrate both the similarity and the differences between the two parameters. Both parameters generally increased during afternoon and decreased during morning. The turbidity time series yielded the following results:

- variability: 4.9–52.4 NTU
- mean: 10.5 ± 5.7 NTU (n = 252)
- daily maximum values: 9.8–22.8 NTU
- daily minimum values: 4.9–10.5 NTU

PSD delivered more detailed information by deciphering the different size classes. Daily fluctuations are much more pronounced in the PSD time series, especially for the period October 2–October 5 and within the small particle size classes (1–2 μm and 2–3 μm). The smallest particle size class (1–2 μm) typically showed the highest concentration and there was a corresponding decrease in concentration with increasing particle size. The following results refer to 1–2 μm particles:

- variability: $2.9 \cdot 10^5$ – $5.8 \cdot 10^5$ particles/10 ml
- mean: $3.9 \cdot 10^5 \pm 5.8 \cdot 10^4$ particles/10 ml (n = 248)
- daily maximum values: $4.2 \cdot 10^5$ – $5.0 \cdot 10^5$ particles/10 ml
- daily minimum values: $2.9 \cdot 10^5$ – $3.9 \cdot 10^5$ particles/10 ml

Since both parameters strongly responded to the rain event on the October 1st, these values were excluded in the range of the maximum values, to demonstrate the daily fluctuations without influences of precipitation. In contrast, almost no response of turbidity and PSD was observed after the rain event on October 3rd, therefore, these values were included.

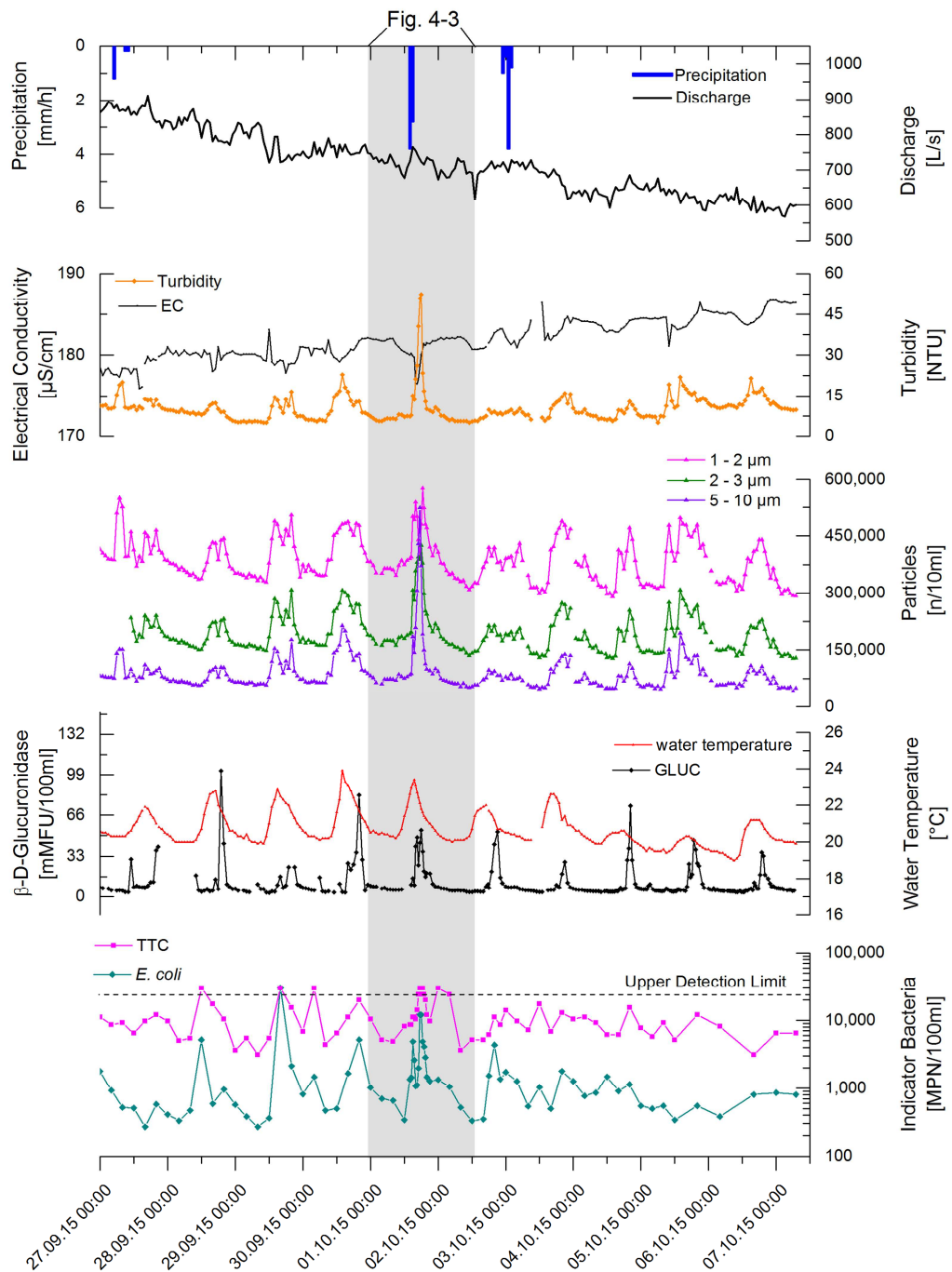


Fig. 4-2 Time series of precipitation, discharge, electrical conductivity, turbidity, concentration of three different particle size classes, and enzymatic activity. Grab samples for the determination of TTC and *E. coli* by using Colisure, were taken every 4 h. The upper detection limit (dotted line) was set to 24,200 MPN/100 ml, due to a dilution factor of 10. The grey bar highlights the period illustrated in Fig. 4-3. Time series signify a strong daily pattern in the data set of particle concentration, turbidity, and enzymatic activity that is not related to precipitation.

The rain event on October 1st appeared to influence a wider area than on October 3rd, which appeared very local and had less of an effect on the springs' recharge area of about 30 km². In this area, precipitation frequently occurs locally and as heterogeneous small rain cells, typical for mountainous regions, where they are affected by large variability in altitude and slope, and, to a lesser extent, by rain shading or wind (Buytaert et al. 2006). Generally, precipitation on October 1st was more intense, with the same amount of rain fall in half the time, leading to higher surface runoff and greater inputs of contaminants and sediments into the river. The daily fluctuations were most likely caused by agricultural activities in the recharge area. Apart from rice harvesting and grazing animals, activities such as fishing caused a sediment remobilization. To catch fish, farmers built small rocky walls inside the riverbed. They sealed the walls with mud from the riverside, resulting in the creation of large turbidity clouds, which entered the cave system. Water temperature that was recorded at the cave entrance and at the Seo Ho spring, indicated a traveling time through the cave passage of 2–3 h. Thus, activities in the vicinity of the cave might have started around 10 am and ended after sunset at 6 pm.

ii. GLUC activity

The time series of GLUC activity is shown together with water temperature measurements in Fig. 4-2 to emphasize the strong similarity in their periodicity. The following results were observed:

- Spring water temperature: 19.0–23.9 °C
- Highest temperatures between 2 and 5 pm
- GLUC activity: 3.1–102.2 mMFU/100 ml (n = 267)
- Daily GLUC activity peaks between 7 and 9 pm

The peaks of GLUC activity appeared much shorter compared to peaks in water temperature and exhibit a temporal delay, which is not observed between GLUC activity and PSD or turbidity. GLUC activity displayed a daily dynamic that was similar to PSD, but with significantly higher values between 7 and 9 pm (Suppl. Figure 4).

iii. E. coli and TTC

E. coli and TTC measurement are displayed together in Fig. 4-2, since TTC concentrations are strongly related to *E. coli* concentrations. However, TTC concentrations are higher than *E. coli* concentrations due to other species present, which may not be of fecal origin (Foppen and Schijven 2006). Since GLUC activity is seen to be specific for *E. coli*, the results for the *E. coli* measurements are summarized:

- Variability: 270 to >24,200 MPN/100 ml
- Values above upper detection limit: one measurement
- Maximum *E. coli* concentrations in the evening: 550–5,170 MPN/100 ml
- Minimum *E. coli* concentrations in the morning: 270–770 MPN/100 ml

E. coli and TTC indicated the strong microbial contamination of the system. Daily fluctuations were noticeable, but the fluctuation pattern looked different than the GLUC activity pattern. However, it has to be considered, that the temporal resolution of *E. coli* and TTC measurements using a sampling interval of 4 h was worse than for other parameters measured every hour.

4.3.2 Variations in time series during one rain event

All measured parameters responded rapidly during the rainfall on October 1st (Fig. 4-3), but differed in the nature of their reactions. The main findings are:

- Double peaks: 1–2 μm , GLUC activity and TTC
- EC minimum (176.5 $\mu\text{S/cm}$) together with first maximum of GLUC activity (47.9 mMFU/100 ml) and 1–2 μm ($5.38 \cdot 10^5$ particles/10 ml)
- Slower response of larger particle size classes, turbidity and *E. coli*
- *E. coli* maximum (12,030 MPN/100 ml) together with turbidity peak (52.4 NTU), larger particle size fractions (2–3 μm : $4.25 \cdot 10^5$ particles/10 ml; 3–4 μm : $3.13 \cdot 10^5$ particles/10 ml; 4–5 μm : $2.34 \cdot 10^5$ particles/10 ml), and second GLUC peak (53.9 mMFU/100 ml)

The first increase of 1–2 μm particles is likely due to the remobilization of river sediments within the cave system and is temporally coupled with the first GLUC activity peak, which may indicate autochthonous bacteria. In this case, the contribution to autochthonous turbidity decreased with increasing particle size, although the rainfall event was only moderate. A stronger rainfall event, with a significant increase in discharge, would probably lead to a remobilization of cave sediments including larger particle size classes. An increase in *E. coli* is coupled with an increase in particle concentrations of larger size classes, turbidity, and the second GLUC activity peak, which may reflect allochthonous turbidity.

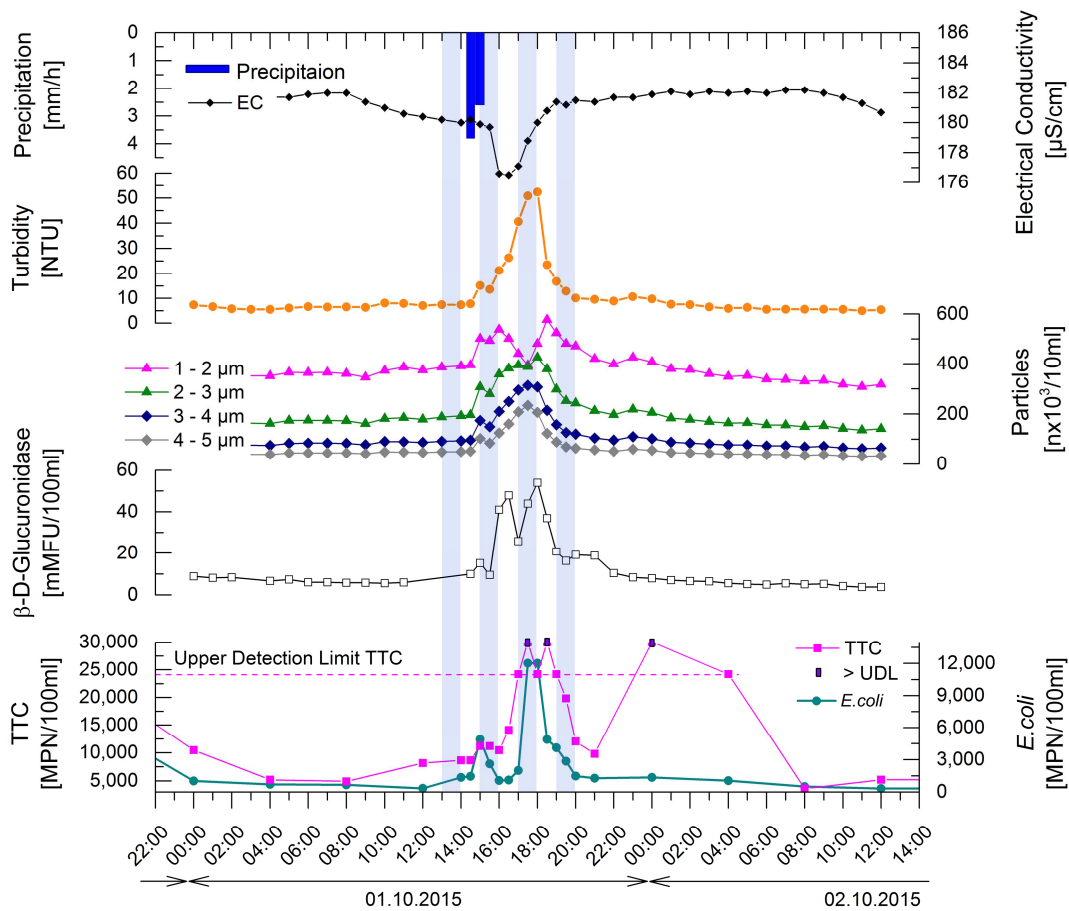


Fig. 4-3 Time series during a moderate rainfall: All parameters, measured with an interval of 30 min (blueish bars = 60 min), display a fast reaction on the precipitation event. However, GLUC activity and small particle concentrations respond faster than *E. coli* and exhibit their first maxima at the minimum of the electrical conductivity, which marks the arrival of the lower mineralized rain water at the spring.

4.3.3 Correlation analysis

i. Autocorrelations

The autocorrelation (AC) was applied to investigate the similarity of the periodicity of the different parameters measured. All parameters displayed clear daily fluctuations with maximum positive correlations after 24 and 48 h, as shown in Fig. 4-4a, with the critical level of correlation for 95% significance ($\alpha = 0.05$) also shown. The highest negative correlations appeared after 12 and 36 h, but were generally lower than positive correlations. Therefore, the positive correlation coefficients were used in the following considerations.

GLUC activity showed a significant correlation coefficient of 0.41 ($\alpha < 0.05$) for a lag time of 24 h, but a distinctly higher correlation after 48 h (0.58, $\alpha < 0.05$). Other significant high correlation coefficients appeared after 3 days (0.46, $\alpha < 0.05$) and 4 days (0.64, $\alpha < 0.05$) (not shown). Although GLUC activity exhibited a higher correlation for 48 h, it is assumed that signal periodicities were primarily caused by a daily pattern, since longer periodicities seem unlikely. Considering the different particle size classes, the correlation coefficients for a time lag of 24 h decreased with increasing particle size (1–2 μm : 0.46; 2–3 μm : 0.44; 5–10 μm : 0.29). For turbidity, the AC was even less significant (0.21, $\alpha < 0.05$) for a time lag of 25 h due to the influence of larger particles.

Although *E. coli* concentration exhibited daily fluctuations (Fig. 4-2), the daily periodicity could not be demonstrated by the AC, probably due to limited number of measurements, which led to a higher interference from the daily pattern by influences of rainfall.

The water temperature displayed an autocorrelation of 24 h, since the spring has a big surface catchment and, therefore, water temperature was clearly affected by air temperature.

ii. Cross-correlations

Cross-correlations (CC) were calculated to compare GLUC activity with different parameters (Fig. 4-4b). Depending on time lag, significant correlation coefficients ranged between -0.31 and 0.54 . In the datasets of GLUC vs. turbidity and GLUC vs. 1–2 μm particles, cross-correlation coefficients were highest without any time lag.

The cross-correlation coefficients for GLUC vs. 2–3 μm and GLUC vs. 5–10 μm increased for positive time lags until 1 h and for GLUC vs. water temperature until 3 h. This suggests that GLUC activity trailed behind water temperatures. Concerning the suspended particles, cross-correlation analysis indicated the highest similarity between GLUC activity and suspended particles of size 2–3 μm .

In general, highest correlation values were found for a time lag between 0 and 2 h, followed by other maxima after 24 ± 2 h, caused by daily periodicity. Negative correlation coefficients are shifted by 12 h and are generally lower than positive correlations. The correlation coefficient between GLUC activity and 2–3 μm was 0.46 ($p < 0.001$) with a time lag of 1 h and slightly increased with 0.49 ($p < 0.001$) at a time lag of 27 h. The cross-correlation for GLUC activity and *E. coli* indicate a correlation with a daily periodicity, however, not as clear as for GLUC activity with other parameters.

Nevertheless, significant cross-correlation coefficients could be found for GLUC activity and *E. coli* without a time lag (0.26, $p < 0.05$) and for a lag in time of 28 h (0.54, $p < 0.001$). The deviation from 24 h could be explained by the greater sampling interval.

Another strong coefficient of 0.54 ($p < 0.001$) was found for the CC of GLUC activity with water temperature and a corresponding time lag of 3 h.

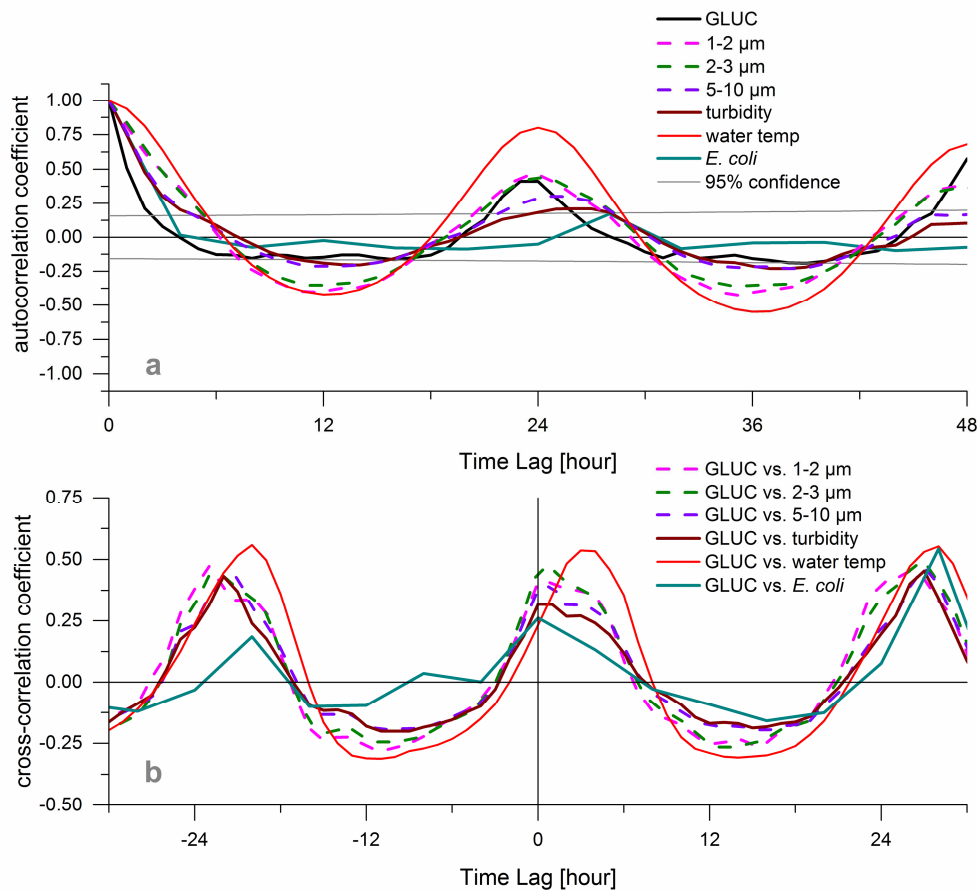


Fig. 4-4 a) Autocorrelation of time series of enzymatic activity (GLUC), turbidity, different particles size classes (1–2 μm , 2–3 μm and 5–10 μm), water temperature (water temp), and *E. coli*. b) Cross correlation between time series of GLUC and different particle size classes, turbidity, water temperature, and *E. coli*. There is no considerable time lag between the maxima of particle concentrations and GLUC.

Stadler et al. (2016) also observed a diurnal fluctuation of enzymatic activity and they assumed a temperature-dependence of bacterial activity. Furthermore, they could exclude that construction-based temperature fluctuations within the ColiMinder triggered any variations in enzymatic activity. Similar to the observations in Vietnam, the maximum enzymatic activity occurs with a delay of 4 to 6 h compared to the daily maximum of water temperature. In this study, it is assumed that GLUC activity is influenced by the daily fluctuations of anthropogenic activities in the recharge area and coupled to this, daily fluctuations of *E. coli* input. Although the water temperature exhibited strong daily fluctuations, the temperature differences were too small (maximum 4 $^{\circ}\text{C}$) to increase the

GLUC activity by a factor of 10–30. Generally enzymatic activity is doubled by a temperature increase of 10 °C (Bergmeyer 2012). A possible contribution of intermediary processes driven by temperature that causes higher enzymatic activity should be part of further detailed investigation.

iii. Spearman's rank order correlations

Correlations for the complete time series

Spearman's rank correlation analysis was applied to determine the correlation coefficients r_s (Table 4-1) between all parameters. For the entire period, a correlation of $r_s = 0.56$ ($n = 62$, $p < 0.001$) was obtained for GLUC activity and *E. coli*.

A similar correlation coefficient was found for 2–3 μm and GLUC activity ($r_s = 0.54$, $n = 231$, $p < 0.001$), which was slightly higher than identified by the CC (0.46). In comparison, *E. coli* displayed weaker correlation with particle concentration, but a still significant $r_s = 0.43$ with 2–3 μm and 5–10 μm . Furthermore, small and significant negative correlations were identified between EC and particle concentration, which were highest for 5–10 μm (-0.34).

Correlations during one rain event

Table 4-1 also depicts the Spearman's rank correlation coefficients for the rain event on October 1st (in blue). For this single precipitation event, the correlation coefficients were higher, especially for GLUC with 2–3 μm and 5–10 μm , with $r_s = 0.87$ ($p < 0.001$, $n = 39$).

Owing to the delayed increase of *E. coli* concentration as a response to the hydrological change, correlation of GLUC with *E. coli* after rainfalls ($r_s = 0.69$, $p < 0.001$, $n = 20$) was not as high as compared to correlations with particle concentrations, but stronger than for the entire period. The best correlation for *E. coli* was obtained with turbidity and 2–3 μm particles ($r_s = 0.81$, $p < 0.001$, $n = 22$), whereas the correlation coefficient was slightly lower for *E. coli* and 5–10 μm ($r_s = 0.79$, $p < 0.001$, $n = 22$) and *E. coli* and 1–2 μm ($r_s = 0.70$, $p < 0.001$, $n = 22$).

Negative correlation coefficients between EC and all other observed parameter emphasized the causal relation between the rainfall event and the increase in microbial contamination and particle transport. The results indicated that there is a significant correlation between particle concentration and GLUC activity or more general, microbial contamination.

Table 4-1 Spearman's rank correlation r_s with significance p and the number of measurements n for the entire period (left, white) and the measurements during the rain event on October 1st (right, blue). The Spearman's rank correlation analysis yielded higher correlation coefficients for a single rain event.

r_s p n	EC	Turbidity	1 - 2 μm	2 - 3 μm	5 - 10 μm	<i>E. coli</i>	TTC	GLUC	r_s p n
GLUC	0.12 0.07 236	0.39 <0.001 236	0.47 <0.001 236	0.54 <0.001 231	0.46 <0.001 231	0.56 <0.001 62	0.43 <0.001 62		GLUC
TTC	-0.13 0.30 64	0.46 <0.001 64	0.45 <0.001 65	0.49 <0.001 62	0.48 <0.001 65	0.65 <0.001 65		0.55 <0.05 20	TTC
<i>E. coli</i>	-0.23 0.06 64	0.35 <0.005 64	0.34 <0.005 65	0.43 <0.001 62	0.43 <0.001 65		0.67 <0.001 22	0.69 <0.001 20	<i>E. coli</i>
5 - 10 μm	-0.34 <0.001 242	0.75 <0.001 242	0.97 <0.001 242	0.98 <0.001 231		0.79 <0.001 22	0.64 <0.005 22	0.87 <0.001 39	5 - 10 μm
2 - 3 μm	-0.30 <0.001 231	0.77 <0.001 231	0.99 <0.001 231		0.98 <0.001 42	0.81 <0.001 22	0.65 <0.005 22	0.87 <0.001 39	2 - 3 μm
1 - 2 μm	-0.31 <0.001 242	0.77 <0.001 242		0.96 <0.001 42	0.91 <0.001 42	0.70 <0.001 22	0.46 <0.05 22	0.82 <0.005 39	1 - 2 μm
Turbidity	-0.16 <0.05 245		0.94 <0.001 42	0.96 <0.001 42	0.92 <0.001 42	0.81 <0.001 22	0.67 <0.001 22	0.79 <0.001 39	Turbidity
EC		-0.62 <0.001 43	-0.55 <0.001 42	-0.64 <0.001 42	-0.71 <0.001 42	-0.53 <0.05 22	-0.30 0.18 22	-0.58 <0.001 39	EC

Nonetheless, an increase in particle concentration does not necessarily mean degradation in water quality, because there are various reasons for sediment remobilization. In low contaminated systems or in better protected groundwater aquifers, PSD might be an inadequate indicator for poor water quality. However in highly polluted catchment areas, an input or remobilization of particles lead to an increase in *E. coli* concentrations and GLUC activity, as shown in this study. This could be explained by the persistence of bacteria attached to particles (Abberton et al. 2016; Mahler et al. 2000). During rain events, the direct bacteria and sediment input from the catchment surface enhance the correlation of PSD and GLUC activity, including larger particle size classes. The combination of PSD and GLUC activity shows the greatest potential for water quality monitoring, because both parameters can be monitored automatically, online and in near real-time. The differentiation of distinct particle size classes allows conclusions of origin and nature of contamination events. While the rain event has led to a mobilization of particles including larger particle

classes, anthropogenic activities in the recharge area caused daily fluctuations that are most distinct in small particle size classes and associated with higher GLUC activities.

4.3.4 Comparison of β -D-glucuronidase activity and *E. coli*

The results presented here indicate that GLUC activity appeared to be a sensitive parameter during water quality monitoring, but was not useful as a surrogate for the conventional cultivation-based method, since a poor correlation between *E. coli* and GLUC activity was observed, both in normal conditions and for a single rain event. In the studies of Tryland and Fiksdal (1998) and Fiksdal and Tryland (2008), interference from viable, but non-culturable (VBNC) target bacteria, algae, plants, and dissolved free enzymes, among others, were discussed. Whilst enumeration of *E. coli* is based on the culturability of cells, rapid enzyme assays including the direct GLUC activity measurements, detect all metabolically active bacterial cells, including VBNC cells (Petit et al. 2000). When allochthonous bacteria enter aquatic environments, they can survive for long periods, but due to nutrient scarcity, temperature, sunlight, and predation by protozoa, they lose their culturability (Baudart et al. 2002; Colwell et al. 1985; Galfi et al. 2016; Goldscheider et al. 2006). This is not necessarily coupled to a loss of enzymatic activity or even a loss of infectivity, and, consequently, pathogenic risk can be maintained without culturability (Petit et al. 2000). Our study indicates that the VBNC may play a major role in enzymatic activity measurements, owing to the complex patterns in parameters directly or indirectly associated with fecal contamination. Furthermore, contributions of non-target bacteria and cell-free substances affecting enzymatic activity measurements cannot be excluded. However, owing to the relatively high concentration of target bacteria, such interference may be limited (Caruso et al. 2002). George et al. (2000) could not find any contribution of false-positive bacteria to GLUC activity, even when the total bacteria abundance was multiplied by 20. Nonetheless, possible interference might depend on different systems and should be further investigated.

Similar results with moderate correlation coefficients for *E. coli* and GLUC activity were recently shown by Stadler et al. (2016) and Ryzinska-Paier et al. (2014) and were also ascribed to the proportion of VBNC and culturable cells.

Due to different *E. coli* assays, the obtained results were not identical, but delivered valuable, complementary information, especially on an event-scale.

Bacteria attached to the cave sediments could comprise a higher proportion of VBNC cells compared to culturable cells due to their age, and may also cause an increase of GLUC

activity, without a corresponding increase in *E. coli*. In contrast, the direct input of bacteria from the catchment area might result in an increase of GLUC activity and *E. coli*, since a larger portion of cells is likely still culturable. This observation could allow one to decipher autochthonous and allochthonous turbidity and bacteria, although further investigations would be necessary to evaluate GLUC activity as an adequate parameter for the differentiation of autochthonous and allochthonous input.

Haack et al. (2016) showed that the number and type of pathogen genes are strongly affected by animal type, human influences and the occurrence and degree of rainfall events.

In this study, *E. coli* also originate from different sources at different time-points with partly continuous and intermittent input and lead to a complex contamination pattern. Consequently, the proportion of VBNC and culturable cells is likely very variable. Nevertheless, the periodical “event-based” evaluation revealed a clear relationship between GLUC activity and *E. coli*. The period analysis in Fig. 4–5 compares means of GLUC activity measurements at different times of the day with corresponding means of *E. coli* measurements.

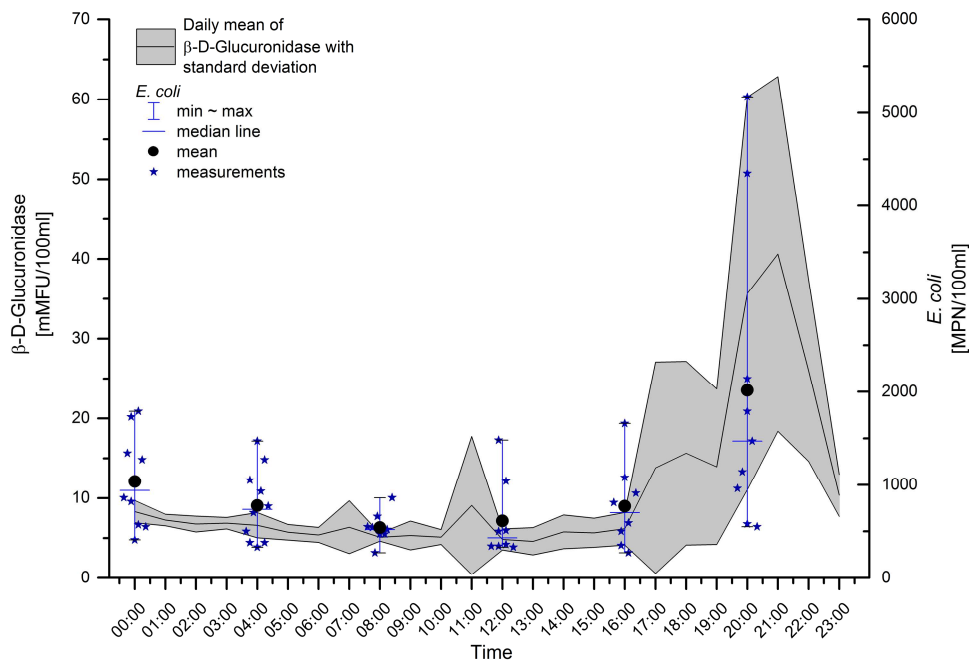


Fig. 4-5 Means at different times of the day of GLUC activity measurements (black line) with its range of values (grey) and the corresponding *E. coli*. Two outliers (4 pm: 5,170 MPN/100 ml and 8 pm: >24,200 MPN/100 ml) are not shown in this graph.

It illustrates that, in general, highest GLUC activities occurred in the evening between 7 and 9 pm and the highest *E. coli* concentrations at 8 pm. Therefore, it can be assumed, that there is a good accordance between the two methods to indicate microbiological contamination patterns. It is noteworthy, that there are glucuronidase-negative *E. coli* strains, which are pathogenic, e.g. *E. coli* O157:H7 and which are not detectable with Colisure or the ColiMinder. Even if the drinking water standards are met by investigating FIB, e.g. *E. coli*, there is a remaining risk for human health due to glucuronidase-negative *E. coli* strains, as shown by Schets et al. (2005).

4.4 CONCLUSION

A ten-day monitoring was performed at a karst spring in a remote area of Northern Vietnam. During a relatively stable recession period, interrupted by smaller rain events, high-resolution field measurements of enzymatic activity and particle size fractions were conducted to characterize contamination patterns.

- This study demonstrates that a near real-time, high resolution monitoring of fecal contamination patterns is possible, even in remote areas without well-established monitoring stations.
- Daily water quality fluctuations could be observed, including turbidity, particle concentration, GLUC activity, and *E. coli*, caused by anthropogenic and agricultural activities within the recharge area. These observations indicate the strong relationship between sediment remobilization and increase in fecal bacteria, even without precipitation events.
- A diurnal GLUC activity dynamic was similar to the dynamic of concentrations of small particle sizes. Nevertheless, a daily peak in GLUC activity is not yet explicable and might be related to an intermediary process driven by water temperature. With the conventional culture-based method of *E. coli* determination, the diurnal contamination dynamic of fecal bacteria in water could be observed, but the AC did not demonstrate daily periodicity, due to a limited number of data points.
- Precipitation events led to an intensified input of fecal bacteria. The GLUC activity responded rapidly to a rain event with an increase, which occurred nearly simultaneously with an increase in concentration of the 1–2 μm particles. A double GLUC activity peak during the event allowed an interpretation of different origins of signal variation. We presume that GLUC activity first displayed an autochthonous signal associated with a high portion of VBNC cells attached to the remobilized cave

sediments. The second increase in GLUC activity within the double peak might originate from allochthonous sediments and *E. coli* from the catchment area, where the portion of culturable cells is likely greater. The combination of GLUC activity and PSD measurement may have a high potential for water quality monitoring, especially for early warning systems in karst areas and warrants further investigation.

- The highest correlations were found between GLUC activity and the particle concentration of the 2–3 μm size class. Although correlation coefficients are only moderate for the whole time series, they are rather strong on an event based scale ($r_s = 0.87$). Considering water quality monitoring in this environment, 2–3 μm particles in combination with GLUC activity could be a powerful tool to investigate contamination patterns of feces.
- It could be shown that there is a significant correlation between GLUC activity and *E. coli*. However, due to rather moderate correlation factors, GLUC activity cannot substitute conventional culture-based determinations of *E. coli*. Instead, measurement of GLUC activity is a complementary assay to identify microbiological contamination, since GLUC activity measurements include VBNC cells which may also pose a threat to human health. The correlation between GLUC activity and *E. coli* should not mark a main concern to assess the direct GLUC activity assay. Instead, an evaluation of risk related to GLUC activities needs further investigation.
- Interference of non-coliform bacteria, algae or other substances is likely negligible due to the high concentrations of target bacteria. However, these contributions to GLUC activity cannot be excluded and require further investigations, especially in low contaminated systems.

The results presented here demonstrated that GLUC activity, in combination with PSD, is a valuable tool to monitor and investigate contamination dynamics in highly variable environmental systems, such as karst areas. Furthermore, this study illustrates the importance of rapid assays for the detection of fecal indicator bacteria, whose extremely high variability in concentration may pose serious threat to human health.

Supplementary data to this article can be found online at <http://dx.doi.org/10.1016/j.scitotenv.2016.12.054>.

ACKNOWLEDGEMENT

The project was funded by the German Federal Ministry of Education and Research (BMBF) [grant number 02WCL1291A]. We want to give our thanks to Ha Giang Peoples Committee, Dong Van Peoples Committee and the Vietnam Institute of Geosciences and Mineral Resources (Hanoi) for their general valuable support during fieldwork. We want to thank VWM GmbH – Vienna Water Monitoring for their friendly and comprehensive support. Special thanks are given to Tobias Zaegel, Christian Weippert, Anh Tran Diep and Tuan Lai Quang for their help during the on-site monitoring as well as to Arica Beisaw for proofreading.

CHAPTER 5

5 CONCLUSIONS AND OUTLOOK

5.1 GENERAL OVERVIEW

The sustainable management of karst water resources is an immense challenge and requires a profound understanding of the karst system and the prevailing conditions. In this thesis, innovative methods and approaches were applied, to characterize a subtropical karst system in Northern Vietnam. In one of the poorest and most remote areas of Vietnam, people suffer from water scarcity and poor water quality. The high variability of water availability and water quality makes the management of the karst water resources difficult. In order to develop a sustainable freshwater supply, the KaWaTech project was initiated and is continued by KaWaTech Solutions. By the implementation of a hydropower-driven water supply system, water is pumped from the Seo Ho River and is distributed to Dong Van City and the mountainous villages. In this context, many hydrogeological aspects must be considered, including general water availability in the region, discharge variability, water quality, contaminant and sediment transport and the vulnerability of karst aquifers.

To address these issues, extensive field work was carried out and the results from three studies, presented in this thesis, emerged. In the following sections, the main findings are presented and perspectives are given. Here, three different levels are considered: (1) from a scientific point of view, each study is discussed and the open research questions are addressed; (2) for the local scale of Dong Van, the project-relevant results are summarised and the future challenges for the Dong Van region are proposed; (3) the transferability of the applied methods and approaches to other karst regions are emphasised.

5.2 SCIENTIFIC ASPECTS

The development of a hydrogeological conceptual model for the Dong Van region was performed to provide a basis for further investigations. To this end, a combination of

different methods was applied, including mapping, artificial tracer tests and hydrochemical analyses. It could be shown, that the different water resources belong to four different physicochemical groups, classified by their $\text{Ca}^{2+}/\text{Mg}^{2+}$ ratio. Furthermore, 72 % of the physicochemical variance of the different water resources could be described by two factors, as indicated by a principal component analysis. While factor 1 is indicative for water-rock interactions, factor 2 can be associated with anthropogenic influences, demonstrating the high impact of human activities. Based on the hydrogeological conceptual model, it could be shown that the strongly karstified Bac Son aquifer, which is the most important aquifer in this region, is particularly vulnerable to contamination. Its karst springs were most highly contaminated with faecal bacteria, with tendentially higher concentrations during rainy season. Springs that are connected to sinking streams exhibited significantly higher contamination levels, especially if they are involved in a polje series, where the closed depressions are extensively used for agriculture (Fig. 5-1). Tracer tests revealed high flow velocities and high tracer recovery rates, which indicate a fast transport of contaminants to the springs. Furthermore, contamination events do not necessarily have to be bound to precipitation events. In fact, discharge of wastewater from households and agriculture to swallow holes strongly reduces the water quality, although usually for a short time. In contrast, springs with a more pristine catchment area in the mountains and/or more diffuse infiltration are less contaminated.

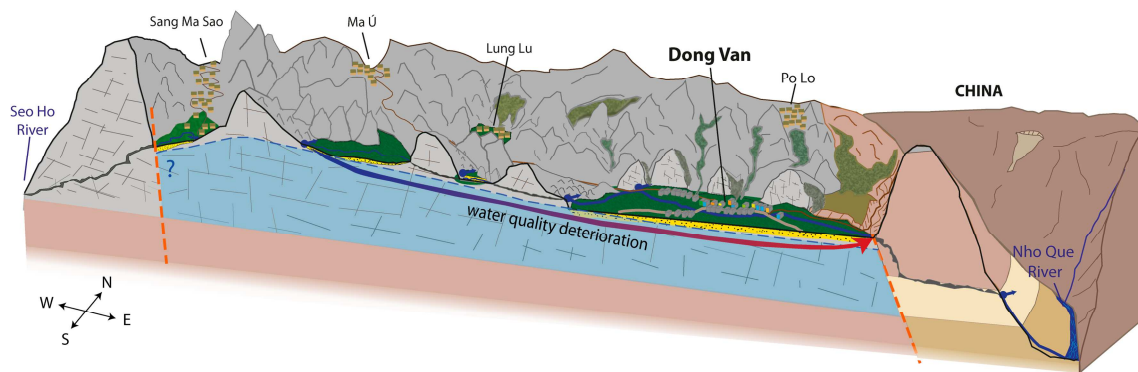


Fig. 5-1 Schematic cross-section from the Seo Ho River in the west to the Nho Que River in the east. Spring water quality decreases from west to east due to the anthropogenic and agricultural impact within the poljes. It is assumed that there is a confining fault in the Sang Ma Sao valley. Otherwise the hydraulic gradient to the Seo Ho River would be too steep. Furthermore, the local occurrence of gabbro gives evidence for a fault zone. Colours correspond to Fig. 2-1b and Fig. 2-4. The geology east of the Nho Que River is not considered.

These observations point to the need of adapted protection strategies that clearly regulate the land use in highly vulnerable areas. In this respect, a long-time monitoring of two representative springs (one with and one without a direct connection to a swallow hole) would be interesting to visualize the impact of different seasons, with their season-dependent cultivation practices on water quality. In addition to the water quality parameters that were studied in this thesis, residuals and metabolites of pesticides and fertilizers could enhance the significance of the study, since the Water Sector Review (2009) emphasised the large problems related to them. It states that most pesticides used in Vietnam were of high toxicity and while their levels of exposures were unnecessarily high, their efficiency was low. Consequently, many farmers were suffering from instances of pesticide poisoning (ADB 2009a). Therefore, monitoring of spring water with regard to pesticides could be useful.

Strong water quality fluctuations cannot only be explained by a variable contaminant input, but by the extremely high variability of flow and transport parameters in karst conduit systems. As shown for the Ma Le cave system in chapter 3, the special hydrological conditions cause highly variable discharge rates (ML 4: 72–1,296 L/s), which result in a wide range of flow velocities (ML 1 to ML 4: 183–1,043 m/h). With increasing discharge, the impact of immobile fluid regions decrease, which could reduce the retention potential, or residence time, of contaminants. The significantly smaller tracer recovery rates under low flow conditions might indicate the retention of tracer within the system. By using the innovative MPI approach, it was possible to obtain a spatial resolution of flow and transport parameter. While the dispersivity for the entire system was found to be smallest at intermediate discharge, the MPI approach enabled the detection of a generally higher dispersivity in the middle cave section (ML 2–ML 3). Furthermore, a higher proportion of immobile fluid regions due to pools, siphons and a larger extent of phreatic passages could be identified by a smaller partition coefficient β for this section.

So far, no tracer test was conducted with a simultaneous injection of two different tracers at different cave segments, which would allow for a direct comparison between Dirac and multiple pulse injection under identical conditions. This comparison would require the use of two tracers with optimally identical transport behaviours, which does not exist. However, at least, these differences have to be taken into account.

Furthermore, studies in other karst conduit systems would be interesting, especially if the system is well known. For example, the tracer tests from the Blue Spring system, described in Lauber et al. (2014) might be suitable to test the MPI approach, since tracer injections were also made within the conduit system. Since the location of the Blue Spring system facilitates field work compared to the cave system in the remote area of Northern Vietnam,

it might be a good alternative test site to perform the direct comparison of Dirac injection and MPI approach. Though, in Germany, the procedure to get permission for a tracer injection is more difficult and time-consuming than in Vietnam.

The high variable transport parameters within the cave system also affect the quality parameters at the spring. To examine the correlations between physicochemical parameters, particles, faecal bacteria concentrations and discharge rates, a high-resolution monitoring was conducted at the karst spring and is presented in chapter 4. With the ColiMinder, an innovative, mobile device was successfully tested for the first time in a remote area without available infrastructure and under subtropical conditions. It enabled a near real-time, on-site monitoring of faecal contamination patterns by field measurements of the enzymatic activity of *E. coli*. Daily water quality fluctuations could be observed through measurements of turbidity, particle concentrations, GLUC activity and *E. coli*. The latter was determined by using a conventional cultivation-based method. These fluctuations were caused by anthropogenic and agricultural activities within the recharge area, which emphasize the strong relationship between sediment remobilization and increase in faecal bacteria, even independent of precipitation events. Since the highest correlations were found between GLUC activity and the particle concentrations of small size classes (<10 µm), particularly on an event based scale, the combination of GLUC activity and PSD presents a powerful tool to investigate contamination patterns of faeces. However, the measurement of GLUC activity cannot substitute conventional culture-based determinations of *E. coli*. The rather moderate correlation factors were ascribed to VBNC cells which exhibit also enzymatic activity, but are not culturable.

This assumption should be proven in future studies by monitoring GLUC activity and *E. coli*, including an assay to determine the presence of VBNC cells. In addition, investigations concerning possible interferences should be carried out, especially if the ColiMinder is applied in less contaminated, natural systems. In this context, the strong daily fluctuations in GLUC activity that could be partly ascribed to anthropogenic activities have to be investigated further, since other research groups also observed similar fluctuations. Finally, to use GLUC activity as an indicator for faecal contamination, a risk evaluation has to be performed with definitions of quality thresholds.

Although, the yielded information represents only pieces of a much bigger research puzzle, they are a valuable contribution to the development of a better understanding of subtropical karst aquifers. In addition, they are of particular importance on a local scale as they provide a basis for the development of adapted water management and groundwater protection strategies.

5.3 PROJECT RELATED ASPECTS

The example of the Dong Van area clearly revealed the water related problems on a local scale in remote, subtropical karst areas. While during dry season, people are burdened by water shortage, strong precipitation events during rainy season lead to a mobilization of sediments and contaminants that deteriorate spring water quality, posing a threat to human health.

The KaWaTech project addressed the problem of water scarcity by implementing the Seo Ho water supply system. Therefore, the detailed investigation and characterization of the upstream located Ma Le cave system was particularly important. The numerous tracer tests revealed not only a high variability of flow and transport parameters, but a very dynamic behaviour concerning inflows, outflows and alternative flow paths. Strong precipitation events can lead to an immense redistribution of cave sediments, which can cause openings and closings of fractures and conduits. During low flow conditions, sediments entering the cave system can be deposited within the cave passage, especially in the section ML 2–ML 3, where the proportion of immobile fluid regions is higher. So, less sediment leaves the cave system than enter and thus, the system acts as a trap, which is a positive effect for the downstream located technical facilities of the supply system in terms of abrasion risk. However, strong precipitation events can intensify the problem, since the deposited sediments will remobilize and reach the water extraction site very quickly. This can be problematic, since the KSB AG, which is designing the pumping system, defined a particle-size of 0.2 mm and a particle concentration of 20 mg/L as threshold. Larger particles and higher concentrations should not enter the pump system to avoid abrasion. Therefore, a reliable and adapted early warning system that leads to a shutdown of the pumps, if the defined limits are exceeded, is essential.

But, also in respect to water quality, an early warning system is necessary. The second project phase KaWaTech Solutions intends to design a water treatment plant to ensure that the supplied water is of good quality. To protect the treatment facilities from overloading and to enhance its resistance, the supply of very turbid raw water should be avoided. The monitoring at the karst spring ML 4 clearly revealed the close relationship between particle concentrations and poor microbial water quality, especially during rain events. Therefore, different particle-size classes should be considered and threshold values defined for an early warning system: small size classes ($<10\ \mu\text{m}$) that might indicate also microbial contamination and a size class of 0.2 mm to protect the technical facilities. In addition, the early warning system can be complemented by a turbidity probe. A turbidity limit can be defined, which corresponds to roughly 20 mg/L. The implementation of the early warning system will be realized within the time frame of KaWaTech Solutions. The Seo Ho supply

system will be completed in the near future and, hopefully, the situation in Dong Van concerning water scarcity will ease.

In order to achieve a sustainable water management, several aspects have to be considered in the future, that are related to the current infrastructure and which are not covered by the KaWaTech projects so far.

- To ensure the supply of high quality water, great efforts have to be invested in improving the Dong Van main system. Measurements of *E. coli* concentrations in water taps at different locations within the distribution network showed strong water quality deteriorations within the main network. Leakages combined with an intermittent water supply, leads to the entrance of contaminants into the main network, if the main network is not under pressure.
- This problem is enhanced due to the absence of an adequate wastewater management strategy. Sewage is partly collected in septic tanks or in small ditches, which contribute to an open channel. Due to leakages or inadequate maintenance of the sewer systems, pathways for contaminants to the freshwater main system could occur in the worst case scenario.
- The sewage channel runs to the cave entrance at the eastern side of the Dong Van polje. After the cave passage, the sewage is discharged to the Nho Que River, from which many people in lower-laying areas depend. Therefore, investments have to be made to implement a wastewater treatment plant in Dong Van to treat the accruing sewage. The amount of wastewater is also likely to increase, due to the increased supply of water to Dong Van, but also due to rising levels of tourism.
- With regard to the current water resources in Dong Van, the development of wastewater management strategies within the recharge areas is also an important issue. For example, by implementing small, decentralized wastewater treatment plants, the input of contaminants could be strongly reduced and therefore, the raw water quality significantly increased. This aspect should also be considered in the catchment area of the Seo Ho plant, since several villages are located in the Ma Le valley.

In addition, one main issue in order to improve the water quality situation in the whole area is awareness-raising within the local population. By enlightenment about the specific characteristics of karst with its high vulnerability, people might be sensitized to avoid a contaminant input. For instance, people could consequently stop to use swallow holes and dolines as wastewater system and dumping site, respectively. In this respect, the handover

of vulnerability and risk maps, which were produced within the KaWaTech project, can support the local government as well as local residents.

Since an increasing amount of groundwater from the karst aquifer below Dong Van is extracted, further investigations would be necessary to gain information about the aquifer extent, confining conditions, aquifer levels, or recharge rates. Although numerous wells have been drilled in the past years, only little information about the underground is available. The drilling of many wells was privately commissioned, consequently they are usually neither registered, nor are there drilling profiles or construction plans. Therefore, as a first step, mapping and geodesic measurements of the numerous wells are highly recommended. On this base, the exact groundwater level can be measured and its fluctuation observed. By knowing the well locations, hydrochemical sampling campaigns could be planned. Natural tracers, e.g. stable isotopes or Cl^-/Br^- ratios might be used to study groundwater mixing within the aquifer or anthropogenic impacts on groundwater. Furthermore, dating of groundwater samples might give information about residence times, which could be important to understand recharge rates. In addition, salt dilution tests within the boreholes could be used to study the underground flow conditions and the location of zones with preferential flow. The application of hydraulic pumping tests could be difficult, since the groundwater level is most likely disturbed by numerous wells that extract groundwater. So, a static water level as a starting point will be unlikely. The resulting superposition of groundwater subsidence might hamper the interpretation of the pumping tests.

This information could help to complement the hydrogeological, conceptual model. Furthermore, it is essential regarding sustainability, if the Vietnamese water management strategy includes the use of the karst aquifer below Dong Van. Otherwise, there might be a high risk of overexploitation and water quality deterioration of the valuable groundwater resource.

5.4 REGIONAL TRANSFERABILITY ASPECTS

The Dong Van area is located at the northeastern rim of the UNESCO Global Geopark (Fig. 5-2) and consists of favourable geological conditions for groundwater availability. In contrast, within the karst plateau south of Dong Van, the groundwater level is very deep. Numerous vertical caves were explored by the Belgian SPEKUL club and by Vietnamese speleologists from VIGMR. They reached depth of up to -341 m in the Hang Ong cave in Pho Bang area or more than -247 m in the Lung Chinh cave, west of Meo Vac (SPEKUL et al. 2005). At the southern rim of the karst plateau, at an elevation of around 250 m asl, the huge Ban Ma karst springs, discharging to the Nhiem River, give evidence of a large

catchment area. This means for most of the cities and villages within the karst plateau, the groundwater table is too deep to extract water with their common methods. Therefore, adapted water supply strategies have to be developed to meet the increasing water demand that has to be expected due to the increasing tourism in the whole Geopark area. But this requires detailed geological and hydrogeological investigations as they were described in this study. Especially artificial tracer tests in combination with natural tracers can help to develop an understanding of the more regional drainage pattern within the karst plateau. In combination with investigations of tectonic structures and speleology surveys, a hydrogeological conceptual model could be developed for larger areas of the karst plateau.



Fig. 5-2 Extent of the Dong Van Karst Plateau Global Geopark (DEM: SRTM, NASA). The Geopark border corresponds to the external borders of the four districts Dong Van, Meo Vac, Yen Minh and Quan Ba.

Not only the Ha Giang province is facing the challenge of water management in subtropical and tropical karst areas, but also other regions within Vietnam, and neighbouring countries. The section of the World Karst Aquifer Map (WOKAM, Fig. 5-3) emphasised the high proportion of carbonate rocks in this part of the world. Especially in South China, wide areas are dominated by karst with similar characteristics to those in Northern Vietnam and comparable challenges in terms of water supply.

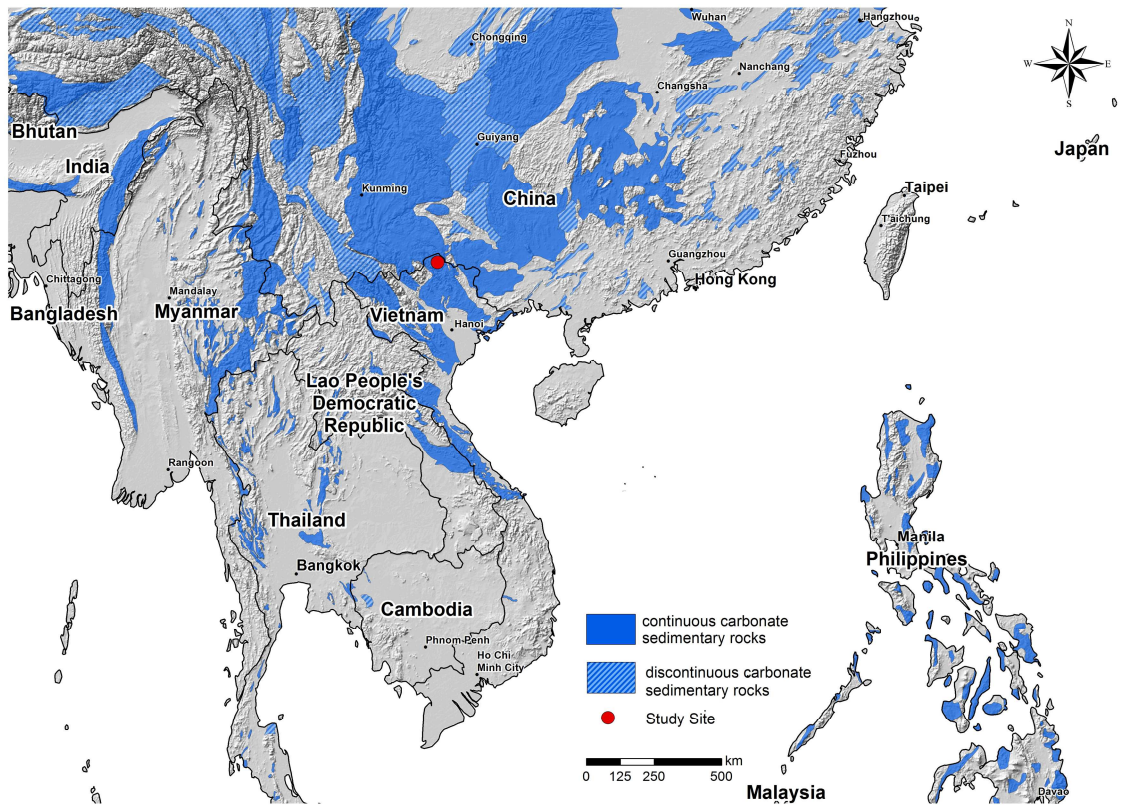


Fig. 5-3 Distribution of carbonate rocks in Southeast Asia (modified after Chen et al. 2017)

The applied approaches and methods used in this study, including tracer tests, hydrochemical studies, on-site monitoring of water quality by using parameters like GLUC activity and particle-size distribution, and analyses of FIB by using Colilert/Colisure are valuable tools to study such areas, even in very remote areas with restricted infrastructure.

In the context of climate change and the increasing world population, the sustainable use and management of karst aquifers will gain more importance and will require profound investigations of the specific karst aquifers, similar to those presented in this thesis. The obtained information are valuable in order to improve the karst water resources management in Dong Van and thus, to enhance the living standards of the local population.

ACKNOWLEDGEMENTS

This work was supported by many people and would not have been possible without their help.

First of all, I want to give my special thanks to Prof. Dr. Nico Goldscheider, who gave me the opportunity to work in this very exciting field of hydrogeology in such an impressive karst area. Many thanks for your support and your advice, that you gave me whenever it was needed. I'm really grateful that you gave me the opportunity to work in this great international project and that you believed in me. I really enjoyed the collaboration with you and I hope to be able to work with you again in the future.

Special thanks go to Nadine Goeppert for her scientific support and her help during the past years. I am very grateful that you joined me on the first two trips to Dong Van and that we can share the unforgettable impressions of Dong Van before the touristic boom began.

I want to thank the whole KaWaTech-Project Team for their support during field work and the great time we spent together in Vietnam. Special thanks go to Arno Hartmann, who spent many weeks with me in Dong Van. Thank you for all the discussions and conversations. Björn Zindler, thank you very much for your support concerning GIS applications and for the great time we spent together in Vietnam and in Karlsruhe. Furthermore, I want to thank Dominik Richter, Georg Kahles, David Walter, Katrin Riester, Daniel Stoffel, Phillip Holz, Pham Tat Thang, Giovanni Banfi, Ulrich Schaaf and Rafael Breiner for the enjoyable and fruitful collaboration on the working level of the KaWaTech project. Prof. Nestmann, Peter Oberle and Philipp Klingel are acknowledged for their great support and their successful coordination of the KaWaTech project. Further thanks go to the SPEKUL team, in particular to David Lagrou, for the great collaboration. Thank you for joining us to the caves and for this great experience!

I would especially like to thank the VIGMR team, namely Ho Tien Chung, Doan The Anh, Tran Diep Anh, Lai Quang Tuan and Do Van Thang. Thanks all of you for your support during my field work, the fruitful discussions and the great time we spent together in Vietnam.

Besides I want to thank Nguyet Vu Thi Minh for the nice meetings and for borrowing the field fluorimeter.

Many thanks go to the students Tra My Nguyen, Marian Bechtel, Tobias Zäge, Christian Weippert, Rainer Schumacher, Luisa Röckel and Matthias Hofer for their commitment, reliable sampling and great time in the field.

Furthermore, I want to thank the laboratory team Daniela Blank, Chris Buschhaus and Christine Roske-Stegemann as well as the secretary Petra Linder for their support and the enjoyable collaboration.

Special thanks are going to Markus Klotz for his great support concerning the particle counters and for his great ideas concerning the applicability under the local conditions in the field.

In addition, many thanks are given to...

... Felix Grimmeisen, for the great collaboration and support during the preparation of my first paper. Our discussions were a big help for me.

...Simon Frank, for the great collaboration concerning the external tracer projects that we have conducted. It was always a pleasure to work together with you.

...Julian Xanke, for reading my manuscript and for the helpful comments and discussions. Furthermore, I want to thank you for the great field work in Jordan.

I would like to thank Simon Frank, Felix Grimmeisen, Julian Xanke, Zhao Chen, Dominik Richter, Tanja Liesch, Nadine Goeppert, Susanne Benz, Michael Augenstein, Daniela Blank, Paulina Alfaro and all other colleagues for the very nice time at the institute and in the field.

Special thanks go to Arica Beisaw, who did the language editing of this work.

The German Federal Ministry of Education and Research (BMBF) are acknowledged for funding the KaWaTech Project [grant number 02WCL1291A] as well as the KaWaTech Solutions Project [grant number 02WCL1415].

Finally, I thank my whole family, especially my parents, for supporting me all time. Many thanks go to my sister-in-law Sabine Frech for reading the manuscript and Marcus Mangeot, who supports, encourages and motivates me since more than a decade.

REFERENCES

- Abberton CL, Bereschenko L, van der Wielen PWJJ, Smith CJ (2016) Survival, Biofilm Formation, and Growth Potential of Environmental and Enteric Escherichia coli Strains in Drinking Water Microcosms. *Applied and Environmental Microbiology* 82: 5320-5331, doi 10.1128/AEM.01569-16
- Abia ALK, Ubomba-Jaswa E, Genthe B, Momba MNB (2016) Quantitative microbial risk assessment (QMRA) shows increased public health risk associated with exposure to river water under conditions of riverbed sediment resuspension. *Science of the Total Environment* 566-567: 1143-1151, doi 10.1016/j.scitotenv.2016.05.155
- Abramson A, Benami M, Weisbrod N (2013) Adapting enzyme-based microbial water quality analysis to remote areas in low-income countries. *Environmental Science & Technology* 47: 10494-10501, doi 10.1021/es402175n
- ADB (2009) Socialist Republic of Viet Nam: Water Sector Review. Asian Development Bank, Ltd. Kellogg Brown & Root Pty, South Australia
- ADB (2009) Water - Vital for Viet Nam's Future. Asian Development Bank, Hanoi, Vietnam
- ADB (2013) Viet Nam - Environment and Climate Change Assessment. Asian Development Bank, Phillipines
- Atkinson TC, Smith DI, Lavis JJ, Witaker RJ (1973) Experiments in tracing underground waters in limestones. *Journal of Hydrology* 19: 323-349, doi 10.1016/0022-1694(73)90106-6
- Bakalowicz M (2005) Karst groundwater: a challenge for new resources. *Hydrogeology Journal* 13: 148-160, doi 10.1007/s10040-004-0402-9
- Barberá JA, Mudarra M, Andreo B, De la Torre B (2017) Regional-scale analysis of karst underground flow deduced from tracing experiments: examples from carbonate aquifers in Malaga province, southern Spain. *Hydrogeology Journal* 26(1):23-40, doi 10.1007/s10040-017-1638-5
- Batiot C, Liñán C, Andreo B, Emblanch C, Carrasco F, Blavoux B (2003) Use of Total Organic Carbon (TOC) as tracer of diffuse infiltration in a dolomitic karstic system: The Nerja Cave (Andalusia, southern Spain). *Geophysical Research Letters* 30, doi 10.1029/2003GL018546
- Baudart J, Coallier J, Laurent P, Prévost M (2002) Rapid and sensitive enumeration of viable diluted cells of members of the family Enterobacteriaceae in freshwater and drinking water. *Applied and Environmental Microbiology* 68: 5057-5063, doi 10.1128/AEM.68.10.5057-5063.2002
- Bear J (1979) *Hydraulics of Groundwater.*, McGraw-Hill, New York
- Bergmeyer H-U (2012) *Methods of enzymatic analysis.* Elsevier

- Bertrand C, Guglielmi Y, Denimal S, Mudry J, Deveze G, Carry N (2015) Hydrochemical response of a fractured carbonate aquifer to stress variations: application to leakage detection of the Vouglans arch dam lake (Jura, France). *Environmental Earth Sciences* 74: 7671-7683, doi 10.1007/s12665-015-4671-5
- Birk S, Geyer T, Liedl R, Sauter M (2005) Process-based interpretation of tracer tests in carbonate aquifers. *Ground Water* 43: 381-388, doi 10.1111/j.1745-6584.2005.0033.x
- BMUB Bundesministerium für Umwelt, Naturschutz, Bau und Reaktorsicherheit (2017) Trinkwasser. <http://www.bmub.bund.de/themen/wasser-abfall-boden/binnengewasser/trinkwasser/>. Cited 09.01.2018
- Brown MC, Wigley TL, Ford DC (1969) Water budget studies in karst aquifers. *Journal of Hydrology* 9: 113-116, doi 10.1016/0022-1694(69)90018-3
- Buytaert W, Celleri R, Willems P, De Bievre B, Wyseure G (2006) Spatial and temporal rainfall variability in mountainous areas: A case study from the south Ecuadorian Andes. *Journal of Hydrology* 329: 413-421, doi 10.1016/j.jhydrol.2006.02.031
- Byappanahalli MN, Nevers MB, Korajkic A, Staley ZR, Harwood VJ (2012) Enterococci in the Environment. *Microbiology and Molecular Biology Reviews* 76: 685-706, doi 10.1128/MMBR.00023-12
- Cai J-X, Zhang K-J (2009) A new model for the Indochina and South China collision during the Late Permian to the Middle Triassic. *Tectonophysics* 467: 35-43 doi 10.1016/j.tecto.2008.12.003
- Caruso G, Crisafi E, Mancuso M (2002) Development of an enzyme assay for rapid assessment of *Escherichia coli* in seawaters. *Journal of Applied Microbiology* 93: 548-556, doi 10.1046/j.1365-2672.2002.01729.x
- Chatfield C (2004) *The analysis of time series: An Introduction*. 6 edn, CRC Press, Taylor & Francis Group
- Chen Z, Auler AS, Bakalowicz M, Drew D, Griger F, Hartmann J, Jiang G, Moosdorf N, Richts A, Stevanovic Z, Veni G, Goldscheider N (2017) The World Karst Aquifer Mapping project: concept, mapping procedure and map of Europe. *Hydrogeology Journal* 25: 771-785, doi 10.1007/s10040-016-1519-3
- Colwell RR, Brayton PR, Grimes DJ, Roszak DB, Huq SA, Palmer LM (1985) Viable but non-culturable *Vibrio cholerae* and related pathogens in the environment: implications for release of genetically engineered microorganisms. *Nature Biotechnology* 3: 817-820, doi 10.1038/nbt0985-817
- Davis JC (2002) *Statistics and data analysis in geology*. John Wiley & Sons, Inc., New York
- Davis JC, Sampson RJ (1986) *Statistics and Data Analysis in Geology*. Wiley, New York
- Day M (2004) Cone Karst. In: Gunn John (ed) *Encyclopedia of caves and karst science*, Taylor & Francis, New York: 495-499

- Dewaide L, Bonniver I, Rochez G, Hallet V (2016) Solute transport in heterogeneous karst systems: dimensioning and estimation of the transport parameters via multi-sampling tracer-tests modelling using the OTIS (One-dimensional transport with inflow and storage) program. *Journal of Hydrology* 534: 567-578, doi 10.1016/j.jhydrol.2016.01.049
- DGMV (2000) Geological Map of Bao Lac: Scale 1:200,000 Department of Geology and Mineral Resources of Vietnam Hanoi
- Dussart-Baptista L, Massei N, Dupont JP, Jouenne T (2003) Transfer of bacteria-contaminated particles in a karst aquifer: evolution of contaminated materials from a sinkhole to a spring. *Journal of Hydrology* 284: 285-295, doi 10.1016/j.jhydrol.2003.08.007
- Emblanch C, Blavoux B, Puig JM, Mudry J (1998) Dissolved organic carbon of infiltration within the autogenic karst hydrosystem. *Geophysical research letters* 25: 1459-1462, doi 10.1029/98GL01056
- Ender A, Goepfert N, Goldscheider N (2018a) Hydrogeological controls of variable microbial water quality in a complex subtropical karst system. *Hydrogeology Journal*, doi 10.1007/s10040-018-1783-5
- Ender A, Goepfert N, Goldscheider N (2018b) Spatial resolution of transport parameters in a subtropical karst conduit system during dry and wet seasons. *Hydrogeology Journal*, doi 10.1007/s10040-018-1746-x
- Ender A, Goepfert N, Grimmeisen F, Goldscheider N (2017) Evaluation of β -d-glucuronidase and particle-size distribution for microbiological water quality monitoring in Northern Vietnam. *Science of the Total Environment* 580: 996-1006, doi 10.1016/j.scitotenv.2016.12.054
- EPA (2009) Statistical Analysis of Groundwater Monitoring Data At RCRA Facilities. U.S. Environmental Protection Agency
- Farnleitner AH, Hocke L, Beiwl C, Kavka GG, Mach RL (2002) Hydrolysis of 4-methylumbelliferyl- β -D-glucuronide in differing sample fractions of river waters and its implication for the detection of fecal pollution. *Water Research* 36: 975-981, doi 10.1016/S0043-1354(01)00288-3
- Ferguson AS, Layton AC, Mailloux BJ, Culligan PJ, Williams DE, Smartt AE, Sayler GS, Feighery J, McKay LD, Knappett PSK (2012) Comparison of fecal indicators with pathogenic bacteria and rotavirus in groundwater. *Science of the Total Environment* 431: 314-322, doi 10.1016/j.scitotenv.2012.05.060
- Field MS, Pinsky PF (2000) A two-region nonequilibrium model for solute transport in solution conduits in karstic aquifers. *Journal of Contaminant Hydrology* 44: 329-351, doi 10.1016/S0169-7722(00)00099-1
- Fiksdal L, Pommepuy M, Caprais MP, Midttun I (1994) Monitoring of fecal pollution in coastal waters by use of rapid enzymatic techniques. *Applied and Environmental Microbiology* 60: 1581-1584

- Fiksdal L, Tryland I (2008) Application of rapid enzyme assay techniques for monitoring of microbial water quality. *Current Opinion in Biotechnology* 19: 289-294, doi 10.1016/j.copbio.2008.03.004
- Filimonau V, Barth JA (2016) From global to local and vice versa: on the importance of the 'Globalization' agenda in continental groundwater research and policy-making. *Environmental Management* 58: 491-503, doi 10.1007/s00267-016-0722-2
- Foppen JWA, Schijven JF (2006) Evaluation of data from the literature on the transport and survival of *Escherichia coli* and thermotolerant coliforms in aquifers under saturated conditions. *Water Research* 40: 401-426, doi 10.1016/j.watres.2005.11.018
- Ford D, Williams P (1989) *Karst geomorphology and hydrology*. 1 edn, Unwin Hyman London
- Ford D, Williams P (2007) *Karst Hydrogeology and Geomorphology*. John Wiley & Sons Ltd, Chichester, UK
- Ford D, Williams P (2013) *Karst hydrogeology and geomorphology*. John Wiley & Sons Ltd
- Fritz J, Rösler W, Schmidt S, Stoffel D, Oberle P, Nestmann F (2012) Using Pumps as Turbines Combined with Pumps for Water Supply in an Efficient Way without the Need of Electrical Power. *GWF Wasser Abwasser* 153: 110-113
- Galfi H, Österlund H, Marsalek J, Viklander M (2016) Indicator bacteria and associated water quality constituents in stormwater and snowmelt from four urban catchments. *Journal of Hydrology* 539: 125-140, doi 10.1016/j.jhydrol.2016.05.006
- Garcia-Armisen T, Lebaron P, Servais P (2005) β -d-glucuronidase activity assay to assess viable *Escherichia coli* abundance in freshwaters. *Letters in Applied Microbiology* 40: 278-282, doi 10.1111/j.1472-765X.2005.01670.x
- George I, Petit M, Servais P (2000) Use of enzymatic methods for rapid enumeration of coliforms in freshwaters. *Journal of Applied Microbiology* 88: 404-413, doi 10.1046/j.1365-2672.2000.00977.x
- Geyer T, Birk S, Licha T, Liedl R, Sauter M (2007) Multitracer test approach to characterize reactive transport in karst aquifers. *Ground Water* 45: 36-45, doi 10.1111/j.1745-6584.2006.00261.x
- Goeppert N, Goldscheider N (2008) Solute and Colloid Transport in Karst Conduits under Low- and High-Flow Conditions. *Ground Water* 46: 61-68 doi 10.1111/j.1745-6584.2007.00373.x
- Goeppert N, Goldscheider N (2011) Transport and variability of fecal bacteria in carbonate conglomerate aquifers. *Ground Water* 49: 77-84 doi 10.1111/j.1745-6584.2010.00741.x
- Goldscheider N, Drew D (2007) *Methods in Karst Hydrogeology*. IAH: International Contributions to Hydrogeology, 26, Taylor & Francis Group, London, UK
- Goldscheider N, Hunkeler D, Rossi P (2006) Review: microbial biocenoses in pristine aquifers and an assessment of investigative methods. *Hydrogeology Journal* 14: 926-941, doi 10.1007/s10040-005-0009-9

- Goldscheider N, Meiman J, Pronk M, Smart C (2008) Tracer tests in karst hydrogeology and speleology. *International Journal of Speleology* 37: 3, doi 10.5038/1827-806X.37.1.3
- Goldscheider N, Pronk M, Zopfi J (2010) New insights into the transport of sediments and microorganisms in karst groundwater by continuous monitoring of particle-size distribution. *Geologia Croatica* 63: 137-142, doi 104154/gc.2010.10
- Gremaud V, Goldscheider N, Savoy L, Favre G, Masson H (2009) Geological structure, recharge processes and underground drainage of a glacierised karst aquifer system, Tsanfleuron-Sanetsch, Swiss Alps. *Hydrogeology Journal* 17: 1833-1848, doi 10.1007/s10040-009-0485-4
- Groves C (2007) Hydrological methods. In: Goldscheider Nico, Drew David (eds) *Methods in Karst Hydrogeology*, Taylor & Francis Group, London, UK:
- Haack SK, Duris JW, Kolpin DW, Focazio MJ, Meyer MT, Johnson HE, Oster RJ, Foreman WT (2016) Contamination with bacterial zoonotic pathogen genes in US streams influenced by varying types of animal agriculture. *Science of the Total Environment* 563: 340-350, doi 10.1016/j.scitotenv.2016.04.087
- Hanoitimes (2017) Ha Giang issues action plan to lure 800,000 visitors by 2020. <http://hanoitimes.com.vn/travel/2017/12/81e0be93/ha-giang-issues-action-plan-to-lure-800-000-visitors-by-2020/>. Cited 08.01.2018
- Hauns M, Jeannin P-Y, Atteia O (2001) Dispersion, retardation and scale effect in tracer breakthrough curves in karst conduits. *Journal of Hydrology* 241: 177-193, doi 10.1016/S0022-1694(00)00366-8
- Heery B, Briciu-Burghina C, Zhang D, Duffy G, Brabazon D, O'Connor N, Regan F (2016) ColiSense, today's sample today: A rapid on-site detection of beta-d-Glucuronidase activity in surface water as a surrogate for *E. coli*. *Talanta* 148: 75-83, doi 10.1016/j.talanta.2015.10.035
- Helsel D, Hirsch R (2002) *Statistical methods in water resources: US Geological Survey Techniques of Water Resources Investigations. Book 4, Chapter A3*, USGS, Reston, VA
- IDEXX Laboratories I (2011) Colisure test procedure. IDEXX, Westbrook, ME. <https://www.idexx.com/en/water/water-products-services/colisure/>. Accessed 27 March 2018
- Jiang Y, Wu Y, Groves C, Yuan D, Kambesis P (2009) Natural and anthropogenic factors affecting the groundwater quality in the Nandong karst underground river system in Yunan, China. *Journal of Contaminant Hydrology* 109: 49-61, doi 10.1016/j.jconhyd.2009.08.001
- Kačaroğlu F (1999) Review of groundwater pollution and protection in karst areas. *Water, Air, & Soil Pollution* 113: 337-356, doi 10.1023/A:1005014532330
- Kaiser HF, Rice J (1974) Little Jiffy, Mark IV. *Educational and psychological measurement* 34: 111-117

- Kapembo ML, Laffite A, Bokolo MK, Mbanga AL, Maya-Vangua MM, Otamonga J-P, Mulaji CK, Mpiana PT, Wildi W, Poté J (2016) Evaluation of Water Quality from Suburban Shallow Wells Under Tropical Conditions According to the Seasonal Variation, Bumbu, Kinshasa, Democratic Republic of the Congo. *Exposure and Health* 8: 487-496, doi 10.1007/s12403-016-0213-y
- Käss W (2004) *Geohydrologische Markierungstechnik*. Gebrüder Borntraeger, Stuttgart, Germany
- KaWaTech (2018) BMBF joint project KaWaTech Solutions. www.kawatech.kit.edu/. Cited 30.01.2018
- Khang P (1985) The development of karst landscapes in Vietnam. *Acta Geologica Polonica* 35: 305-324
- Kilian M, Bülow P (1979) Rapid identification of Enterobacteriaceae. *Acta Pathologica Microbiologica Scandinavica Section B Microbiology* 87: 271-276
- Koschelnic J, Vogl W, Epp M, Lackner M (2015) Rapid analysis of β -D-glucuronidase activity in water using fully automated technology. Paper presented at the 8th International Conference on Sustainable Water Resources Management Development, A Coruna, Spain 2015
- Kostyla C, Bain R, Cronk R, Bartram J (2015) Seasonal variation of fecal contamination in drinking water sources in developing countries: A systematic review. *Science of the Total Environment* 514: 333-343, doi 10.1016/j.scitotenv.2015.01.018
- Kumpel E, Nelson KL (2013) Comparing microbial water quality in an intermittent and continuous piped water supply. *Water Research* 47: 5176-5188, doi 10.1016/j.watres.2013.05.058
- Kumpel E, Nelson KL (2014) Mechanisms affecting water quality in an intermittent piped water supply. *Environmental Science & Technology* 48: 2766-2775, doi 10.1021/es405054u
- Kumpel E, Nelson KL (2016) Intermittent Water Supply: Prevalence, Practice, and Microbial Water Quality. *Environmental Science & Technology* 50: 542-553, doi 10.1021/acs.est.5b03973
- Lauber U, Ufrecht W, Goldscheider N (2014) Spatially resolved information on karst conduit flow from in-cave dye tracing. *Hydrology and Earth System Sciences* 18: 435-445, doi 10.5194/hess-18-435-2014
- Lepvrier C, Faure M, Van VN, Van Vu T, Lin W, Trong TT, Hoa PT (2011) North-directed Triassic nappes in Northeastern Vietnam (East Bac Bo). *Journal of Asian Earth Sciences* 41: 56-68, doi 10.1016/j.jseaes.2011.01.002
- Linh K (2017) Continue to improve the law on water resources. MONRE <http://www.monre.gov.vn/wps/portal/news>. Cited 07.01.2018
- Liu Y, Batelaan O, Huong N, Tam VT, De Smedt F (2004) Flood prediction in the karstic Suoimuoi catchment, Vietnam. *Trans-KARST* 2004: 139

- Luhmann AJ, Covington MD, Alexander SC, Chai SY, Schwartz BF, Groten JT, Alexander EC (2012) Comparing conservative and nonconservative tracers in karst and using them to estimate flow path geometry. *Journal of Hydrology* 448: 201-211, doi 10.1016/j.jhydrol.2012.04.044
- Mahler BJ, Personné JC, Lods GF, Drogue C (2000) Transport of free and particulate-associated bacteria in karst. *Journal of Hydrology* 238: 179-193, doi 10.1016/S0022-1694(00)00324-3
- Maliva RG (2016) *Karst Aquifer Characterization Techniques*, Springer International Publishing: 545-570
- Massei N, Wang HQ, Field MS, Dupont JP, Bakalowicz M, Rodet J (2006) Interpreting tracer breakthrough tailing in a conduit-dominated karstic aquifer. *Hydrogeology Journal* 14: 849-858, doi 10.1007/s10040-005-0010-3
- McKinney RE (2004) *Environmental pollution control microbiology: a fifty-year perspective*. Marcel Dekker, Inc., New York
- MONRE (2006) *National Water Resources Strategy - Towards the year 2020*. Ministry of Natural Resources and Environment. Culture-Information Publishing House, Hanoi
- Montgomery MA, Elimelech M (2007) Water and sanitation in developing countries: including health in the equation. *Environmental Science & Technology* 41: 17-24
- Morales T, de Valderrama IF, Uriarte JA, Antigüedad I, Olazar M (2007) Predicting travel times and transport characterization in karst conduits by analyzing tracer-breakthrough curves. *Journal of Hydrology* 334: 183-198, doi 10.1016/j.jhydrol.2006.10.006
- Mouret C (2004) Asia, southeast In: Gunn John (ed) *Encyclopedia of Caves and Karst Science*. Fitzroy Dearborn, New York: 210-217
- Nguyen NT, Pham NH, Pham XC, Nguyen TTH, Duong TTT (2013) Application of multimedia methodology for investigation of karst water in highland regions of Ha Giang Province, Vietnam. *Environmental Earth Sciences* 70: 531-542, doi 10.1007/s12665-013-2617-3
- Nguyen TPL (2013) *The Legal Framework of Vietnam's Water Sector: Update 2013*. ZEF Zentrum für Entwicklungsforschung, Bonn, Working Paper 116
- Nguyet VTM, Goldscheider N (2006) Tracer tests, hydrochemical and microbiological investigations as a basis for groundwater protection in a remote tropical mountainous karst area, Vietnam. *Hydrogeology Journal* 14: 1147-1159, doi 10.1007/s10040-006-0038-z
- Nguyet VTM, Thanh VP, Hai VD, Roi ND, Tra DTT (2016) Hydrogeochemical characterization and groundwater quality of the Dong Giao karst aquifer in Tam Diep, Ninh Binh, Vietnam. *Acta Carsologica* 45: 233
- Nicod J (2003) A little contribution to the karst terminology: special or aberrant cases of poljes? *Acta Carsologica* 32(2): 29-39
- Noble RT, Weisberg SB (2005) A review of technologies for rapid detection of bacteria in recreational waters. *Journal of Water and Health* 3: 381-392, doi 10.2166/wh.2005.051

- Oberle P, Stoffel D, Walter D, Breiner R, Vogel M, Müller HS, Nestmann F (2017) Innovative Technologien zur Wasserförderung und-verteilung in Gebirgsregionen. *Bautechnik* 94: 514-525, doi 10.1002/bate.201700066
- Parkhurst DL, Appelo C (1999) User's guide to PHREEQC (Version 2): A computer program for speciation, batch-reaction, one-dimensional transport, and inverse geochemical calculations. US Geological Survey Techniques of Water Resources Investigation Report 99-4259
- Petit M, George I, Servais P (2000) Survival of *Escherichia coli* in freshwater: β -D-glucuronidase activity measurements and characterization of cellular states. *Canadian Journal of Microbiology* 46: 679-684 doi 10.1139/w00-040
- Press WH, Teukolsky SA, Vetterling WT, Flannery BP (1992) *Numerical Recipes in C*, 2nd edit. Cambridge University, New York
- Pronk M, Goldscheider N, Zopfi J (2006) Dynamics and interaction of organic carbon, turbidity and bacteria in a karst aquifer system. *Hydrogeology Journal* 14: 473-484, doi 10.1007/s10040-005-0454-5
- Pronk M, Goldscheider N, Zopfi J (2007) Particle-size distribution as indicator for fecal bacteria contamination of drinking water from karst springs. *Environmental Science & Technology* 41: 8400-8405, doi 10.1021/es071976f
- Prüss A (1998) Review of epidemiological studies on health effects from exposure to recreational water. *International Journal of Epidemiology* 27: 1-9, doi 10.1093/ije/27.1.1
- Reshes G, Vanounou S, Fishov I, Feingold M (2008) Cell shape dynamics in *Escherichia coli*. *Biophysical Journal* 94: 251-264, doi 10.1529/biophysj.107.104398
- Richardson M, Moore RD, Zimmermann A (2017) Variability of tracer breakthrough curves in mountain streams: Implications for streamflow measurement by slug injection. *Canadian Water Resources Journal/Revue Canadienne des Ressources Hydriques* 42: 21-37, doi 10.1080/07011784.2016.1212676
- Rompré A, Servais P, Baudart J, de-Roubin M-R, Laurent P (2002) Detection and enumeration of coliforms in drinking water: current methods and emerging approaches. *Journal of Microbiological Methods* 49: 31-54, doi 10.1016/S0167-7012(01)00351-7
- Runkel RL (1998) One-dimensional transport with inflow and storage (OTIS): A solute transport model for streams and rivers US Department of the Interior, US Geological Survey, Reston, VA
- Runkel RL, Broshears RE (1991) One-dimensional transport with inflow and storage (OTIS): a solute transport model for small streams. CADSWES, University of Colorado, Boulder, CO
- Ryzinska-Paier G, Lendenfeld T, Correa K, Stadler P, Blaschke AP, Mach RL, Stadler H, Kirschner AKT, Farnleitner AH (2014) A sensitive and robust method for automated on-line monitoring of enzymatic activities in water and water resources. *Water Science and Technology* 69: 1349-1358, doi 10.2166/wst.2014.032

- Schets FM, During M, Italiaander R, Heijnen L, Rutjes SA, Van der Zwaluw WK, de Roda Husman AM (2005) *Escherichia coli* O157: H7 in drinking water from private water supplies in the Netherlands. *Water Research* 39: 4485-4493, doi 10.1016/j.watres.2005.08.025
- Schillinger JE, Gannon JJ (1985) Bacterial adsorption and suspended particles in urban stormwater. *Journal Water Pollution Control Federation* 57: 384-389
- Schnegg P-A (2002) An inexpensive field fluorometer for hydrogeological tracer tests with three tracers and turbidity measurement. XXXII IAH and ALHSUD congress on Groundwater and Human Development, Mar del Plata, Argentina, Balkena, Rotterdam, The Netherlands, pp. 1484-1488
- Servais P, Garcia-Armisen T, Lepeuple AS, Lebaron P (2005) An early warning method to detect faecal contamination of river waters. *Annals of Microbiology* 55: 151-156
- Sigma-Aldrich (1998) Enzymatic Assay of β -GLUCURONIDASE (EC 3.2.1.31) from *E. coli*. Sigma-Aldrich <http://www.sigmaaldrich.com/technical-documents/protocols/biology/enzymatic-assay-of-b-glucuronidase-from-ecoli.html>. Cited 09.08.2016
- SPEKUL, BVKCA, RIGMR (2005) Belgian - Vietnamese Speleological Expedition 2003 - 2004. Report of the seventh expedition in the provinces (district) of Hoa Binh (Tan Lac), Bac Kan (Ba Be) and Ha Giang (Dong Van and Meo Vac). (not published)
- Stadler P, Blöschl G, Vogl W, Koschelnik J, Epp M, Lackner M, Oismüller M, Kumpan M, Nemeth L, Strauss P (2016) Real-time monitoring of beta-d-glucuronidase activity in sediment laden streams: A comparison of prototypes. *Water Research* 101: 252-261, doi 10.1016/j.watres.2016.05.072
- Stallard MA, Otter RR, Winesett S, Barbero M, Bruce M, Layton A, Bailey FC (2016) A Watershed Analysis of Seasonal Concentration-and Loading-based Results for *Escherichia coli* in Inland Waters. *Bulletin of Environmental Contamination and Toxicology* 97: 838-842, doi 10.1007/s00128-016-1928-y
- Stevanovic Z (2015) *Karst aquifers-characterization and engineering*. Springer, Cham, Switzerland
- Tam V, Vu T, Batelaan O (2001) Hydrogeological characteristics of a karst mountainous catchment in the northwest of Vietnam. *Acta Geologica Sinica (English Edition)* 75: 260-268
- Tam VT, Batelaan O (2011) A multi-analysis remote-sensing approach for mapping groundwater resources in the karstic Meo Vac Valley, Vietnam. *Hydrogeology Journal* 19(2): 275-287, doi 10.1007/s10040-010-0684-z
- Tang G, Mayes MA, Parker JC, Jardine PM (2010) CXTFIT/Excel—A modular adaptable code for parameter estimation, sensitivity analysis and uncertainty analysis for laboratory or field tracer experiments. *Computers & Geosciences* 36: 1200-1209, doi 10.1016/j.cageo.2010.01.013

- Togo CA, Wutor VC, Pletschke BI (2006) Properties of in situ *Escherichia coli*-D-glucuronidase (GUS): evaluation of chemical interference on the direct enzyme assay for faecal pollution detection in water. *African Journal of Biotechnology* 5: 2338-2344
- Toride N, Leij FJ, Van Genuchten MT (1993) A comprehensive set of analytical solutions for nonequilibrium solute transport with first-order decay and zero-order production. *Water Resources Research* 29: 2167-2182, doi 10.1029/93WR00496
- Toride N, Leij FJ, Van Genuchten MT (1995) The CXTFIT code for estimating transport parameters from laboratory or field tracer experiments. US Salinity Laboratory, Riverside, CA
- Toride N, Leij FJ, Van Genuchten MT (1999) The CXTFIT code for estimating transport parameters from laboratory or field tracer experiments. Research Report No. 137. US Salinity Laboratory, USDA, ARS, Riverside, CA
- Tran HT, Van Dang B, Ngo CK, Hoang QD, Nguyen QM (2013) Structural controls on the occurrence and morphology of karstified assemblages in northeastern Vietnam: a regional perspective. *Environmental Earth Sciences* 70: 511-520, doi 10.1007/s12665-011-1057-1
- Tryland I, Fiksdal L (1998) Enzyme Characteristics of β -d-Galactosidase and β -d-Glucuronidase-Positive Bacteria and Their Interference in Rapid Methods for Detection of Waterborne Coliforms and *Escherichia coli*. *Applied and Environmental Microbiology* 64: 1018-1023
- Tuyet D (2001) Characteristics of karst ecosystems of Vietnam and their vulnerability to human impact. *Acta Geologica Sinica (English Edition)* 75: 325-329, doi 10.1111/j.1755-6724.2001.tb00539.x
- UNDP (2017) United Nations Development Programme in Viet Nam. About Viet Nam. <http://www.vn.undp.org/content/vietnam/en/home/countryinfo/>. Cited 10.01.2018
- UNESCO (2017a) 2017 UN World Water Development Report, Wastewater: The Untapped Resource. <http://www.unesco.org/new/en/natural-sciences/environment/water/wwap/wwdr/2017-wastewater-the-untapped-resource/>. Cited 10.01.2018
- UNESCO (2017b) Dong Van Karst Plateau UNESCO Global Geopark (Viet Nam). <http://www.unesco.org/new/en/natural-sciences/environment/earth-sciences/unesco-global-geoparks/list-of-unesco-global-geoparks/viet-nam/dong-van-karst-plateau/>. Cited 08.01.2018
- UNICEF (2017) Water and Sanitation: Current Status + Progress. <https://data.unicef.org/topic/water-and-sanitation/sanitation/>. Cited 10.01.2018
- US Environmental Protection Agency E (2012) Recreational Water Quality Criteria. EPA-820-F-12-061, US EPA, Washington, DC
- USCB (2017) United States Census Bureau, International Programs. World Population, www.census.gov/population/international/data/worldpop/table_population.php

- van Genuchten MT, Šimůnek J, Leij FJ, Toride N, Šejna M (2012) STANMOD: model use, calibration, and validation. *American Society of Agricultural and Biological Engineers* 55(4): 1353-1366, doi 10.13031/2013.42247
- Van Nguyen L, Nguyen NK, Van Hoang H, Tran TQ, Vu NT (2013) Characteristics of groundwater in karstic region in northeastern Vietnam. *Environmental Earth Sciences* 70: 501-510, doi 10.1007/s12665-012-1548-8
- Viet Nam News (2015) Ceaseless drought plagues Dong Van. <http://vietnamnews.vn/environment/268602/ceaseless-drought-plagues-dong-van.html#fuFREuqxKTkaMphY.97>. Cited 08.01.2018
- Vietnam Law & Legal Forum (2006) Decision No. 81/2006/QĐ-TTg of April 14, 2006, Approving the national strategy on water resources to 2020.
- VIGMR (unpublished) Geological Map of Ha Giang; Scale 1:50,000 Vietnam Institute of Geosciences and Mineral Resources, Hanoi
- Vogel LJ, Edge TA, O'Carroll DM, Solo-Gabriele HM, Kushnir CS, Robinson CE (2017) Evaluation of methods to sample fecal indicator bacteria in foreshore sand and pore water at freshwater beaches. *Water Research* 121: 204-212, doi 10.1016/j.watres.2017.05.021
- Waibel G (2010) State management in transition: understanding water resources management in Vietnam. ZEF Working Paper Series, Bonn
- Waltham T (2008) Fengcong, fenglin, cone karst and tower karst. *Cave Karst Science* 35: 77-88
- WB World Bank (2017) Vietnam Data. <https://data.worldbank.org/country/vietnam>. Cited 07.01.2018
- White WB (1988) *Geomorphology and hydrology of karst terrains*. Oxford University Press, New York
- WHO (2008) *Guidelines for drinking-water quality: Recommendations*. 3 edn, WHO, Geneva
- WHO (2017) *Drinking-water*. <http://www.who.int/mediacentre/factsheets/fs391/en/>. Cited 10.01.2018
- Wildeboer D, Amirat L, Price RG, Abuknesha RA (2010) Rapid detection of *Escherichia coli* in water using a hand-held fluorescence detector. *Water Research* 44: 2621-2628, doi 10.1016/j.watres.2010.01.020
- Williams PW (1987) Geomorphic inheritance and the development of tower karst. *Earth surface processes and landforms* 12: 453-465
- Worthington SR (2009) Diagnostic hydrogeologic characteristics of a karst aquifer (Kentucky, USA). *Hydrogeology Journal* 17: 1665-1678, doi 10.1007/s10040-009-0489-0
- Wutor VC, Togo CA, Pletschke BI (2007) Comparison of the direct enzyme assay method with the membrane filtration technique in the quantification and monitoring of microbial indicator organisms—seasonal variations in the activities of coliforms and *E. coli*, temperature and pH. *Water SA* 33: 107-110

- WWAP (2015) The United Nations World Water Development Report 2015: Water for a sustainable world. United Nations World Water Assessment Programme, UNESCO, Paris
- Zech A, Attinger S, Cvetkovic V, Dagan G, Dietrich P, Fiori A, Rubin Y, Teutsch G (2015) Is unique scaling of aquifer macrodispersivity supported by field data? *Water Resources Research* 51: 7662-7679, doi 10.1002/2015WR017220
- Zindler B, Degen A, Stolpe H (2015) Übersichtskarte Flusseinzugsgebiet Ma Le Fluss, Ha Giang, Vietnam. Unpublished project results KaWaTech. RUB Bochum
- Zindler B, Stolpe H (in preparation) Methodenhandbuch. FuE-Verbundvorhaben KaWaTech, Teilprojekt 7: Ländliche Entwicklung, Ressourcenschutz und sozio-kulturelle Aspekte

SUPPLEMENTARY INFORMATION

SUPPLEMENTARY MATERIAL – CHAPTER 2

Suppl. Table 1 Physicochemical parameters for the different sampling points, which were used for the principal component analysis (Fig. 2–3).

Sampling point	Statistical Analysis	pH	EC	O ₂	Temp	Ca ²⁺	Mg ²⁺	HCO ₃ ⁻	K ⁺	Na ⁺	Cl ⁻	SO ₄ ²⁻	NO ₃ ⁻
		[-]	[μS/cm]	[mg/L]	[°C]	[mg/L]	[mg/L]	[mg/L]	[mg/L]	[mg/L]	[mg/L]	[mg/L]	[mg/L]
CSP1	n	5	5	5	5	5	5	5	5	5	5	5	5
	Min	7.26	292.00	7.78	18.70	45.12	8.20	183.05	0.15	0.18	0.42	1.72	1.63
	Max	7.81	321.00	7.97	18.90	57.22	9.19	237.97	0.27	0.49	0.93	6.17	6.99
	Mean	7.51	306.20	7.86	18.80	50.14	8.63	208.07	0.20	0.27	0.56	2.73	5.46
	Std. deviation	0.18	11.02	0.06	0.09	3.99	0.39	17.94	0.04	0.12	0.19	1.72	1.94
CSP2	n	5	5	5	5	5	5	5	5	5	5	5	5
	Min	7.67	231.00	8.10	18.20	34.20	6.48	131.19	0.35	0.26	0.82	1.68	1.52
	Max	8.02	249.00	8.21	18.30	39.61	7.79	173.90	0.46	0.49	1.43	6.62	8.47
	Mean	7.77	239.80	8.16	18.24	37.01	6.96	152.66	0.39	0.35	0.97	2.82	6.33
	Std. deviation	0.13	7.30	0.05	0.05	2.28	0.54	14.05	0.04	0.08	0.23	1.91	2.47
CSP3	n	5	5	5	5	5	5	5	5	5	5	5	5
	Min	8.02	169.40	8.03	14.30	30.80	2.56	115.93	0.41	0.44	0.59	2.86	2.05
	Max	8.20	217.00	9.30	21.80	37.20	3.03	143.39	0.90	1.07	0.95	4.11	4.94
	Mean	8.14	193.56	8.58	18.66	33.83	2.75	128.14	0.58	0.89	0.73	3.26	3.73
	Std. deviation	0.07	16.71	0.42	2.60	2.12	0.18	9.25	0.19	0.23	0.13	0.45	0.93
CSP4	n	4	4	4	4	4	4	4	4	4	4	4	4
	Min	7.96	187.00	8.00	14.30	34.14	2.48	112.88	0.43	0.41	0.58	2.93	3.69
	Max	8.11	217.00	9.24	21.00	37.00	3.11	152.54	0.88	1.86	2.12	4.10	5.03
	Mean	8.06	199.48	8.56	17.95	34.87	2.86	129.66	0.59	1.06	1.07	3.34	4.22
	Std. deviation	0.06	12.64	0.44	2.39	1.23	0.24	14.39	0.17	0.52	0.62	0.45	0.49
CST1	n	4	4	4	4	4	4	4	4	4	4	4	4
	Min	7.92	169.40	7.62	13.80	30.38	2.52	118.98	0.37	0.54	0.59	2.93	1.88
	Max	8.18	211.00	9.25	24.30	36.00	3.03	140.34	0.83	1.02	0.78	4.18	4.84
	Mean	8.07	190.68	8.29	19.53	32.98	2.71	127.37	0.53	0.85	0.68	3.54	3.43
	Std. deviation	0.10	16.28	0.62	4.05	2.00	0.21	7.89	0.18	0.18	0.07	0.55	1.07
CST2	n	4	4	4	4	4	4	4	4	4	4	4	4
	Min	8.02	169.00	7.60	18.10	30.56	2.53	112.88	0.34	0.50	0.63	2.91	2.02
	Max	8.21	216.00	8.51	24.30	37.00	3.11	137.29	0.95	1.05	0.92	3.94	4.83
	Mean	8.15	190.00	8.09	21.25	32.57	2.76	121.27	0.56	0.83	0.75	3.42	3.52
	Std. deviation	0.07	16.81	0.32	2.20	2.60	0.23	9.97	0.23	0.21	0.10	0.39	1.05
CST3	n	5	5	4	5	5	5	5	5	5	5	5	5
	Min	7.23	290.00	5.77	18.10	46.39	4.02	192.20	0.51	0.53	0.42	0.50	2.92
	Max	7.70	337.00	6.67	19.80	60.83	5.92	219.66	1.90	2.24	0.98	1.77	6.44
	Mean	7.39	311.80	6.21	19.32	55.35	5.00	203.80	0.83	1.70	0.79	1.12	5.35
	Std. deviation	0.17	15.92	0.33	0.63	4.82	0.78	10.81	0.53	0.62	0.19	0.40	1.27
FS1	n	5	5	5	5	5	5	5	5	5	5	5	5
	Min	7.53	254.00	7.59	17.70	47.22	1.05	149.49	0.18	0.12	0.26	4.59	7.02
	Max	7.80	270.00	7.88	18.10	54.20	1.32	173.90	0.49	0.45	0.67	9.24	10.37
	Mean	7.66	264.60	7.75	17.88	51.45	1.23	157.42	0.40	0.20	0.39	6.48	8.99
	Std. deviation	0.11	5.78	0.10	0.16	2.46	0.10	8.97	0.11	0.12	0.14	1.56	1.25

Continuation of Suppl. Table 1

Sampling point	Statistical Analysis	pH	EC	O ₂	Temp	Ca ²⁺	Mg ²⁺	HCO ₃ ⁻	K ⁺	Na ⁺	Cl ⁻	SO ₄ ²⁻	NO ₃ ⁻
		[-]	[μS/cm]	[mg/L]	[°C]	[mg/L]	[mg/L]	[mg/L]	[mg/L]	[mg/L]	[mg/L]	[mg/L]	[mg/L]
FS2	n	5	5	5	5	5	5	5	5	5	5	5	5
	Min	7.56	298.00	6.98	16.90	56.64	1.44	180.00	0.15	0.13	0.24	5.79	5.62
	Max	7.81	318.00	7.80	18.30	73.53	1.76	201.36	0.55	0.51	0.48	7.78	8.49
	Mean	7.64	305.00	7.41	17.60	61.59	1.55	189.76	0.45	0.24	0.37	6.68	7.36
	Std. deviation	0.09	7.38	0.28	0.57	6.39	0.11	7.81	0.15	0.14	0.09	0.68	1.17
FS3	n	5	5	5	5	5	5	5	5	5	5	5	5
	Min	7.30	306.00	7.67	18.80	57.32	1.26	183.05	0.12	0.11	0.24	5.16	6.29
	Max	7.62	327.00	7.97	19.10	62.40	1.78	198.30	0.71	0.39	0.52	9.95	13.25
	Mean	7.44	317.00	7.83	18.94	60.24	1.64	190.98	0.49	0.20	0.37	7.59	10.40
	Std. deviation	0.15	7.40	0.12	0.14	1.85	0.20	4.96	0.20	0.11	0.09	1.61	2.37
FS4	n	5	5	5	5	5	5	5	5	5	5	5	5
	Min	7.11	296.00	7.46	17.00	55.07	1.82	192.20	0.31	0.23	0.46	2.31	4.62
	Max	7.98	338.00	8.50	19.30	66.96	2.14	207.46	0.65	0.46	0.57	9.26	9.95
	Mean	7.52	313.20	7.86	18.48	60.61	2.02	198.91	0.47	0.35	0.50	4.77	8.59
	Std. deviation	0.34	15.99	0.37	0.89	3.89	0.13	5.92	0.11	0.09	0.04	2.38	2.00
FS5	n	3	3	3	3	3	3	3	3	3	3	3	3
	Min	7.50	372.00	7.85	16.70	67.80	1.44	225.76	0.17	0.23	0.27	2.14	4.86
	Max	7.83	377.00	8.12	18.00	75.80	1.79	244.07	0.33	0.33	0.40	10.16	12.95
	Mean	7.71	374.33	7.99	17.53	70.95	1.56	236.95	0.24	0.28	0.35	6.68	8.14
	Std. deviation	0.15	2.05	0.11	0.59	3.48	0.16	8.01	0.06	0.04	0.06	3.36	3.48
FS6	n	5	5	5	5	5	5	5	5	5	5	5	5
	Min	7.09	303.50	7.22	19.20	54.06	3.29	189.15	0.38	0.18	0.35	2.37	3.43
	Max	7.46	320.00	7.73	19.30	61.00	4.20	207.46	0.51	0.44	0.64	6.02	7.93
	Mean	7.28	312.70	7.39	19.28	57.84	3.70	197.69	0.42	0.31	0.50	3.42	6.42
	Std. deviation	0.13	5.58	0.19	0.04	2.63	0.38	7.06	0.05	0.10	0.10	1.36	1.59
KS1	n	5	5	5	5	5	5	5	5	5	5	5	5
	Min	7.17	360.00	6.54	18.50	63.07	4.27	222.71	0.30	0.36	0.94	2.10	1.35
	Max	7.58	390.00	6.99	20.60	71.38	4.59	259.32	1.46	1.39	1.55	3.23	6.86
	Mean	7.42	368.60	6.76	19.70	67.80	4.40	244.07	0.66	0.96	1.11	2.53	4.77
	Std. deviation	0.14	11.43	0.16	0.77	3.15	0.14	13.09	0.44	0.37	0.23	0.51	2.14
KS2	n	5	4	5	5	5	5	5	5	5	5	5	5
	Min	7.40	356.00	6.93	18.90	60.03	4.64	216.61	0.31	0.43	1.15	2.03	1.97
	Max	7.81	377.00	7.89	20.90	71.16	5.39	266.64	1.28	2.01	3.28	3.08	6.97
	Mean	7.62	367.00	7.40	20.06	66.18	4.96	240.04	0.65	1.38	1.71	2.48	5.02
	Std. deviation	0.15	9.57	0.33	0.72	4.05	0.31	18.71	0.38	0.58	0.80	0.43	1.88
KS3	n	5	5	5	5	5	5	5	5	5	5	5	5
	Min	7.18	325.00	2.65	19.90	49.25	7.20	213.56	0.47	0.47	1.77	1.31	1.53
	Max	7.62	360.00	5.42	20.60	56.60	8.19	228.81	2.35	2.63	2.69	4.66	7.43
	Mean	7.39	339.00	4.63	20.18	52.89	7.89	219.36	1.03	2.07	2.14	2.27	4.98
	Std. deviation	0.15	13.62	1.00	0.34	2.89	0.38	6.57	0.72	0.80	0.30	1.24	2.19
KS5	n	4	4	4	4	4	4	4	4	4	4	4	4
	Min	7.54	295.00	5.53	15.70	54.50	3.44	180.00	0.08	0.05	0.38	3.38	6.04
	Max	8.14	346.00	8.35	20.10	66.00	4.32	237.97	0.23	0.40	0.77	8.42	7.93
	Mean	7.92	328.75	7.22	18.03	59.80	3.80	207.46	0.14	0.25	0.53	5.36	7.03
	Std. deviation	0.23	20.44	1.04	1.87	4.88	0.34	21.25	0.06	0.13	0.15	2.07	0.72
KS6	n	5	5	5	5	5	5	5	5	5	5	5	5
	Min	7.11	353.00	6.61	19.60	62.04	2.99	244.07	0.32	0.36	0.77	1.76	1.93
	Max	7.34	408.00	9.38	20.10	77.80	5.40	286.78	1.02	1.62	1.17	5.38	7.79
	Mean	7.18	381.80	7.54	19.72	71.17	4.31	261.76	0.54	1.03	0.99	3.01	5.49
	Std. deviation	0.08	18.56	1.02	0.19	5.36	0.91	14.75	0.25	0.47	0.14	1.32	2.02

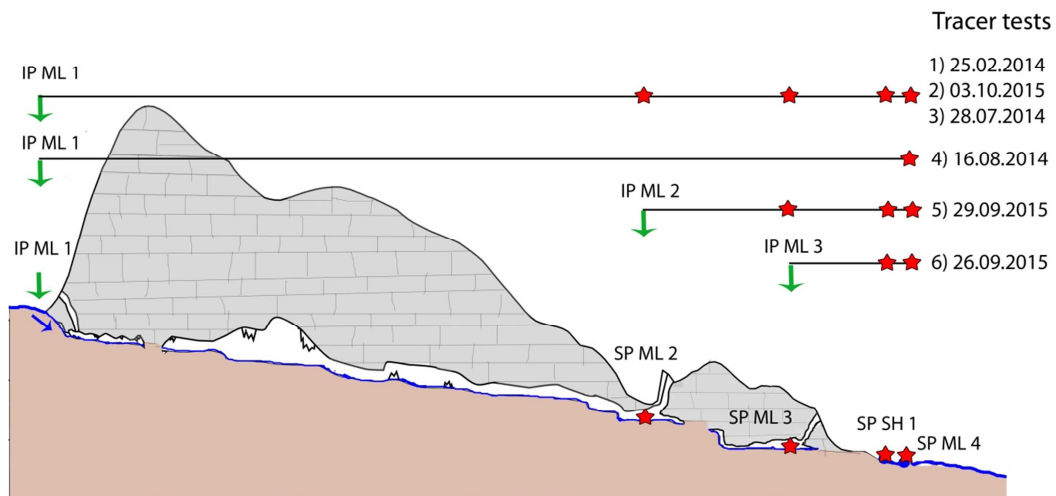
Continuation of Suppl. Table 1

Sampling point	Statistical Analysis	pH	EC	O ₂	Temp	Ca ²⁺	Mg ²⁺	HCO ₃ ⁻	K ⁺	Na ⁺	Cl ⁻	SO ₄ ²⁻	NO ₃ ⁻
		[-]	[μS/cm]	[mg/L]	[°C]	[mg/L]	[mg/L]	[mg/L]	[mg/L]	[mg/L]	[mg/L]	[mg/L]	[mg/L]
OS1	n	4	4	4	4	4	4	4	4	4	4	4	4
	Min	7.57	168.00	7.71	16.70	18.56	8.04	106.78	0.12	0.22	0.17	1.71	1.78
	Max	8.14	227.00	8.53	21.60	24.20	8.94	128.14	0.63	0.66	0.69	2.67	12.55
	Mean	7.83	197.05	8.13	19.08	22.19	8.61	112.88	0.40	0.36	0.42	2.17	7.02
	Std. deviation	0.23	21.51	0.29	1.87	2.16	0.34	8.89	0.21	0.18	0.18	0.37	4.95
OS2	n	3	3	3	3	3	3	3	3	3	3	3	3
	Min	5.92	55.00	6.10	18.30	8.53	1.08	33.56	0.31	0.28	0.17	0.00	0.35
	Max	6.60	97.40	7.57	19.60	16.60	1.57	73.22	0.62	1.69	0.34	0.59	1.37
	Mean	6.21	69.53	6.80	19.03	11.64	1.26	48.81	0.44	0.85	0.23	0.24	0.72
	Std. deviation	0.29	19.71	0.60	0.54	3.54	0.22	17.44	0.14	0.60	0.08	0.25	0.46
OS3	n	2	2	2	2	2	2	2	2	2	2	2	2
	value	6.55	85.80	7.86	18.90	12.80	1.27	67.12	1.32	0.31	0.19	0.61	0.24
	value	6.44	100.00	7.24	19.50	13.40	1.47	64.07	0.37	1.57	0.20	0.53	0.19
OS4	n	2	2	2	2	2	2	2	2	2	2	2	2
	value	7.27	150.60	5.67	23.00	17.80	2.14	79.32	0.09	2.10	0.31	0.11	0.54
	value	7.17	93.30	7.26	18.50	13.20	1.54	61.02	1.51	0.40	0.37	0.81	0.59
OS5	n	1	1	1	1	1	1	1	1	1	1	1	1
	value	7.25	236.00	7.53	20.10	16.00	1.49	79.32	2.98	0.35	0.22	0.62	0.26
OS6	n	4	4	4	4	4	4	4	4	3	4	4	4
	Min	7.57	291.00	7.22	18.30	58.16	0.67	183.05	0.05	0.11	0.16	1.76	2.49
	Max	7.88	344.00	7.78	20.10	72.80	0.78	216.61	0.32	0.28	0.57	5.39	7.71
	Mean	7.78	318.75	7.57	19.05	64.03	0.74	199.83	0.16	0.18	0.29	3.35	4.67
	Standard deviation	0.12	18.78	0.21	0.69	5.89	0.05	13.03	0.10	0.07	0.16	1.31	2.02
SRDV	n	5	4	4	5	5	5	5	5	5	5	5	5
	Min	7.94	246.00	7.68	18.20	49.50	5.99	207.46	1.19	2.20	3.14	2.83	3.00
	Max	8.22	366.00	8.30	22.20	56.00	7.54	237.97	2.69	3.69	4.26	7.54	9.74
	Mean	8.02	316.25	8.08	20.26	53.86	6.98	223.93	1.66	2.79	3.49	3.97	6.98
	Std. deviation	0.10	44.84	0.25	1.45	2.39	0.60	9.76	0.54	0.58	0.40	1.81	2.26
SSDV	n	4	4	4	4	4	4	4	4	4	4	4	4
	Min	7.88	244.00	6.80	13.00	44.98	4.84	176.95	1.70	3.20	3.12	2.90	3.07
	Max	8.11	393.00	7.97	24.60	56.00	8.01	256.27	3.99	9.84	9.82	5.00	8.20
	Mean	7.95	315.25	7.42	18.40	49.88	6.94	212.03	2.85	5.87	6.13	3.88	6.22
	Std. deviation	0.09	56.13	0.43	4.15	4.04	1.24	28.50	0.83	2.79	2.40	0.79	2.06
SSML	n	4	4	4	4	4	4	4	4	4	4	4	4
	Min	8.04	159.50	7.44	17.80	27.08	2.24	88.47	0.40	0.46	0.50	2.38	2.25
	Max	8.49	196.00	8.51	26.30	32.40	2.71	128.14	1.14	0.95	0.69	4.48	4.43
	Mean	8.29	177.15	8.02	20.85	30.07	2.46	108.30	0.60	0.81	0.60	3.60	3.22
	Std. deviation	0.16	14.17	0.40	3.49	2.22	0.17	14.39	0.31	0.20	0.08	0.79	0.92
W1	n	1	1	1	1	1	1	1	1	1	1	1	1
	Value	7.42	368.00	6.20	20.80	62.88	3.14	237.97	0.44	1.10	1.02	0.75	4.34
W2	n	1	1	1	1	1	1	1	1	1	1	1	1
	Value	7.47	302.00	7.87	18.80	49.20	8.47	204.41	0.27	0.18	0.50	2.03	6.36

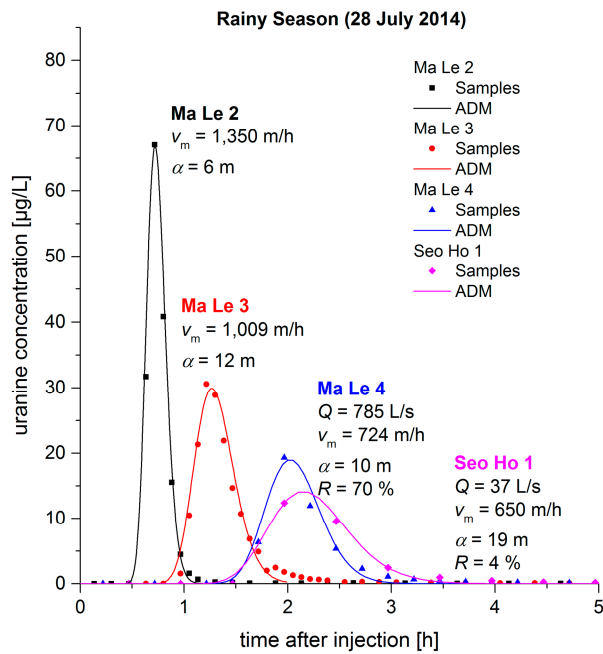
Suppl. Table 2 Results of the microbiological analysis for *Escherichia coli* (*E. coli*), thermotolerant coliforms (TTC) and enterococci (ENT). Two sampling campaigns were carried out during dry season in 2014 (DS1) and in 2015 (DS2) and two further during rainy season in 2014 (RS1) and in 2016 (RS2). One campaign took place at transient time in October 2015 (TS).

Sampling point	TTC [MPN/100ml]					<i>E. coli</i> [MPN/100ml]					ENT [MPN/100ml]				
	DS1	DS2	RS1	RS2	TS	DS1	DS2	RS1	RS2	TS	DS1	DS2	RS1	RS2	TS
CSP1	411	153	2,420	172	74	51	17	6	165	3	n.d.	46	10	452	9
CSP2	162	5	365	125	250	<1	<1	91	78	91	n.d.	<1	4	130	8
CSP3	1,120	>2,420	>2,420	>2,420	3,440	96	206	>2,420	>2,420	310	n.d.	1,733	>2,420	1,414	240
CSP4	770	>2,420	>2,420	>2,420	2,990	78	219	435	>2,420	360	n.d.	1,553	89	1,300	411
CST3	>2,420	1,300	>2,420	2,420	649	>2,420	517	1,986	687	166	n.d.	416	1,986	173	17
KS1	205	1,203	>2,420	>2,420	>2,420	14	7	219	>2,420	727	n.d.	320	66	>2,420	178
KS2	2,420	11,200	>2,420	>2,420	1,553	2,420	2,360	866	>2,420	1,120	n.d.	204	1,414	>2,420	1,414
KS3	112	42	225	>2,420	261	1	<1	19	>2,420	16	n.d.	<1	14	>2,420	2
KS4	n.d.	n.d.	n.d.	1,300	1,986	n.d.	n.d.	n.d.	1,203	130	n.d.	n.d.	n.d.	8	411
KS5	>2,420	117	n.d.	1,553	2,420	1,203	6	n.d.	435	178	n.d.	2	n.d.	228	687
KS6	165	>2,420	>2,420	196	1,046	93	<1	727	90	23	n.d.	2	188	<1	81
SRDV	1,733	649	>2,420	8,160	24,200	173	155	>2,420	2,050	4,610	n.d.	n.d.	3	1,010	3,610
FS1	2,420	16	>2,420	136	144	501	3	4	16	1	n.d.	<1	2	41	6
FS2	>2,420	>2,420	>2,420	248	>2,420	<1	49	261	248	122	n.d.	242	58	1,413	770
FS3	1,300	517	>2,420	1,360	579	58	15	4	579	<1	n.d.	<1	38	2,420	<1
FS4	>2,420	>2,420	1,986	687	1,733	866	64	461	387	99	n.d.	98	1,986	59	n.d.
FS5	361	107	n.d.	106	60	<1	93	n.d.	1	1	n.d.	16	n.d.	<1	2
FS6	51	49	727	1,046	93	<1	37	18	387	15	n.d.	<1	3	59	2
OS1	>2,420	>2,420	n.d.	1,553	>2,420	28	387	n.d.	172	1	n.d.	19	n.d.	41	57
OS2	n.d.	n.d.	980	187	70	n.d.	n.d.	17	51	16	n.d.	n.d.	7	980	n.d.
OS3	n.d.	n.d.	435	214	150	n.d.	n.d.	23	105	<1	n.d.	n.d.	31	10	21
OS4	n.d.	>2,420	15	727	2,420	n.d.	20	9	17	2	n.d.	37	13	344	56
OS5	n.d.	n.d.	>2,420	921	n.d.	n.d.	n.d.	2	28	n.d.	n.d.	n.d.	13	23	n.d.
OS6	>2,420	157	>2,420	1,553	>2,420	61	<1	57	326	921	n.d.	21	70	250	233
SSDV	10,960	9,600	n.d.	>48,400	>48,400	2,920	530	n.d.	24,060	31,060	n.d.	70	n.d.	2,880	634
SSML	>2,420	>2,420	n.d.	976	14,140	517	131	n.d.	320	1,270	n.d.	104	n.d.	142	240
W1	n.d.	n.d.	n.d.	<1	<1	n.d.	n.d.	n.d.	<1	<1	n.d.	n.d.	n.d.	<1	n.d.
W2	n.d.	n.d.	n.d.	205	166	n.d.	n.d.	n.d.	85	18	n.d.	n.d.	n.d.	28	n.d.
W3	n.d.	n.d.	n.d.	1	>2,420	n.d.	n.d.	n.d.	<1	62	n.d.	n.d.	n.d.	<1	n.d.
W4	n.d.	n.d.	n.d.	1	102	n.d.	n.d.	n.d.	<1	2	n.d.	n.d.	n.d.	<1	n.d.

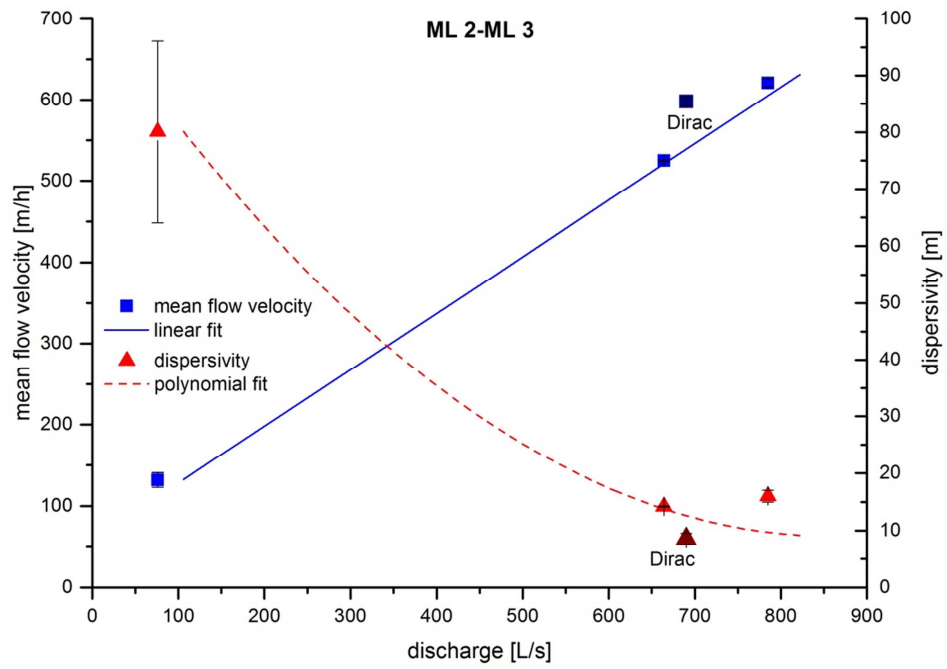
SUPPLEMENTARY MATERIAL – CHAPTER 3



Suppl. Figure 1 Tracer tests conducted in the Ma Le system with the different injections points (IP) and sampling points (SP). Cross section follows the course of the caves (Fig. 2–1b).

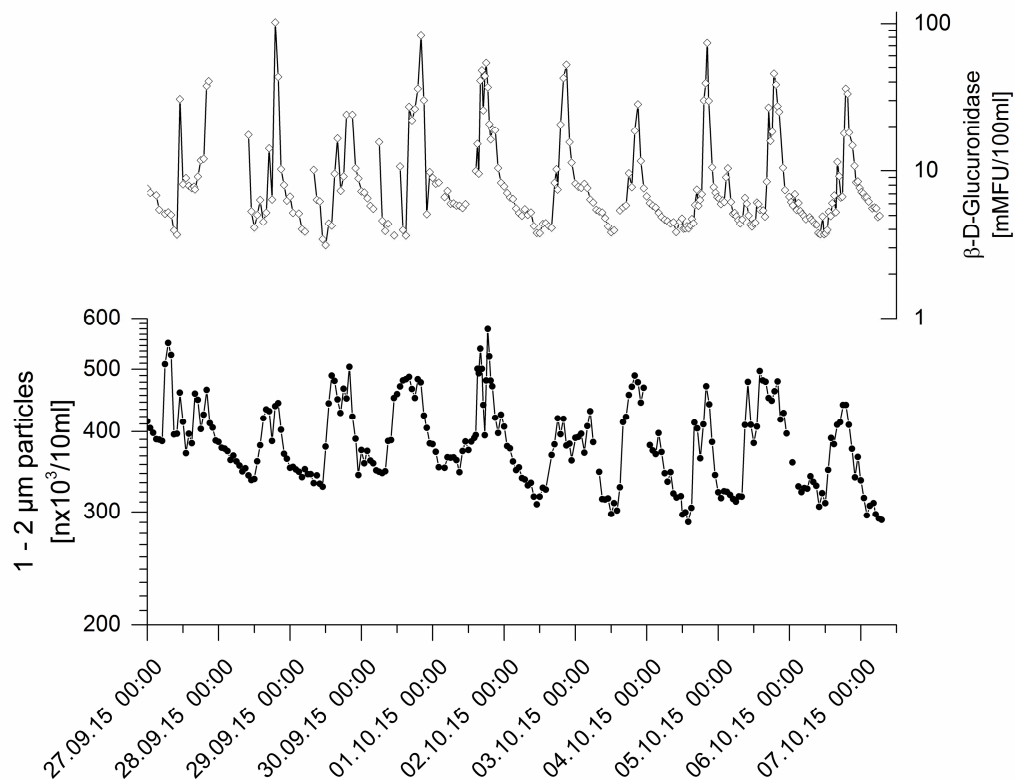


Suppl. Figure 2 Breakthrough curves for the tracer test under high flow conditions (test No. 4 in Table 3–1) on 28 July 2014 (Q = discharge, v_m = mean flow velocity, α = dispersivity, R = recovery rate). The Dirac input function was applied.



Suppl. Figure 3 Flow and transport parameters as a function of spring discharge (ML 4), exemplified with the section ML 2–ML 3 obtained by a multiple pulse injection approach and a Dirac injection.

SUPPLEMENTARY MATERIAL – CHAPTER 4



Suppl. Figure 4 Comparison of the daily variations between β -D-Glucuronidase activity and the particle concentration of particle size $1 \leq x < 2 \mu\text{m}$.